

# Ionic sweat analysis for health monitoring in real-time exercise

**Master thesis in Biomedical Engineering**

Luis del Río García







# Ionic sweat analysis for health monitoring in real-time exercise

by

Luis del Río García

to obtain the degree of Master of Science  
at the Delft University of Technology,  
to be defended publicly on Friday, November 26th, 2021, at 13:00.

Student number: 4994167  
Supervisor: Prof.dr. P.J. French  
Daily supervisor: MSc A.S.M. Steijlen  
Project Duration: March, 2021 - November, 2021

Thesis committee:	Prof.dr. P.J. French	TU Delft
	Dr.ir. A. Bossche	TU Delft
	Prof.dr.ir. F.P. Widdershoven	TU Delft
	MSc A.S.M. Steijlen	TU Delft

An electronic version of this dissertation is available at  
<http://repository.tudelft.nl/>.

Cover Image: Sweat on the surface of the skin. Source: <http://www.shutterstock.com/>







# Preface

This thesis was carried out as part of my Biomedical Engineering (BME) masters program at TU Delft. This project interested me from the beginning, as it combined two of my biggest passions in life: sports and biomedical engineering. I was greatly motivated to contribute with my engineering skills to develop a new device in the market of wearable devices in sports. The great potential sweat analysis can have in health monitoring has pushed me to work hard through out a very unusual year. Coronavirus times have imposed extra challenges in a research project where drawbacks are already found daily. I would like to take this space to thank everyone who has helped me achieve the completion of this work.

First of all I want to thank my supervisor Prof. dr. Paddy French for trusting me to carry this research project. He welcomed me in the CAS-P1 group, in which I have felt as part of a big group for the first time in my short researcher life. I very much appreciated all the discussions and feedback I got from the weekly meetings we have had for an entire year every Tuesday. I also had the chance to participate in the ProRISC & SAFE 2021 conference, presenting a poster of my research project and obtaining insightful critiques. That is why I would like to thank for all this help to Paddy, Andre, Sybrand, Jeroen, Annemarijn, Dimos, and all master and graduate students that I had the privilege to co-work with. Special thank you to Annemarijn and Jeroen for advising me with the day-to-day practical problems I have encountered in my work, I appreciate your willingness to help me every time I have struggled.

In addition, this project has also been hosted by Holst Centre, providing their facilities and knowledge in the field of wearable devices and supervised by C. Kjellander through the process. Thank you Charlotte for the help you gave me through out the whole internship period, your input in the wearable device market allowed me to move forward at a great pace when corona measures tried to slow down my work. I also want to thank Peter Zallar for his help at the chemical lab, very much needed to build those sticky membranes that drove us just a little crazy.

I would not be where I am right now if it was not for the company of my flatmates at Kloksteeg 17. Thank you Alberto, Nria, Paula, Mateo, David and Irene for all the laughs and tears we shared together every single day in the house. Your warming company made me realize I had a home in Delft. Also thank you Pablo, Amaia, Alvaro, Karl and Chu-Hsuan for the fun times when we were able to leave our homes.

Last but not least, thank you to my family for your warm support through our FaceTime calls, and physically tasted via boxes full of cheese sent from Spain. Mom, dad, I am proud to be called your son.

*Luis del Ro Garca  
Delft, November 2021*





# Abstract

Sweat analysis has the potential to become a new method in the wearable monitoring technology market by providing new and more precise physiological parameters. The need for more accurate sweat sensors has not allowed setting a correlation between sweat constituents and a person's health status. The development of this research field could lead to the creation of a new non-invasive method in the medical sector.

This study provides a new sweat analysis method for real-time health monitoring while performing physical activity. A sweat analysis system has been developed for the analysis of sodium and chloride ions found in sweat. A patch is adhered to the skin, wicking sweat by capillary action into a microchannel system. The integration of a potentiometric sensor inside this patch allows for the analysis of sweat *in situ*. Two ion-selective electrodes and a reference electrode are produced and tested for the correct functioning of the sensor. In addition, a read-out circuit is used for the real-time monitoring of sweat ion concentrations during physiological experiments carried on an ergometer.

The developed sweat analysis system proved to be a functional device capable of collecting and analyzing sweat in real-time. Wireless data transmission would avoid malfunctions in the system's connection and allow new tests in different sports environments. Future research should focus on validating the sensor with further physiological tests to set a stronger relationship between ionic sweat concentrations and the health status of a person.





# Contents

<b>Preface</b>	<b>iii</b>
<b>Abstract</b>	<b>v</b>
<b>Nomenclature</b>	<b>ix</b>
<b>List of Figures</b>	<b>xi</b>
<b>List of Tables</b>	<b>xiii</b>
<b>1 Introduction</b>	<b>1</b>
1.1 Wearable monitoring technology in sports . . . . .	1
1.1.1 Physiological sensors for real-time monitoring . . . . .	2
1.2 Sweat monitoring . . . . .	3
1.2.1 Sweat monitoring in medicine . . . . .	4
1.3 Project objectives. . . . .	5
1.4 Project outline . . . . .	5
1.4.1 Literature study . . . . .	5
1.4.2 Study, building and validation of the sweat analysis system . . . . .	6
1.4.3 Final discussion and conclusion . . . . .	6
<b>2 Monitoring of sweat</b>	<b>7</b>
2.1 Perspiration process . . . . .	7
2.1.1 Types of sweat glands . . . . .	7
2.1.2 Sweat production . . . . .	9
2.2 Sweat composition . . . . .	11
2.3 Sweat sensing system . . . . .	12
2.3.1 Requirements. . . . .	13
2.3.2 Validation . . . . .	13
<b>3 Sweat sensor</b>	<b>15</b>
3.1 Analytical techniques in sweat sensing . . . . .	15
3.1.1 Potentiometry. . . . .	20
3.1.2 Ion-selective electrodes in sweat sensors. . . . .	21
3.1.3 Conclusion . . . . .	22
3.2 Methods. . . . .	23
3.2.1 Design. . . . .	23
3.2.2 Screen-printing of the sensors . . . . .	25
3.2.3 Chemical composition of the membranes . . . . .	27
3.2.4 Production steps . . . . .	31
3.3 Sensor validation . . . . .	33
3.3.1 Experimental set up . . . . .	33
3.3.2 Results . . . . .	35
3.4 Discussion . . . . .	38
<b>4 Sweat collector</b>	<b>41</b>
4.1 Sweat collection techniques . . . . .	41
4.1.1 Capillary action in sweat collectors . . . . .	44
4.1.2 Conclusion . . . . .	46

4.2	Methods . . . . .	47
4.2.1	Design . . . . .	47
4.2.2	Materials and structure . . . . .	50
4.2.3	Surface treatment of TPU . . . . .	53
4.2.4	Production steps . . . . .	53
4.3	Collector validation . . . . .	54
4.3.1	Experimental set up . . . . .	54
4.3.2	Results . . . . .	56
4.4	Discussion . . . . .	57
<b>5</b>	<b>Sweat analysis system</b>	<b>59</b>
5.1	System integration . . . . .	59
5.1.1	Read-out circuit. . . . .	59
5.1.2	Design and structure . . . . .	60
5.1.3	Production steps . . . . .	62
5.2	Sweat analysis system validation . . . . .	63
5.2.1	Syringe pump experiment . . . . .	64
5.2.2	Physiological experiment. . . . .	66
5.3	Discussion . . . . .	69
<b>6</b>	<b>Final discussion</b>	<b>71</b>
6.1	Design and production steps. . . . .	71
6.1.1	Sweat sensor . . . . .	71
6.1.2	Sweat collector . . . . .	72
6.1.3	Sweat analysis system . . . . .	73
6.2	Results . . . . .	73
6.2.1	Sweat sensor . . . . .	73
6.2.2	Sweat collector . . . . .	74
6.2.3	Sweat analysis system . . . . .	74
<b>7</b>	<b>Conclusion and future work</b>	<b>77</b>
	<b>Bibliography</b>	<b>89</b>
<b>A</b>	<b>Additional results of physiological experiments</b>	<b>91</b>
<b>B</b>	<b>Read-out software code</b>	<b>95</b>
<b>C</b>	<b>Pictures of physiological experiments</b>	<b>97</b>
<b>D</b>	<b>Informed consent form and study information</b>	<b>101</b>

# Nomenclature

## Abbreviations

Abbreviation	Definition
<b>Ag/AgCl</b>	Silver/Silver-Chloride
<b>ATP</b>	Adenosine triphosphate
<b>DMPP</b>	Photoinitiator 2,2-dimethoxy-2-phenylacetophenone
<b>FISA</b>	Flexible integrated sensing array
<b>FFC</b>	Flexibile Printed Circuit
<b>IC</b>	Ion chromatography
<b>ISE</b>	Ion-selective electrode
<b>PDMS</b>	Polydimethylsiloxane
<b>PEDOT</b>	Poly(ethylenedioxythiophene)
<b>PET</b>	Polyethylene terephthalate
<b>pHEMA</b>	Poly(2-hydroxietil methacrilato
<b>PSS</b>	Poly(sodium styrenesulfonate)
<b>PVA</b>	Polyvinyl Acetate
<b>PVB</b>	Polyvinyl Butyral
<b>PVC</b>	Polyvinyl Chloride
<b>THF</b>	Tetrahydrofuran
<b>TPU</b>	Thermoplastic polyurethane
<b>WBW</b>	Whole-body washdown
<b>WMT</b>	Wearable monitoring technology





# List of Figures

1.1	Wearable technology in different industries [9] . . . . .	2
1.2	Effect of dehydration on physical performance [22] . . . . .	4
2.1	Different types of glands in the axilla [17] . . . . .	8
2.2	Mouse eccrine sweat gland and cellular constituents. The eccrine gland comprises a secretory coil in the deep dermis and a relatively straight duct open to the skin surface (left panel). The secretory coil contains three types of cells, clear, dark and myoepithelial. Clear and dark cells are secretory cells, and myoepithelial cells form a major niche for sweat gland stem/progenitor cells (right lower panel). The sweat duct consists of luminal and basal layers where ions are partially reabsorbed (right upper panel). [41] . . . . .	9
2.3	Mechanisms of sweat secretion in the secretory coil (left). Reabsorption of ions in the proximal duct (right). [17] . . . . .	10
2.4	Overview of the parts needed for the sweat sensing system. . . . .	12
3.1	Chromatograms of chloride (left) and sodium (right) [62] . . . . .	17
3.2	Sweat-Chek™ Analyzer using ion conductivity technique [66] . . . . .	17
3.3	Schematic explanation of the flame photometry process [67] . . . . .	18
3.4	Images of the epidermal microfluidic biosensor (left) before and (right) after injecting artificial sweat [72] . . . . .	19
3.5	Response mechanism of complete solid-contact ion-selective electrode for detection of common ions in sweat. [55] . . . . .	20
3.6	A) Ion-selective electrodes of the sensor. B) Illustration of the electronics and sensor of the device [80] . . . . .	21
3.7	A) Wearable FISA on a subject's wrist, integrating the multiplexed sweat sensor array and the wireless FPCB. B) Schematic of the sensor array [31] . . . . .	22
3.8	<i>Final sweat sensor version made by T. Bakker [56]</i> . . . . .	23
3.9	<i>Layer by layer design of the sweat sensor</i> . . . . .	24
3.10	<i>Sensor FFC connector [56]</i> . . . . .	25
3.11	<i>Production steps of screen-printing [84]</i> . . . . .	26
3.12	<i>Incomplete adhesion of the insulation layer (left) and carbon ink (right)</i> . . . . .	27
3.13	<i>Screen-printed sweat sensors on PET</i> . . . . .	27
3.14	<i>Sweat patch containing an array of AgCl sensing electrodes and reference electrode. The pHEMA hydrogel layer was drop casted within an O-ring, which was glued on top of the reference electrode. Holes were punched through the collection area to allow the sweat to be absorbed. [82]</i> . . . . .	29
3.15	<i>Potentiometric responses of PVA/KCl-Ag/AgCl solid reference electrode vs double-junction Ag/AgCl/KCl (3 M) containing a 1 M LiAcO salt bridge in (A) 3 M KCl solution and (B) different concentration solutions of ions range from 10<sup>-1</sup> M to 10<sup>-6</sup> M. (C) pH response and (D) light sensitivity of PVA/KCl-Ag/AgCl RE. Potential responses in panels B and C have been vertically shifted for clarity of presentation [76]</i> . . . . .	30
3.16	<i>Multi-channel measurement setup running four experiments at the same time [56].</i> . . . .	34
3.17	<i>Stability test for the sensors using four different NaCl concentrations.</i> . . . .	35
3.18	<i>Stability test for pre-wetted sodium sensors using four different NaCl concentrations.</i> . . . .	36
3.19	<i>Comparison between a polarized and non-polarized chloride electrode</i> . . . . .	37
3.20	<i>Calibration curve for the Na sensor</i> . . . . .	37
3.21	<i>Time constant estimation using 10 and 75 mmol/L concentrations.</i> . . . .	38
4.1	Whole-body washdown technique. A: intact system; B: a section of the bag has been cut away to show subject cycling on the ergometer. [54] . . . . .	42

4.2	Absolute regional median sweat rates of male athletes during high intensity exercise [81]	43
4.3	Example of the capillary action process in a rapid COVID-19 antigen test [101]	44
4.4	Megaduct sweat collector (Wescor® Inc., Logan, UT) [102]	45
4.5	Working principle of the hydrophobic valve to route liquid into the one-opening chamber in the microfluidic device. (a) Schematic of the one-opening chamber with the hydrophobic valve and a bridging channel in a microfluidic device. (b) Optical images (i–iv) and (c) numerical simulations of the hydrodynamic flow process into the one-opening chamber with a hydrophobic valve [106]	46
4.6	Lateral view of the skin structure. Sweat is wicked from the inlet hole to the microchannel due to capillary pressure.	47
4.7	Principle of operation of a Tesla valve. The upper figure shows flow in the blocking direction: at each stage, part of the fluid is turned around (red) and interferes with the forward flow (black). The lower figure shows flow in the forward direction (blue) [113].	49
4.8	Final design for the sweat collector	50
4.9	Sweat collector structure showing the three different TPU layers.	51
4.10	Schematic of the different layers of TPU and double sided tape.	52
4.11	Final design and structure of the sweat collector	54
4.12	Sweat collector using double-sided tape without an inlet hole. Dye artificial sweat can be observed flowing inside the microchannel.	55
4.13	Explanatory drawing of the different dimensions of the microchannel in the sweat collector.	56
4.14	Sweat flow rate of the four different collectors.	56
4.15	Sequential images showing the sweat flow inside the collector during a 30 minute exercise.	57
5.1	Read-out circuit application overview [56]	59
5.2	Hardware abstraction layer (HAL) of the read-out circuit developed by T. Bakker [56]	60
5.3	Final design for the sweat patch	61
5.4	Final structure for the sweat patch. The sweat sensor is integrated within the collector	62
5.5	Sweat patch system. Sweat sensor and collector integrated together.	62
5.6	A) Response of the sodium membrane in a long-term stability test [85]. B) Potential stability dependency on the electrode's surface [76].	63
5.7	Calibration curve for the Na sensor with larger electrodes.	64
5.8	Stability test sweat sensor in 10 $\mu\text{l}/\text{min}$ , 20 $\mu\text{l}/\text{min}$ , 30 $\mu\text{l}/\text{min}$ , Concentration=30mM	65
5.9	Sensitivity test sweat sensor in 20mM, 50mM, 90mM, Rate=10 $\mu\text{l}/\text{min}$	65
5.10	Sensitivity test sweat sensor from 30mM to 90mM and back to 30mM	66
5.11	Sweat system output signals for the three sensors in a 45 minutes exercise period	67
5.12	Sweat system output for all sensors in a 45 minutes exercise period with no shielding of the sensors	68
5.13	Sweat system output signal for sensor 2	69
A.1	Sweat system output for all sensors in a 45 minutes exercise period for subject 2	91
A.2	Sweat system output for all sensors in a 45 minutes exercise period for subject 3	92
A.3	Sweat rate for subject 1	92
A.4	Sweat rate for subject 4	93
C.1	All three sensors and the sweat patch attached to the back of the subject	97
C.2	Strong adhesion of the sensor in a subject with abundant body hair	98
C.3	Sweat sensing patch during the exercise period	98
C.4	Slight skin irritation right after detachment of the patch	99

# List of Tables

2.1	Concentrations of sweat micronutrients and non-micronutrients. . . . .	11
3.1	Analytical techniques for measuring ion concentrations in sweat . . . . .	20
3.2	Chemical materials used to produce the sodium-selective membrane . . . . .	28
3.3	Chemical materials used to produce the reference membrane . . . . .	30
3.4	Total quantities of each material for the production of the sodium membrane . . . . .	31
4.1	Analysis of possible materials for the sweat collector . . . . .	51
4.2	Analysis of possible double sided tapes . . . . .	52





# Introduction

The study of sweat during physical activity lacks health monitoring systems capable of collecting sweat constituents without contamination and effectively analysing them in real-time. This graduation project will aim to expose this problem statement and propose a novel engineering solution for it.

This section will first focus on the clinical background information related to the problem statement previously exposed. Current technologies on the real-time monitoring of athletes during exercise will be overlooked, especially regarding sweat monitoring. Afterwards, the project objectives will be presented and the thesis outline exposed.

## 1.1. Wearable monitoring technology in sports

Sports have a crucial role in the society nowadays. It influences the economy, politics, racism, religion and every other aspect of modern life [1]. Just in the USA, a total of 100 billion dollars are spent per year by Americans on sports equipment, sporting events or gym memberships [2]. In the Netherlands, it was observed that Dutch people spend an average of 1000€ per year on sports. This expenditure contributes to almost 1,5% of gross income in the Netherlands [3]. This investment keeps increasing as people are more concerned about the importance of exercising to stay healthy. Therefore, there is a great interest from companies to invest and participate in this big market worldwide.

Attention has lately been focused on improving athletes' health quality to enhance their performance and offer a better show. In order to do so, technology has recently taken an essential role in the process [4–6]. Technology helped to understand better the chemical and mechanical processes the body of a professional athlete goes through when performing to their maximum [7]. Teams are constantly pushing athletes to test the maximum physical strength their bodies can withstand. Thus, this industry needs to be constantly updated to achieve sporting perfection and it uses the latest technology to do so.

Until very recent years, the research concerning the study of biometric and physiological signals has been limited in laboratories with many types of equipment and of big sizes. The introduction of wearable technology in the market allows for acquiring and studying long periods of exercise with an in-person approach. This progress is mainly thanks to sensors, as well as integrated circuits, textiles and other elements. This wearable monitoring technology (WMT) is already making significant progress and it will have a great impact on the sports market shortly [8]. Currently, technological companies are already entering the marketing of wearable sensors to measure physiological signals (see Figure 1.1).

WMT can be divided into two types of categories depending on the parameters measured by the device. Firstly, some aim to measure the athlete's body movement using technology such as accelerom-

Wearable	Accelerometer	Gyroscope	Heart Rate Monitor	GPS	Smart Category	Application	Body Place	Other Sensors
Apple Watch 2	x		x	x	Watch	Lifestyle	Wrist	Speaker
Fitbit	x		x	x	Watch	Fitness	Wrist	Photodiode
Nintendo Joycon	x	x			Controller (modular)	Gaming	Hand *	IR sensor, NFC
PlayStation VR	x	x			Eye wear	Gaming	Head	Microphone, speaker
OM Bra	x		x	x	Clothing	Medical	Upper body	Pedometer
RealWear HMT	x	x		x	Ear wear	Industrial	Head	Microphone, Speaker, camera
HexoSkin	x		x		Clothing	Fitness	Upper body	Pedometer, ECG sensor, Thermometer
Vuzix AR3000	x	x		x	Headwear	Medical	Head	Camera, Magnetometer, microphone
Google Glass	x	x		x	Eye wear	Industrial	Head	Magnetometer, microphone, speaker, light sensors, IR sensor, Camera
Samsung Gear S3	x	x	x	x	Watch	Lifestyle	Wrist	Barometer, Light sensor

Figure 1.1: Wearable technology in different industries [9]

eters, magnetometers or Global Positioning System (GPS). Secondly, other types of sensors focus on measuring the physiological parameters in the athletes' body during exercise. These last types of sensors measure signals such as heart rate, muscle activity or even brain signals.

Physiological sensors will be the focus of this project to understand how much feedback WMT can give on an athlete's health status during physical activity.

### 1.1.1. Physiological sensors for real-time monitoring

Sensors can acquire different physiological signals emitted by the body during physical activity. As previously mentioned, the heartbeat or muscle activity are signals of interest to get the body's real-time health status. Besides these examples, a new method for measuring physiological signals comes through the analysis of sweat.

The monitoring of these signals can be critical to avoid injuries and body breakdowns during high-intensity periods. In the early 21st century, a study tried to measure the socioeconomic costs resulting from sports injuries in Flanders. This study showed that Flanders' direct and indirect medical costs involved in acute insurance-claimed injuries to over €100 million per year. Results showed how necessary it is to have a development on the research for sports injury prevention. Even though the benefits of doing sports outweigh the costs of injuries, their prevention can have a considerable impact on the socioeconomic consequences [10].

#### Heart rate monitoring

Heart rate sensors are an excellent method to indicate the physiological adaptation and intensity of effort. These types of sensors currently use light in order to measure the heart rate of the athlete. The method behind is called photoplethysmography and consists of the emission of light to measure blood flow, and therefore linking it to heartbeat [11]. Heart rate sensors can be very relevant in sports as they show the athlete's heartbeat and directly derive the oxygen consumption ( $VO_2$ ) and the energy expenditure. This method requires calibration of the heart rate data, which powerful wearable devices can do precisely [12].

Heart rate feedback can be effective to know the intensity of the exercise and check any abnormalities on the pulse. However, it does not give any information on other essential aspects as hydration

levels or salt concentration in the body.

### **Muscle monitoring**

By using sensors attached to the different muscles of the body, much information can be derived from them. Electromyography (EMG) can be used not only to analyse the performance of an athlete's muscles and in order to avoid injuries [13]. Regarding the first objective, there have been recent improvements in data analysis by using wearable surface electromyography (sEMG). This method can give real-time data to analyse the motion of the muscle [14]. Muscle injuries are the most common type of injury in sports, constituting between 20% to 55% of all injuries [15]. There is a great interest in both avoiding and faster treating these types of injuries. That is the case in football, where sEMG allowed us to understand better how hamstring injuries were produced and how to avoid them by proximal neuromuscular control [16].

Muscle monitoring can help prevent injuries once they are close to happening. However, as with heart rate monitoring, many injuries could be early predicted if more physiological characteristics of the body were known.

This lack of more precise physiological feedback on an athlete's health status leads this project to focus on a new approach to the problem: sweat monitoring. Section 1.2 will expose the potential of this process in the real-time health monitoring of sports, as well as in other medical applications.

## **1.2. Sweat monitoring**

In addition to the last examples, there has been a rising interest in the study of perspiration. Sweat is present on the skin of every person during physical activity. It regulates the body's temperature when exercising, but sweat composition can also be fundamental to monitor the body's status. Research in the last decades has shown the potential of sweat analysis for measuring hydration of the body as well as to avoid extreme salt loss [17–19].

In high-competition sports, dehydration is considered the primary challenge to physiological homeostasis and performance. Most people lose as much as two litres of body fluid during one hour of exercise. However, an athlete may lose as much as three litres of fluid an hour during an intense workout. Fluid loss in endurance activities such as distance running, cycling, strenuous hiking, or cross-country skiing can be severe. These types of activities can quickly lead to heat exhaustion. In endurance athletes, dehydration can cause symptoms called post-extreme endurance syndrome (PEES). Symptoms of PEES include decreased body temperature, nausea, vomiting, diarrhoea, dizziness, headache, muscle cramps, and an inability to drink fluids [20].

However, dehydration usually does not cause symptoms, so it is commonly thought that water intake could be done once the exercise is over. However, hydration can have a significant impact on the performance of the sport even if no symptoms appear. A loss of sweat equal to 2% of body weight causes a noticeable decrease in physical and mental performance. Losses of 5% or more of body weight during physical activities may decrease the capacity for work by roughly 30% [21]. Dehydration could be avoided by monitoring sweat during a long and exhaustive period of exercise where high quantities of sweat were secreted.

Moreover, losing high quantities of sweat does not only derive from water loss. The body also loses salts present in the substance through sweat, mainly sodium (Na) and chloride (Cl) ions. When blood sodium concentration falls to an abnormally low level, there is a rapid and dangerous brain swelling that can result in seizures, coma, and even death. This condition is called hyponatremia, and despite being rare to occur in athletes, it has taken the lives of marathon runners and military recruits. Thus, athletes should be more aware of their levels of salt loss in sweat in order to replace it with sodium-containing beverages or food during the physical exercise [23].

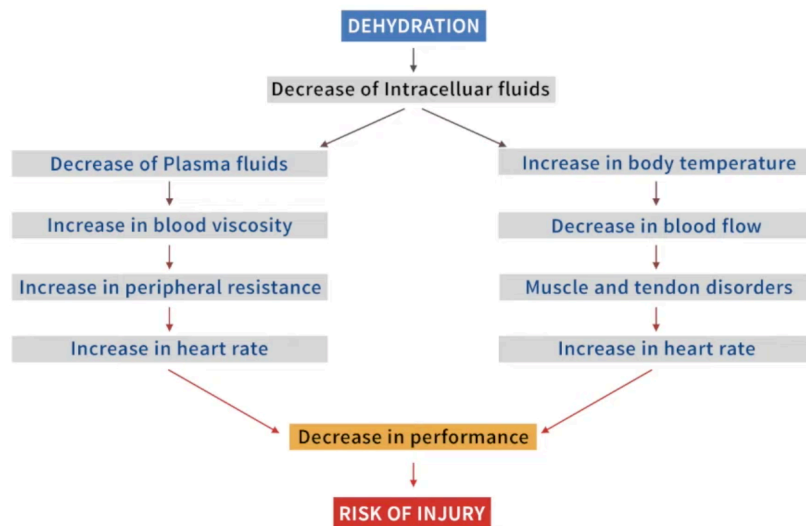


Figure 1.2: Effect of dehydration on physical performance [22]

As previously mentioned, current research is on track to develop a system capable of monitoring the health status of the athlete during exercise. Regarding dehydration, recent studies have shown a correlation between electrolyte concentration and the athlete's dehydration. Changes in this concentration can relate to the amount of sweat being lost [24]. In the case of salt losses during exercise, reading of trim concentration levels of electrolytes in sweat can relate to low levels of salt in the body [17]. These studies will be exposed in chapter 2.

The current barrier for sweat monitoring during physical activity is the lack of devices to collect and analyse sweat in situ. Literature research carried before this project came to show the obstacles for more efficient sweat analysis. Sweat analysis methods nowadays first try to collect sweat to analyse it in the lab later on. This process shows the inability of the athlete to react in time if suffering dehydration or extreme salt loss. In addition, concentrations of sweat constituents are low, so minimum contamination of the sample leads to its inaccurate analysis [25]. Finally, sweat production occurs at a low rate ( $\text{nl min}^{-1} \text{mm}^{-2}$ ) and the incapability of sensors to measure such reduce amount of analyte bring inaccurate results [26].

### 1.2.1. Sweat monitoring in medicine

This project will be mainly focusing on the analysis of sweat during physical activities. However, sweat analysis has the potential to become a monitoring tool in other fields. Sweat monitoring can also help cystic fibrosis patients and correlate constituents found in sweat and blood.

*Cystic fibrosis* is a genetic disease that affects people who have inherited two faulty versions of a gene for CFTR (cystic fibrosis transmembrane conductance regulator), a protein necessary to remove chloride in cells. Having such a mutation is shown in sweat, which possesses a much more elevated concentration of chloride than in a healthy patient [27]. Progress in sweat research has allowed creating a fast and efficient test that can determine if a patient most probably is carrying this mutation in its DNA without the necessity of going through a genetic test. The test is simple, as it only requires the stimulation of sweat (called iontophoresis) and the following collection of it using a patch. The sweat is then analysed in the laboratory and the concentration of chloride is obtained. Average values of [Cl] are less than 30 mmol/L, but a patient with cystic fibrosis will have values above 60 mmol/L [28]. This process shows how sweat monitoring can contribute to the medical and physical condition of a patient.

In addition, other constituents besides sodium and chloride can be found in sweat, such as glucose.

This molecule has always been the main blood constituent for the diagnosis and monitoring of diabetic patients. However, to analyse diabetes, there needs to be an estimation of the glucose concentration in blood using invasive methods, with the pain, inconvenience, and blood waste such as the fingerstick blood glucose testing. Thus, new methods are trying to analyse glucose through sweat [29, 30]. It has been observed that sweat glucose concentration is much lower than such in blood, being in the micromolar range; usually less than 100  $\mu\text{M}$ . Sweat glucose seemed to rise at the beginning of constant-rate exercise, to then fall [31]. Studies show that high levels of glucose injected in blood lead to double normal sweat glucose concentration [32]. However, the utility of glucose as a sweat biomarker is still controversial, especially as an actual correlation between blood and sweat is not yet established.

Another example where sweat analysis can be helpful is measuring alcohol levels present in the body. As a non-invasive method, this method could accurately provide a convenient means to monitor alcohol consumption [33]. These processes show the tremendous potential sweat monitoring can have not only in sports but also in other areas of health monitoring.

### 1.3. Project objectives

Literature research on sweat analysis devices has shown a lack of health monitoring systems capable of acquiring and analysing perspiration in real-time. Perspiration during exercise allows for the cooling down in the body, leading to dehydration and a loss of salts in high-performance athletes. Attempts have been made to monitor sweat constituents, but it has not yet been able to constantly obtain sweat data feedback related to the athlete's health status.

A precise measurement of sweat constituents can lead to the regulation of body electrolytes, especially for sodium and chloride ions, being the most abundant in sweat. This controlled analysis can also avoid the dehydration and muscle exhaustion of athletes. Addressing this issue will also help to monitor diseases which can be detected through sweat (cystic fibrosis) [27], as well as to monitor substances present in the body (glucose or alcohol) [33]. This step forward in sweat analysis will help it to be considered as a non-invasive health monitoring process.

This project aims to determine and build a precise system capable of collecting and analysing sweat chloride and sodium concentration during physical activity. The most suitable collecting and sweat analysis methods will be chosen to build this non-invasive device using cutting edge technology. The research question that wants to be answered in this project is:

**How can sweat sodium and chloride ions be effectively collected and analysed using a precise sensing system during physical activity for real-time health monitoring?**

Throughout this project, the first aim will be to answer this research question. In addition, this report will show all the work done to design and build this system and show the results obtained after testing the device. Finally, an evaluation of the project will be stated, together with an orientation for future research on this field.

### 1.4. Project outline

The structure of this project will be as follows:

#### 1.4.1. Literature study

Chapter 2 will first focus on explaining the process of perspiration. In order to collect and analyse sweat, it is first necessary to understand its process and composition. By the end of the chapter, a conclusion



will be stated, specifying on which aspect of sweat analysis this project will focus on.

### **1.4.2. Study, building and validation of the sweat analysis system**

This section will be divided into the two main structures of the sweat analysis system: the sweat sensor and collector. Chapters 3 and 4 are focused on the process for building the sweat sensor and collector, from a small literature review to its final validation. The integration of the sweat collector and sensor, as well as the final process of physiologically testing the sweat analysis system and the results obtained is explained in Chapter 5.

### **1.4.3. Final discussion and conclusion**

The discussion and conclusion derived from the results obtained are shown in chapters 6 and 7. In this section, the recommendations for future development of the sweat analysis device are included.

# 2

## Monitoring of sweat

In this chapter, all the necessary information for the accurate monitoring of sweat is presented. Firstly, the entire perspiration process is evaluated and explained. Secondly, Section 2.2 will review the composition of sweat, showing the main constituents found in it. Finally, Section 2.3 will introduce the main focus points of this research for analyzing sweat during physical activity, the requirements needed in the project and the validation process.

### 2.1. Perspiration process

Sweat is a very complex substance in which there is a great variety of chemical compounds [17]. Our skin is filled with tiny glands that segregate sweat onto the skin's surface for several reasons. However, not all sweat glands are the same and sweat from different parts of the body is produced in different ways. When exercising, sweat segregation occurs in the face and upper body, while hands tend to sweat more under emotional strain. This event is due to the different sweat glands activation system [34].

The nervous system is in charge of the thermoregulation of the body. When working hard or feeling hot, the body communicates these feelings to the brain through nerves. In response, the brain sends messages back along the nerves to the sweat glands, telling them to increase the operation of the body's cooling system. However, other sweat glands are controlled by hormones instead of nerves. Most of these sweat glands are on the palms of the hands and the soles of the feet and start producing sweat due to hormonal changes on the body (such as the activity of adrenalin).

This project aims to study the sweat produced during physical activity for thermoregulatory purposes. Thus, it is necessary first to understand the differences between types of sweat glands in the skin. It is also essential to study this fluid from a biological point of view to see where it is produced and segregated and its composition.

#### 2.1.1. Types of sweat glands

There are three main types of sweat glands: eccrine, apocrine and apoecrine [35]. Eccrine glands are the most abundant type of glands in the skin, and they are responsible for most of the sweat secreted. However, apocrine and apoecrine glands also play a role in the final chemical composition of sweat, so it is necessary to understand their function in the production of sweat.

Eccrine sweat glands are located almost everywhere in the skin, except for the ear canal and some parts in the genital areas. These glands rely on the dermis, and they can excrete directly onto the skin's surface or through hair pores. There are approximately between 1.6 and 4 million eccrine glands

distributed on the body surface. They are most numerous on the sole ( $\sim 620/\text{cm}^2$ ), then the forehead ( $\sim 360/\text{cm}^2$ ), the cheek ( $\sim 320/\text{cm}^2$ ) and the palms ( $\sim 300/\text{cm}^2$ ). Eccrine sweat glands are least numerous on the trunk ( $\sim 65/\text{cm}^2$ ) and the extremities ( $\sim 120/\text{cm}^2$ ) [36]. Under sweltering conditions, the body can produce up to 10 L of sweat per day, but the normal production is around 0.5-1 ml/min. Also, it is known that at least 5% of all sweat glands are constantly active, which shows the enormous role of sweat production [37].

Eccrine glands begin to develop in palms and soles when the embryo is 3 months old and around 5 months in the rest of the body [35]. These glands keep forming during the early months of childhood, until approximately 2-3 years of age, when the total number of eccrine glands stops increasing [17]. It is crucial to take into account that the skin surface has kept increasing for many more years. Thus, babies have a higher density of eccrine glands than human adults. However, it is common to think that higher sweat gland density will result in a higher sweating rate. As F. Sato *et al.* showed, sweat rate is not related to the sweat gland density, but more to the differences in sweat secretion per gland [38]. Eccrine sweat is mainly formed of water and salt (NaCl), but it also possesses a mixture of other chemicals compounds. The structure and function of eccrine glands and their chemical composition will be explained thoroughly in the following sections.

Besides eccrine glands, there are also two other types of sweat glands: apocrine and apoecrine glands. Apocrine glands are related to the production of pheromones to emit body odour, secreting its viscous substance through hair follicles. In the case of apoecrine glands, they are a mixture of eccrine and apocrine glands. They secrete directly onto the skin but are only found in the axilla, probably necessary for its better thermoregulation.

Lastly, there is a fourth type of gland, sebaceous glands. These glands are not considered sweat glands, but they also secrete a substance called sebum into the skin's surface. Little is known about these glands, but the accepted conclusion of why humans developed them is thought to be related to the importance in the thermoregulation process of hunter-gatherers groups developed thousands of years ago [39].

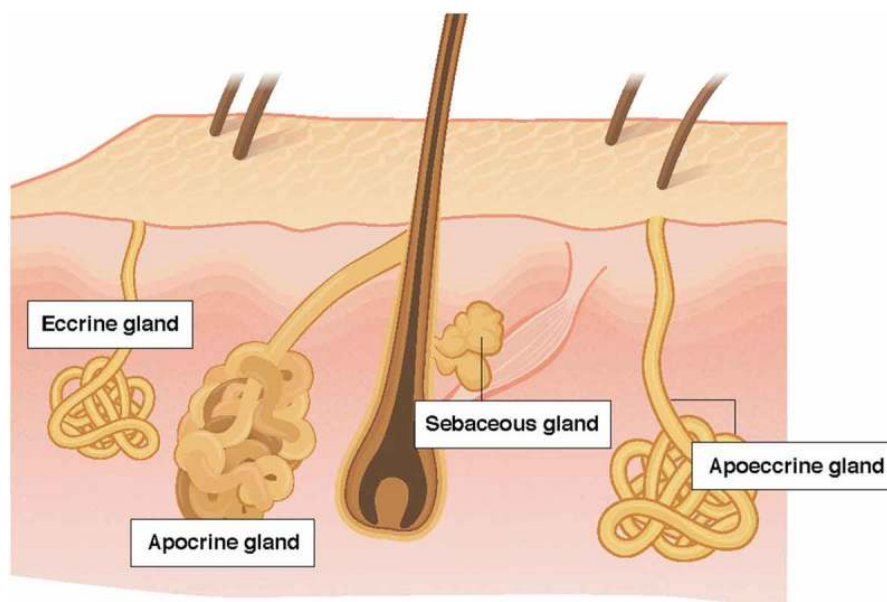


Figure 2.1: Different types of glands in the axilla [17]

After knowing what type of glands are in charge of secreting sweat into the skin's surface, it is crucial now to understand the composition of the sweat and how it is produced. Eccrine glands are the most abundant in our body and the major contributors to final sweat composition during physical activity.

Thus, from further on, the attention will be focused on the sweat production and composition of eccrine glands.

### 2.1.2. Sweat production

Eccrine sweat glands have an average size of around 3 to 5 mm in length, located in the skin's dermis. It is composed of a secretory coil and a relatively straight sweat duct that opens to the skin's surface. The sweat gland is composed of two types of secretory cells: dark and clear cells and a type of structure supporting cell: myoepithelial cells. Regarding the duct (also divided into proximal and distal), we can find luminal and basal cells in it [17, 40]. For all these types of cells, it can be defined as an apical membrane facing the lumen, and a basolateral membrane, in contact with the blood or other cells. Figure 2.2 shows the previously explained structure visually.

Clear cells are in charge of the secretion of primary sweat, mainly composed of isotonic and blood plasma. They have many mitochondria and membrane villi, extending to excessive sweating in patients with local hyperhidrosis. On the other hand, dark cells barely have any mitochondria and membrane villi, and they were long thought to have a small role in the secretion of sweat [41]. However, it has recently been discovered that dark cells can rapidly change their ion concentration due to stimulation with methacholine [42]. Thus, besides the contribution of dark cells on secreting glycoproteins and antimicrobial dermcidin, they also play an essential function in sweat secretion by assisting clear cells. Dark cells can be easily differentiated from clear cells as they have an abundance of dark cell granules in their cytoplasm [17]. Myoepithelial cells' function is to support the gland against the hydrostatic pressure produced during sweat secretion.

Regarding the function of the duct, it mainly focuses on the reabsorption of  $\text{Na}^+$  and  $\text{Cl}^-$  ions in sweat, especially in the proximal duct, as cells here have more mitochondria and Na-K-ATPase activity than those at the distal duct [43]. The different anatomy structures previously mentioned can be observed in Figure 2.2.

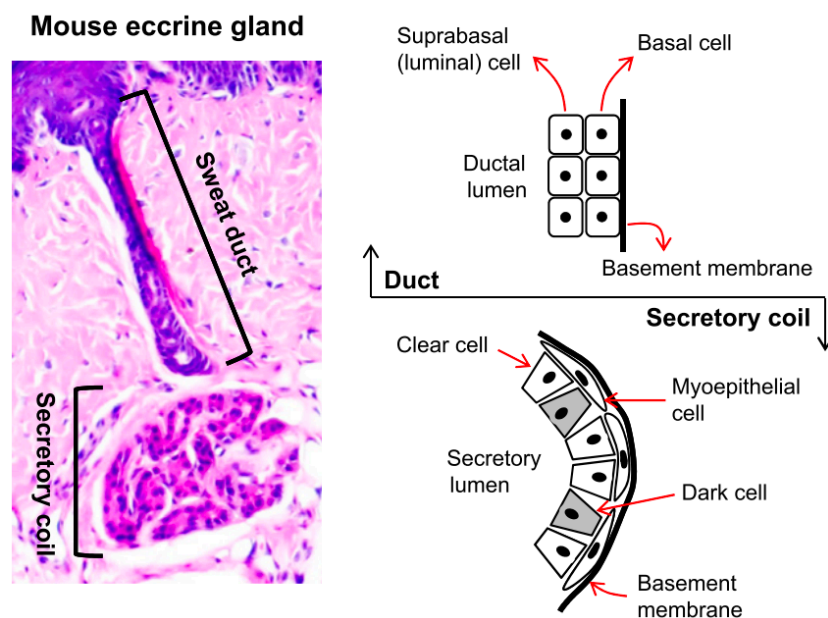


**Figure 2.2:** Mouse eccrine sweat gland and cellular constituents. The eccrine gland comprises a secretory coil in the deep dermis and a relatively straight duct open to the skin surface (left panel). The secretory coil contains three types of cells, clear, dark and myoepithelial. Clear and dark cells are secretory cells, and myoepithelial cells form a major niche for sweat gland stem/progenitor cells (right lower panel). The sweat duct consists of luminal and basal layers where ions are partially reabsorbed (right upper panel). [41]

## Sweat secretion

Sweat secretion is controlled by the central nervous system, and depending on which type of sweating is occurring, specific neural centres control them. For example, an external stimulus can induce sweat secretion, as it happens in response to emotions, causing sweat secretion in palms and soles. When eating spicy food, sweat is also secreted due to gustatory stimulus, especially in the glands located on the face. However, the most important one is the action of hypothalamic sweating, in charge of the thermoregulation of the body, responding to elevations in body temperature [44]. Eccrine sweat glands can respond to both core temperatures (in the case of fever) or peripheral temperatures due to an elevation of the skin temperature.

The neural order to start producing sweat arrives at the glands through acetylcholine. This neurotransmitter attaches to the muscarinic receptors in the basolateral membrane of the clear cells, triggering a release of intracellular Ca stores and an influx of extracellular Ca into the cytoplasm [17]. This influx produces the contrary efflux of KCl through  $\text{Cl}^-$  channels in the apical membrane and  $\text{K}^+$  channels in the basolateral membrane. The cell shrinks, which triggers an influx of  $\text{Na}^+$ ,  $\text{K}^+$ , and  $\text{Cl}^-$  via Na-K-2Cl cotransporters on the basolateral membrane. Subsequently, there is  $\text{Na}^+$  and  $\text{K}^+$  efflux via Na-K-ATPase and  $\text{K}^+$  channels on the basolateral membrane and  $\text{Cl}^-$  efflux via  $\text{Cl}^-$  channels on the apical membrane. Cl concentration increase in the lumen creates an electrochemical gradient for the movement of Na across the cell junction [45]. The primary process of sweat secretion is illustrated in Figure 2.3.

## Ion reabsorption

After ions are secreted into the lumen, they have to travel through the duct, where a proportion of them will be reabsorbed through the luminal and basal cells, especially in the proximal duct where there are more mitochondria and Na-K-ATPase activity. Na reabsorption occurs passively through amiloride-sensitive epithelial Na channels (ENaC). The transport of Na across the basolateral membrane in the basal cells occurs through Na-K-ATPase. This process also triggers the passive efflux of K onto the basal cells through the basolateral membrane [46] as seen in Figure 2.3.

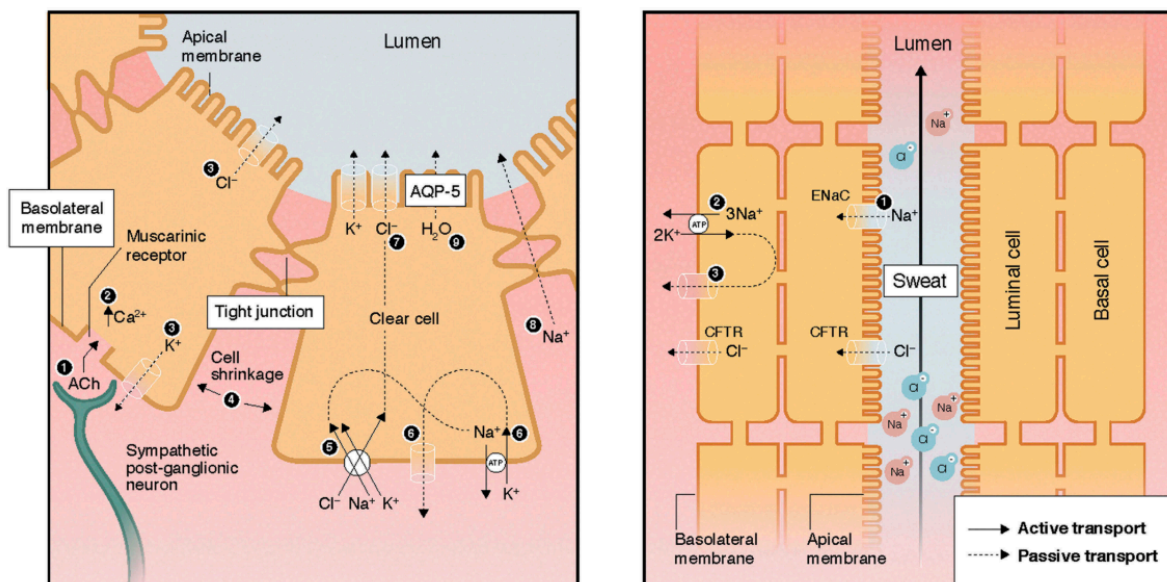


**Figure 2.3:** Mechanisms of sweat secretion in the secretory coil (left). Reabsorption of ions in the proximal duct (right). [17]

Regarding the absorption of  $\text{Cl}^-$ , it is also produced passively through cystic fibrosis membrane channels (CFTR) on both the apical and basolateral membranes (see Figure 2.3). These membranes

are thought to be intercorrelated, and work as a syncytium [17]. The rate of reabsorption for Na<sup>+</sup> and Cl<sup>-</sup> has also been investigated, and it seems to show that the higher the sweating rate, the lower re-absorption rate of ions, making the final concentration of ions in sweat higher [47].

On a similar note, the secretion of sweat in the clear cell and the reabsorption of Na require energy consumption (ATP activity). The primary source of this energy is thanks to the oxidative phosphorylation of plasma glucose, making the sweat glands depend almost exclusively on exogenous substrates [48]. Studies have shown that exclusion of glucose and blood from isolated sweat glands have inhibited the secretion of sweat, which comes to show there is a significant dependency on oxygen supply for the secretion of ions as well as for its reabsorption [49].

## 2.2. Sweat composition

In order to study the composition of sweat, many previous steps need to be set and taken into account. Regarding the methodological considerations when measuring sweat, it has been widely studied how methodology affects sweat secretion and its composition. Two important conclusions were taken out from the research done by L. Baker. The first one highlights the importance of ensuring the same conditions during the sweat measurements, especially the stimulation method and the location of sweat collection. The second point shows that even after a thorough skin cleaning and preparation, some residual contents coming from the sweat duct and sebum secretions or skin surface contaminants can be collected. These components will lead to contamination of sweat which can overestimate the amount of some of those particles [17]. The structure of this methodology should also have some main stages to consider when interpreting and studying the sweat composition. These stages can be divided into skin cleaning/preparation, sweat stimulation, sweat collection, sample storage and analytical technique.

	Concentration [mmol/L]	Sweat-rate dependence	Biomarker for physiology	Reference
Sodium	10-90	Yes	Dehydration, indirect sweat-rate	[17–19]
Chloride	10-90	Yes	Dehydration, indirect sweat-rate	[17–19]
Potassium	4-24	No, proportional to blood	Muscle activity	[19, 50]
Calcium	0.5-3	No	Homeostasis, stress fractures	[19, 51]
Magnesium	0.02-0.4	Various	Muscle strength, aerobic performance	[19, 51]
Iron	0.0001–0.03	No	Muscle activity, anemia	[17, 52]
Lactate	5-40	No	Muscle activity, acid-base equilibria	[17, 49]
Urea	4-12	No	Acid-base equilibria	[17, 49]
Ammonia	0.5-8	No	Exercise intensity	[19, 53]
Bicarbonate	0.2-2.5	Various	Acid-base equilibria	[19]
pH	4-7	Dependence from other species	Acid-base equilibria	[19]

**Table 2.1:** Concentrations of sweat micronutrients and non-micronutrients.

The exact composition of all sweat constituents is still far from being precisely defined, both for micronutrients and non-micronutrients. The first ones relate to main ions and vitamins and trace minerals, while non-micronutrients refer to products of metabolism, proteins, amino acids and toxicants. Except for the higher concentration micronutrients (Na, Cl and K), the lack of data does not allow for setting precise normative ranges for sweat constituents at this time. Instead, literature can give broad ranges for all constituents, which can provide a particular order of magnitude, from the lowest concentrations (minerals and heavy metals) to the highest ones (NaCl). These differences in concentration for sweat constituents can be observed in Table 2.1, as well as its dependency on sweat rate and its role as a



biomarker. It needs to be understood that not all components of sweat are mentioned in the table, but they constitute the main ones in sweat.

Even if the concentration of sweat's constituents can be more or less set in a specific range, the secretion process of these components is still unknown except for Na and Cl. Some mechanisms may be active and others passive, as well as it has been observed that some particles are secreted due to the actual process of sweat gland metabolism (lactate and urea) [49]. Thus, only the mechanism of Na and Cl can be further explained in detail.

Regional [Na] is usually between 10 to 90 mmol/L, whereas whole-body sweat [Na] is measured, the final concentration is 20 to 80 mmol/L approximately. In the case of [Cl] the regional measurements have shown to be similar to [Na], but whole-body concentration seems to be slightly lower, reporting values of between 20-70 mmol/L [54]. Table 2.1 explains how these two ions' concentrations act as biomarkers for showing body dehydration.

### 2.3. Sweat sensing system

After reviewing the physiology of sweat and its composition, the main focus of this project will be on its accurate analysis during physical activity. As observed, chloride and sodium are the principal ions in sweat, and they can provide high information monitoring physical activity. The relationship between these ions concentrations and the athlete's health status can provide a deep understanding of whether or not the athlete is suffering from dehydration or salt loss.

Sweat analysis requires building a sensing system capable of acquiring and analyzing sweat in real-time using electrochemistry. An electrochemical sweat sensor is composed of three main parts essential for the analysis: microfluidic device, sensing system, and electronic component [55]. The microfluidic device will acquire sweat from the skin and guide it to the sensing system. In this system, the electrochemical reaction will occur in order to analyze the sweat constituents. Finally, the electronic component will read the signal from the sensing system and convert it into the final result, the ion concentrations in sweat.

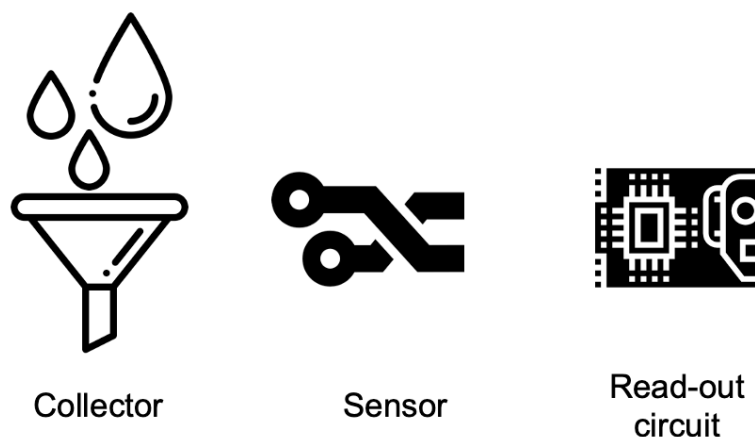


Figure 2.4: Overview of the parts needed for the sweat sensing system.

As observed in Figure 2.4, the three main parts for the sweat sensing system are:

- A sweat sensor capable of measuring chloride and sodium ions for small quantities of sweat.

- A sweat collector to reduce contamination of the sample and provide time for the sensor to analyze sweat.
- An read-out circuit for the sweat sensor.

As already mentioned, previous work done by T. Bakker developed a functional read-out system, the electronic component of the system [56]. Bakker also developed a sweat sensor, encountering some issues during the production stage. Considering the project's goal, time constraints, and background knowledge, it was decided to focus on the improvement of the sensor and use the same read-out circuit, which was still fully functional. In addition, this project will focus on the design of a sweat collector capable of acquiring and guiding sweat through microfluidic channels.

### 2.3.1. Requirements

As the sweat analysis system is a complex structure, some requirements are set before building the sweat sensor and collector. The aim will be to fulfil these conditions to build the most efficient sweat sensing system.

- The system should be capable of reliably monitoring a patient for one hour of exercise.
  - The region of interest for measuring chloride and sodium concentration should be between 10 *mmol/L* and 100 *mmol/L*.
  - Measurements should have an accuracy of  $\pm 2$  *mmol/L*.
- Sweat collection must avoid the contamination of sweat samples.
  - Accuracy in sweat analysis directly depends on the invariability of the sample during its collection.
- The system should reduce the sweat flow speed to increase the time for sampling.
  - Response time of the sensor should be estimated.
  - Reducing sweat flow should not influence on the accurate analysis of ion concentrations.
- The materials and techniques used to build the system should enable the end product to become a comfortable and wearable device
  - Biocompatible materials should be used to avoid skin irritation.
  - Any electronics must be isolated from the patient.
  - The system should be condensed into a single wearable device.

### 2.3.2. Validation

The validation of the sweat sensing system is divided into four steps:

1. The three sub-parts are validated on themselves in a laboratory setting.

2. The sweat sensor and collector are integrated with the read-out circuit and validated in a laboratory setting.
3. The entire sweat sensing system is validated on human volunteers.

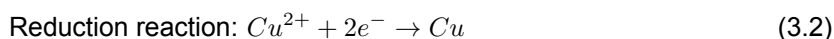
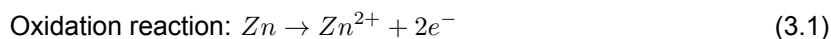
# 3

## Sweat sensor

Sweat needs to be analysed in order to measure the different constituents in it. For this project, it is of particular interest to estimate ion concentrations found in sweat. This chapter will start by evaluating and selecting the most suitable analytical technique found in literature to analyse sweat. Afterwards, the design and fabrication methods for building the sweat sensor will be exposed. Finally, the validation results of the sensor will be shown.

### 3.1. Analytical techniques in sweat sensing

All electrochemical techniques for analysing sweat have in common the use of reduction and oxidation reactions, known as *redox* reactions. Electrons travel from one reactant to the other, one chemical species losing these electrons (called the *reducing agent*), and the other species gains those electrons (the *oxidising agent*). An example of this type of reaction is shown below.



From equations 3.1 and 3.2, it can be observed how Zn is the reducing agent (loses electrons), while Cu is the oxidation agent (gains electrons). In a redox reaction, the side where the oxidation takes place is called the *anode*, whereas the side where reduction occurs is called the *cathode*. These two processes take place simultaneously, as they cannot happen independently, and each of them is called a *half-reaction*. The two half-reactions together form the complete redox reaction. Each half-cell has a standard electrode potential ( $E^0_{cell}$ ), which corresponds to the driving forces occurring at the electrode during the reaction process. The total potential difference of the redox reaction is the difference between both half-cells, and it is called the Electromotive Force (see equation 3.3).

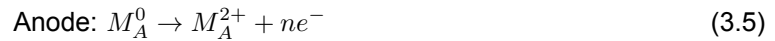
$$E^0_{cell} = E^0_{cathode} - E^0_{anode} \quad (3.3)$$

However, to measure the potential differences between each half-cell, the reaction needs a complete loop for electrons to jump from one half-cell to the other. Thus, a salt bridge connecting the anode and the cathode is used to close this gap. The redox reaction allows measuring the electrons being transferred. In order to link these electrical properties into chemical features, the total charge in the

redox reaction can be linked to the number of moles ( $n$ ) involved in the reaction and the Faraday constant ( $F$ ), as shown in equation 3.4.

$$q = n \cdot F \quad (3.4)$$

Taking into account the previous information, the reaction on each half-cell can be standardised, as seen in equation 3.5 and 3.6. Where  $M_A$  and  $M_B$  are the two elements involved in the solution. In this case, the reaction occurs between a membrane (electrode) and the ionic solution (electrolyte).



Finally, when measuring the specific concentration of an ion inside a solution, it is possible to calculate the potential on one half-cell by making the other half-cell the reference electrode (by convention, the anode). This reference half-cell has to provide always a known and stable potential to measure the potential on the other half-cell (by convention, the cathode). In section 3.2.3 the most common materials for reference membranes will be listed, and the reasoning for choosing the most suitable one for this project will be explained.

As already mentioned, there are different techniques available nowadays in order to analyse sweat. The criteria to choose between them depend on several factors, such as whether the analysis is done in the laboratory or on the field. Several studies have investigated and compared different techniques such as ion chromatography, flame photometry, direct and indirect ion-selective electrode (ISE) or ion conductivity. In particular, a study compared sweat [Na] using some of these different analytical techniques [57]. Results showed variability of around 12% between them, which concluded that they should not be used interchangeably.

Sweat [Na] has been the most abundant constituent analysed in many different methods [17]. Regarding the precise measurement of sweat [Na], there is a specific ranking that most studies coincide with when accuracy is compared. Having variations between 4% and 30% depending on the technique, ion chromatography and ion-selective electrodes seem to be the least accurate of all of them. Afterwards, flame photometry provides higher accuracy for the sweat [Na]. Finally, ion conductivity shows the most accurate results for estimating the total [Na] in sweat [58–60]. Once these methods have been presented, it would be interesting to briefly understand how they work before choosing a specific technique for our project.

### **Ion chromatography**

This technique is a variation of liquid chromatography, which measures concentrations of ionic species by separating them based on their interaction with a resin. Ionic species are separated differently depending on the type and size of the particles. The solutions go through a pressurised chromatographic column where column constituents absorb ions. Eluent is used as an ion extraction liquid, which runs through the column and makes the absorbed ions separate from the column. The retention time of different species determines the ionic concentrations in the sample [61].

Ion chromatography has been widely used for the study of sweat [62, 63]. In order to better understand the role of sweat [Cl] and [Na] in the diagnosis and treatment of cystic fibrosis, ion-chromatography is a beneficial method. A recent study came to show a newly developed ion chromatography method for the determination of these ion concentrations, in combination with the Macroduct sweat collection further described in section 4.1.1. The method showed excellent results for a method that requires a simple setup and presents high precision [62]. Figure 3.1 shows how the concentration of chloride and

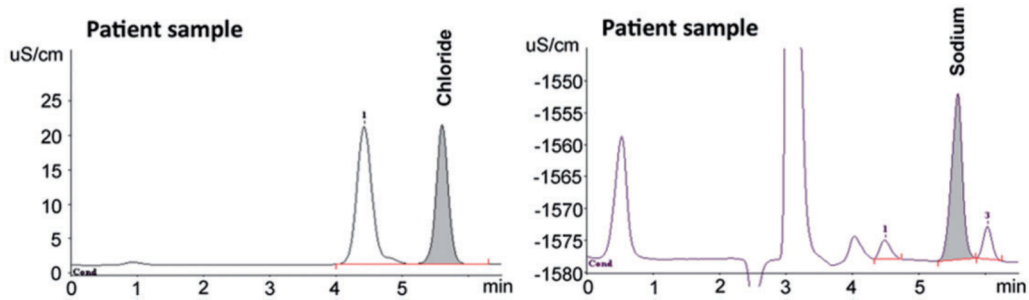


Figure 3.1: Chromatograms of chloride (left) and sodium (right) [62]

sodium are obtained from the ion chromatography process.

### Ion conductivity

The idea behind this method is to measure the ability of a substance to conduct electricity. Highly ionised substances are vital electrolytes, as they allow the flow of electrons throughout the entire solution. The electrical conductivity of the solution is measured by acquiring the resistance (measured by a conductivity meter) of the solution between two electrodes separated by a fixed distance [64]. Metals dissolved in the solution allow for better conductivity. whereas on the other hand, distilled water is an inferior conductor (weak electrolyte) [65].

Research for measuring sweat ions have been carried out using ion conductivity as the analytical technique. Paul Boisvert and Victor Candas already tried in 1993 to use ion conductivity to measure sweat [Na] and [Cl]. They chose a specific device called Sweat-Chek analyser (model 3100, Wescor, Logan, Utah, USA), which was already available in the market and displayed the total NaCl concentration. After previously collecting the sweat samples, they introduced them inside the analyser. Results showed an overestimation of sweat [Na] and [Cl]. However, as estimations followed a linear behaviour, they were able to recalculate ion concentrations by subtracting a specific number from what the analyser had estimated [60].



Figure 3.2: Sweat-Chek™ Analyzer using ion conductivity technique [66]

As observed in Figure 3.2, the Sweat-Chek™ Analyser has been developed and improved in the last decades. It is now commercially available by ELITechGroup for complete electrolyte analysis of sweat samples [66]. The sweat sample was previously collected by the Macroduct (explained in section

4.1.1). The sample is then transferred into the cell by using a syringe plunger. When the specimen contacts both cell electrodes (less than 10 microliters are required), the conductivity of the specimen is measured, converted to equivalent NaCl molarity, and the result is displayed. Results are very accurate, but as observed, a big device is required to implement ion conductivity, making it an impedence for measuring sweat in real-time.

### Flame photometry

Flame photometry is a technique used to detect and display specific metal ions (K, Na, Li, Ca, and Ba) and accurately determine each concentration within a given substance. It works by measuring the intensity of light emitted when the element is exposed to a flame, as the metals are dissociated due to the thermal energy [67, 68]. This dissociation will result in the emission of some radiation (measured using emission techniques) due to the movement of excited atoms (measure using direct absorption techniques). The wavelength of the emitted light is specific for specific elements, allowing for measuring the specific concentration of each of them [67].

Flame photometry is a very accurate analytical technique, and it can provide excellent results in any sweat analysis study [17]. However, the equipment necessary for it is pretty expensive and heavy, making the analysis of sweat on the field very tedious. Thus, this type of process is reserved for the study of sweat in the laboratory for better understanding.

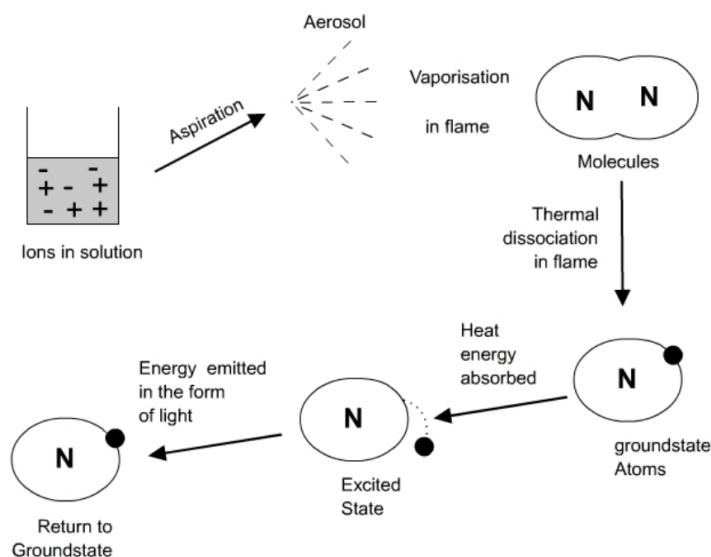


Figure 3.3: Schematic explanation of the flame photometry process [67]

### Colorimetric sensing

Sensing of sweat constituents can also be done by colourimetric sensing. This technique can detect a colour change associated with a specific chemical reaction between an analyte and sensing materials [69]. This colour change will allow calculating the specific concentration of the analyte in the solution. By using imaging processing, the differences in colour intensity will predict the final analyte's concentration. This technique is widely used in different fields and allow for the detection of organic dyes and drugs due to their easy fabrication, quick detection, and high sensitivity and selectivity [69–71].

A recent sweat sensing device using colourimetric sensing was developed by Ahyeon Koh *et al.* in 2017. This thin and soft device acquired sweat from the skin using a closed microfluidic system open through some inlet holes. The device then routes sweat into different channels and reservoirs for multiparametric sensing of markers of interest [72]. The sweat collection mechanism in this device uses five different inlet holes to acquire the substance from the skin's surface. Each inlet hole drives sweat

through microchannels using PDMS and arrives at a specific chamber or collection area. The exterior "curly" channel seen on the most outer part of the device (see Figure 3.4) allows measuring sweat rate and volume, thanks to a dye that turns transparent as sweat keeps advancing.

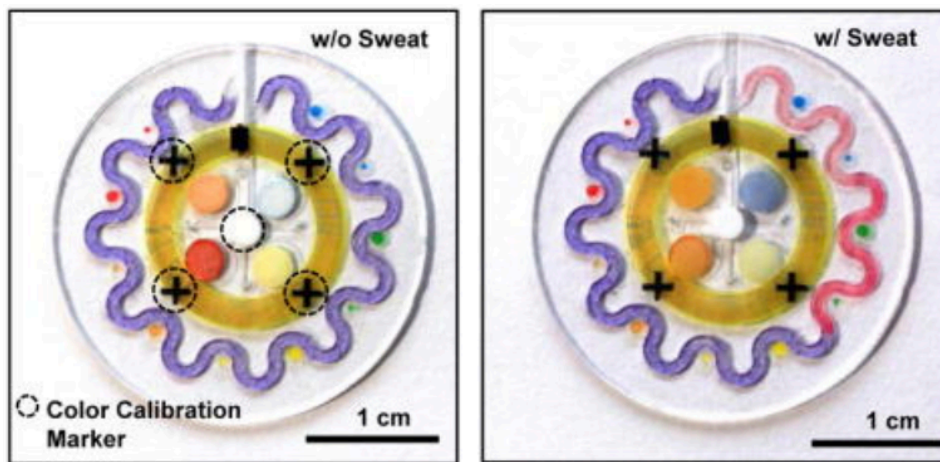


**Figure 3.4:** Images of the epidermal microfluidic biosensor (left) before and (right) after injecting artificial sweat [72]

The previously mentioned chambers are filled with reagents for colourimetric analysis. It allowed for rapid quantitative assessment of sweat rate, total volume loss, sweat pH, and the concentration of Cl, lactate and glucose in sweat. The value of these parameters was obtained by recording colour changes and converting them into quantitative information. This process was possible thanks to digital image capture and analysis. This type of system for sweat analysis seems to have some advantages, such as its simple fabrication, the lack of need for power, or its low cost. It can also measure sweat rate and volume, parameters that can give critical information during perspiration. However, the need to constantly analyse the enzymatic reaction by taking pictures and filling the chambers again with the proper reagents are drawbacks to consider. The device must be used in sports where the athlete is in a fixed position, having many disadvantages for sweat analysis during physical activity in an open area.

### Ion-selectivity

This type of method consists of a thin membrane across which only the intended ion can be transported. This selectivity will produce a potential difference in the membrane, which will allow determining the activity of ions in an aqueous solution. The ion-selective electrode allows measured ions to interact with the membrane but excludes the passage of the other ions. There is an internal reference electrode within this electrode embedded in a filling solution (containing the same ions as the one to be measured). A voltmeter connects the ion-selective electrode and the reference electrode. Both electrodes are immersed in the same test solution to measure the potential difference [73].

Ion-selective electrodes are widely used when measuring sweat parameters during field analysis, especially for Cl and Na as they are the most abundant sweat ions [74–76]. A study wanted to make a comparison between ion-chromatography and ion-selective electrode (ISE) techniques regarding its validity and reliability for measuring [Na] and [K] during exercise in a hot environment. The experiment came to show that based on typical error of the measurement results, sweat [Na] and [K] obtained with the ion-selective method showed less accurate results than ion chromatography performed in the lab. However, it concluded that the field ion-selective method of extracting and analysing sweat from regional absorbent patches could help obtain sweat [Na] when fast estimations in a hot-humid field setting are needed [77].

Despite being less precise than other methods, ion-selective electrodes estimate sweat [Na] and [Cl] with some accuracy. The most important advantage of this analytical technique is the possibility of reducing the system into a small and flexible device. The simplicity of placing electrodes close to the



sweat area makes this technique suitable for building a sweat sensor. The different criteria for choosing ion-selectivity is shown in Table 3.1.

ANALYTICAL TECHNIQUE	Real-time	Reliable results	Small	Flexible	References
Ion chromatography	-	++	+	-	[61–63]
Ion conductivity	+	++	--	-	[60, 64–66]
Flame photometry	-	++	--	-	[67, 68]
Colorimetric sensing	++	-	++	+	[69–72]
Ion-selectivity	++	+	++	++	[73–77]

Orange highlighted was used in this study

**Table 3.1:** Analytical techniques for measuring ion concentrations in sweat

### 3.1.1. Potentiometry

After choosing the ion-selective technique as the method that best fits the interest of this project, it can be studied in more detail the chemical process behind this method. As previously explained, the ISE method measures the potential difference between these electrodes to estimate the ion concentration. The electrochemical technique behind this method is potentiometry. This technique measures the potential difference under static conditions, which means it is very little or even zero current in the system. The relation between an electrochemical cell's potential and the concentration of electroactive species in the cell is described by the Nernst equation, which was formulated in 1889 [78]. The Nernst equation is described in equation (3.7).

$$\varphi = \varphi^0 - \frac{RT}{zF} \ln a \quad (3.7)$$

Where  $\varphi$  is the measured potential,  $\varphi^0$  is the potential overall interfaces except for the membrane/sweat interface.  $R, T, F, z, a$  are, respectively, gas constant, absolute temperature, Faraday constant, charge number of ion, and activity of the target sweat ion [55]. Thanks to this equation, the total amount of ions in the analyte can be obtained by measuring the potential difference between the working electrode and the reference electrode.

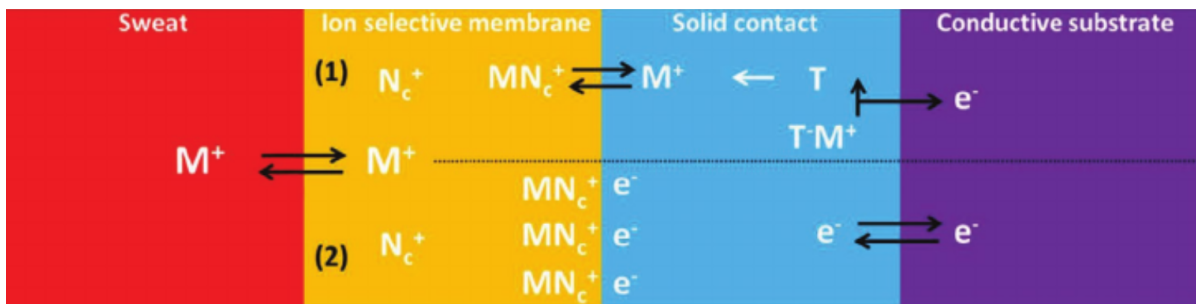


**Figure 3.5:** Response mechanism of complete solid-contact ion-selective electrode for detection of common ions in sweat. [55]

The process of Nernst response in an ion-selective electrode (ISE) is illustrated in Figure 3.5. When interacting with sweat, the ions  $M^+$  are selectively absorbed by the ionophore  $N_C$  in the selective membrane to form  $MN_C^+$ . This molecule then reaches the membrane and solid contact interface and transfers the electrons to the conductive substrate [79]. The overall interfaces induce a difference in potential when the ion concentration reaches a certain amount. Ideally, the variations in potential would only depend on the interface between sweat with the selective membrane due to potential constants of other

interfaces.

### 3.1.2. Ion-selective electrodes in sweat sensors

After explaining the chemical principles of ion-selective electrodes, an overview of the most significant wearable sweat sensors in research is presented using this analysis technique. This state-of-the-art section will expose the main sweat analysis principles as well as the fabrication process and the materials used.

#### Adhesive potentiometric sensor patch for monitoring sweat electrolytes

This type of system can collect and analyse sweat, as well as transmit the data recorded using an RFID (radio frequency identification) chip which can be read by a smartphone [80]. Regarding the collection of sweat, there are two possibilities for the system to obtain it. It is mentioned that paper microfluidics can collect sweat by wicking it from the skin into the sensors. The other method would disregard the collection of sweat, as the sensing electrodes could be folded over and directly contact the skin.

The second topic worth mentioning is related to the analysis of sweat. This system uses a  $\text{Na}^+$  selective membrane to analyse the concentration of this ion. By placing both a reference electrode and a working electrode, the system can measure the potential difference. It is also stated by the research group that any other relevant ion in sweat could also be sensed using appropriate commercially available ionophores from Sigma-Aldrich [80]. Both reference and working electrodes have the first few layers in common by electrodeposition of Pd and Ag on a previously defined bare copper electrode. The working membrane was made from a cocktail of sodium Ionophore X, bis(2-Ethylhexyl) sebacate (DOS), potassium tetrakis (p-chlorophenyl)borate (KTPC1PB), PVC, and cyclohexanone, then manually mixed until the PVC was fully dissolved. On the other hand, the reference electrode was completed by chloridization of an Ag layer in 1 M KCl with a  $3 \text{ mA/cm}^2$  anodic current for 30 s to form such a reference (see Figure 3.6A). The membrane solution was placed carefully over the working electrode using a modified screen-printing process.

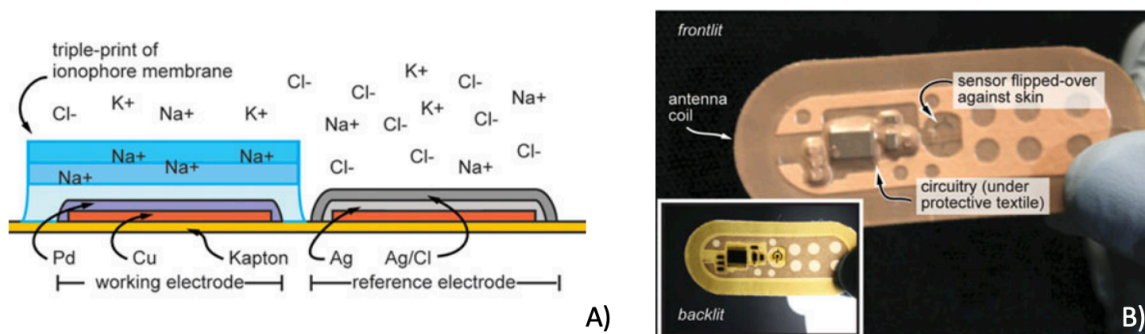


**Figure 3.6:** A) Ion-selective electrodes of the sensor. B) Illustration of the electronics and sensor of the device [80]

Regarding the electronics of the system for the necessary analysis and data transmission, it was necessary to print a flexible electronic circuit board. Flexibility is vital for wearable electronics, which allows for a comfortable attachment to the skin. Thus, the board is built from Dupont Pyralux, a combination of flexible, conformal polyimide and a thin copper foil. In order to protect the patch, a medical textile covered the area, as well as to improve the visual aesthetics. A double-sided medical adhesive tape was used below the patch in order to attach it to the skin (see Figure 3.6B).

This device stands out for its ability to gather all the necessary technology to analyse sweat and transmit the data wirelessly while being flexible, wearable, and low-cost. However, the performance of

this device to analyse sweat constituents can be improved, only giving rough estimations of the most relevant ions in sweat. A higher sampling frequency is needed and improved power management or better stability of the reference electrode to improve this efficiency. On a parallel note, the device is only able to measure one ion concentration of sweat at a time, which gives little information about the health status.

### Flexible integrated sensing array (FISA) for multiplexed *in situ* perspiration analysis

It is presented a mechanically flexible and fully integrated sensor array for multiplexed *in situ* perspiration analysis. The device can simultaneously and selectively measure sweat metabolites (such as glucose and lactate) and electrolytes (such as sodium and potassium ions), as well as skin temperature [31]. Compared to the previous device, it follows similar analytical principles to measure ion concentrations and other constituents, but the amount of information obtained from sweat is much more significant in this system.

Sensors were fabricated on a mechanically flexible polyethylene terephthalate (PET) substrate. Also, a flexible printed circuit board (FPCB) technology was developed to incorporate the critical signal conditioning, processing, and wireless transmission functionalities. This device uses electrodes open to the skin surface to analyse sweat, so no collection mechanism is necessary. This multiplexed sensor array is very complex and has many different components, as shown in Figure 3.7B. The system uses ion-selective electrodes for measuring  $\text{Na}^+$  and  $\text{K}^+$  coupled with a polyvinyl butyral (PVB) coated reference electrode. There are also amperometric glucose and lactate sensors immobilised within a porous film. The Ag/AgCl electrode serves as a shared reference electrode and counter electrode for both sensors in this case. In order to insulate the sensor, parylene is used to ensure reliable reading and preventing electrical contact of the metal lines with skin and sweat.

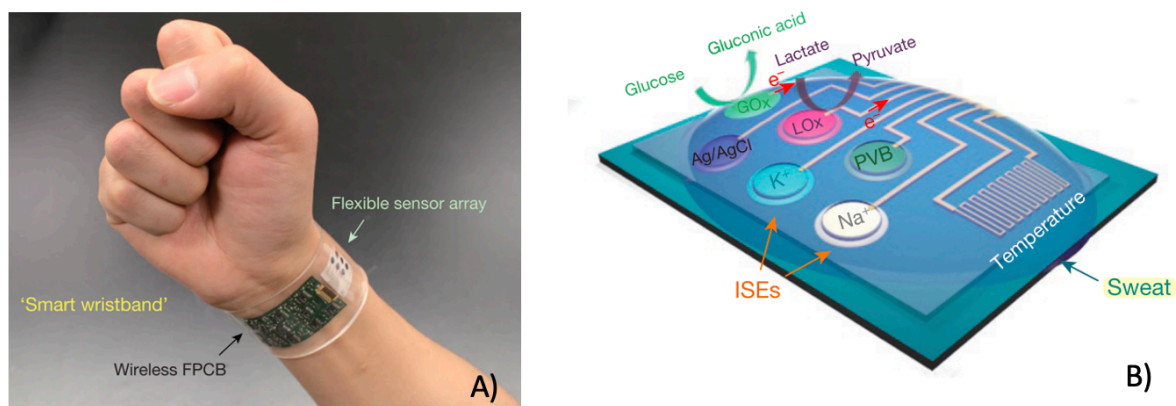


**Figure 3.7:** A) Wearable FISA on a subject's wrist, integrating the multiplexed sweat sensor array and the wireless FPCB. B) Schematic of the sensor array [31]

The whole device can be fixed around the wrist for the proper collection of sweat and its analysis (see Figure 3.7A). The device can also be strapped around the head, as it has a higher sweat rate than on the wrist [81]. All the data analysed is collected thanks to the wireless transmission via a Bluetooth transceiver. This system shows a complete outcome than the previous system, being able to monitor sweat during physical activity while measuring many different parameters in sweat. Nevertheless, sweat constituents are not the only parameters to measure during perspiration, such as sweat rate or sweat volume. Thus, even if the device seems to be complete, further improvements can be made.

### 3.1.3. Conclusion

The sensing of sweat is a complex electrochemical process. There are different analytical techniques

available, but choosing between them depends on the final goal of the analysis. All these techniques have in common the use of *redox* reactions to acquire a potential difference between each half-cell. For the accurate measurement of  $[\text{Na}^+]$  and  $[\text{Cl}^-]$  during real-time activity, a process capable of miniaturisation and excellent wearability was needed.

Ion-selectivity is chosen as the analytical technique to measure  $\text{Na}^+$  and  $\text{Cl}^-$  ions in sweat. This technique allows building a small and wearable sensor capable of analysing sweat constituents in real-time. In addition, measuring each ion's concentration specifically instead of total concentrations will bring more accurate results. As observed, this technique is already being used in literature [31, 80] with promising results. The following section focuses on the design and production of the sweat sensor using ion-selective electrodes to analyse sweat ions.

## 3.2. Methods

Once literature was reviewed to find the most suitable sweat sensing system, it was time to design the sweat sensor. This section will discuss all the decisions taken for designing and building the sweat sensor.

### 3.2.1. Design

The design of the sweat sensor is greatly influenced by the previous work done by T. Bakker [56]. He designed several prototypes for his sweat sensor focused on the diagnosis of sweat in cystic fibrosis patients. As the working principles are the same as the one used for this project, our sweat sensor has many similarities to the last version of his sensor, observed in Figure 3.8.

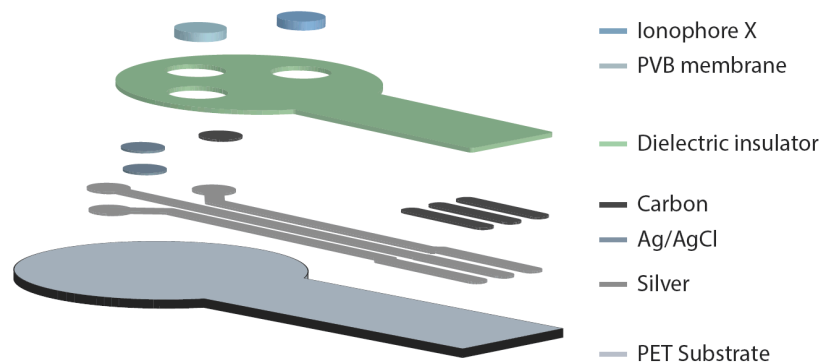


Figure 3.8: Final sweat sensor version made by T. Bakker [56]

However, a new version was designed already thinking on the possibility of the final integration between the sweat sensor and collector (refer to section 5). Figure 3.9 shows the new sensor version of the sweat sensor. As already mentioned, the most significant change related to the structure was the reduction in the size of the electrodes, so sweat could easily cover their surface to be analysed.

As observed in Figure 3.9, the sweat sensor is divided into four different layers:

- The substrate
- The conducting layer

- The sensing electrodes
- The insulation layer

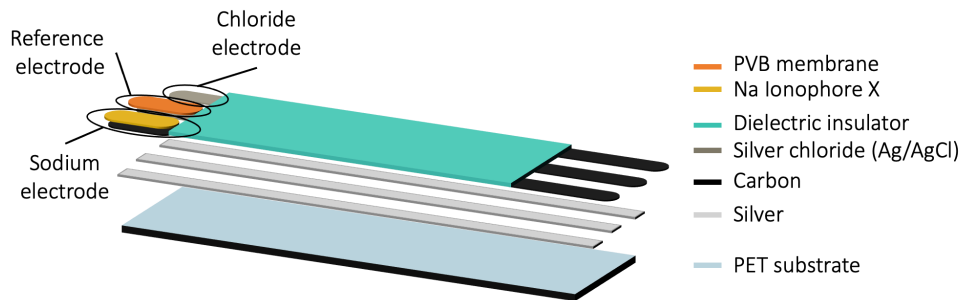


**Figure 3.9:** Layer by layer design of the sweat sensor

The substrate of the sensor was made of Polyethylene Terephthalate (PET). This material is most commonly used in literature as a substrate for sensors and the chosen material for these devices at Holst Centre. The same reason followed the material chosen for the reference electrode: Ag/AgCl. This Silver/Silver Chloride ink is widely used as a reference membrane [82], and it will also be used as the chemical material for the chloride electrode, as this element is already present in the ink.

The conducting layer is made put of silver, as it is an excellent conductive material. This layer will be used as the line of connection between the electrodes and the read-out circuit.

Special attention was taken for the sensing electrodes, as they are responsible for the proper analysis of sweat. These electrodes aim to be sensitive to both chloride and sodium. Their chemical composition will be discussed in subsection 3.2.3.

The last essential layer involved the usage of carbon ink at the end of the sensor. These three layers are necessary for the connection between the sensor and the read-out circuit. Without this layer, the silver ink could be scratched off by reconnecting the sensor multiple times. A Flexible Printed Circuit (FFC) 8-pin connector will be used for this connection, which will be further explained in chapter 5. As observed in Figure 3.10, pin 3 and 6 are removed from the connector and serve as an isolation barrier.

The following considerations were taken into account in order to minimise the error during the printing process [56]:

- The conducting paths have to be wide enough to obtain good conduction.
- The conducting paths have to be isolated with a water-resistant insulation layer to separate the paths from each other when placed underwater.
- The carbon layers at the end of the conducting paths are necessary for the connection to wires using an FFC connector.
- Sharp corners are avoided in order to facilitate the printing process.

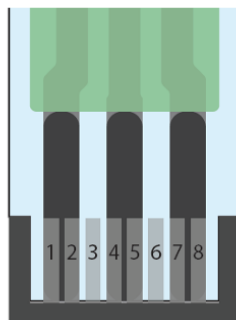


Figure 3.10: Sensor FFC connector [56]

These layers are built using screen-printing technology, on which each layer is deposited on top of each other using different stencils for the process. In the next section, this printing technique will be further explained.

### 3.2.2. Screen-printing of the sensors

Screen-printing is one of the most promising approaches towards simple, rapid and inexpensive production of biosensors [83]. The process is quite simple, requiring the substrate, the vinyl stencil and the ink for each layer. The production of the sweat sensor was made at Holst Centre due to the collaboration we had for this project. The facilities provided by the company allowed to build sensors with much more precision, using cutting edge technology. This fact allowed the use of the screen-printing machines, which made the process much more straightforward than doing it by hand (as T. Bakker had to do). The process of screen-printing is illustrated in Figure 3.11 and has the following four steps [84]:

- Step 1: the substrate is fixed onto the screen-printing table. The ink is poured onto the screen mesh at one end.
- Step 2: The squeegee with a rubber blade drags across the mesh to fill all mesh openings.
- Step 3: The screen mesh now filled with ink is pressed onto the substrate, and the squeegee is again dragged from one end to the other end. Steps 2 and 3 may be repeated several times to ensure the ink has adhered to the substrate.
- Step 4: The screen is released, and the printed substrate is taken out and left to dry at ambient temperature in a good ventilation environment.

There was the first process of screen-printing of the sensor. The prints were of excellent quality, and a significant step forward was already done compared to the screen-prints hand made by T. Bakker. However, this first print had a few issues. The insulation layer was not surrounding the electrodes of T. Bakkers' sensors. Also, the carbon ink of the sodium-selective membrane was not covering the entire surface of the Ag/AgCl layer (see Figure 3.12), which could affect the conductivity of the sensor. As already mentioned, sometimes the ink does not adhere completely to the substrate, and the ink has to be pressed a few extra times to assure adhesion. Extra caution was taken on the adhesion of the carbon and insulation layer in the new printing process.

The final screen-prints are observed in Figure 3.13. There were made three different designs for the sensors. The above version was the third one made by T. Bakker, and the versions shown on the



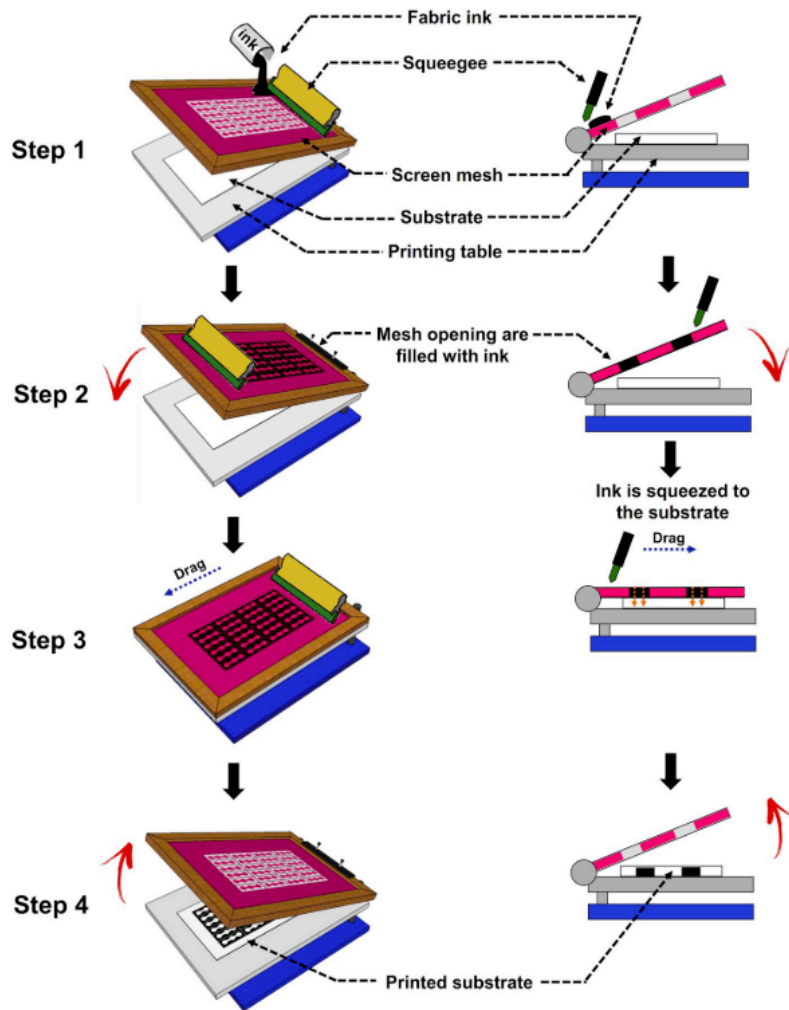
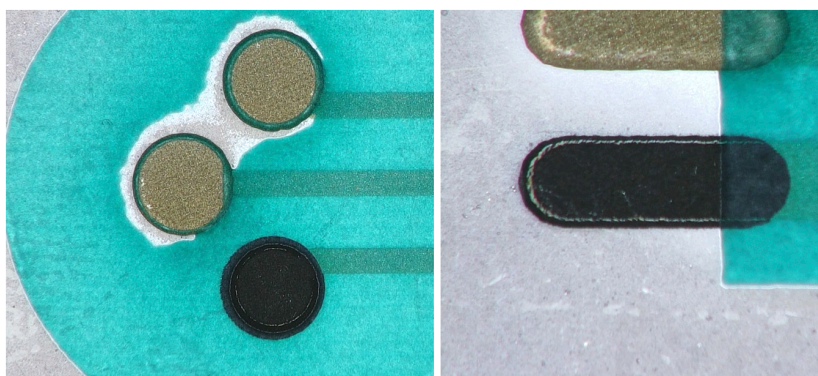


Figure 3.11: Production steps of screen-printing [84]

bottom were made thinking already on the possibility of integrating the sensor's electrodes inside the sweat collector. The chosen substrate for all of the sensors was PET. As already mentioned, on top of this substrate, there were three additional layers, shown in Figure 3.9. The specific materials used for these screen-prints were the following:

- First layer (L1): silver (Ag), one layer, *DuPont 5025*.
- Second layer (L2): carbon (C), two layers, *DuPont BQ226*.
- Third layer (L3): silver chloride (AgCl), one layer, *DuPont 5876*.
- Fourth layer (L4): dielectric insulator, two layers, *DuPont BQ10*.

As Holst Centre is already experienced with the screen-printing of sensors, the lab technicians suggested most inks. In addition, they already had partnerships with different chemical providers, so the margin to choose different brands than the ones available was limited. Regardless of these limitations, these inks were already used in literature for the building of sweat sensors using screen-printing techniques [31, 55, 80]. Only in the case of the Ag/AgCl ink there is a difference in composition. Whereas T. Bakker used an Ag/AgCl ratio of 60/40, the silver chloride provided by Holst Centre had a ratio of



**Figure 3.12:** Incomplete adhesion of the insulation layer (left) and carbon ink (right)

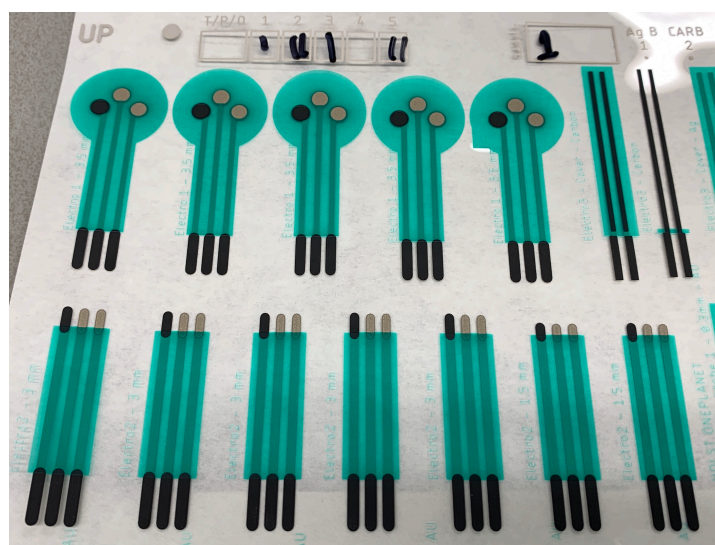


**Figure 3.13:** Screen-printed sweat sensors on PET

32/68. This difference in ratio will be mentioned in the sensor validation section 3.3 when referring to the chloride electrode.

### 3.2.3. Chemical composition of the membranes

As already mentioned, potentiometry is a widespread electrochemical technique due to its low costs and the broad spectrum of ions that can be measured using it. It works by a zero current technique that measures the potential difference between the reference electrode and the sensing electrode in an electrochemical cell.

In this project, silver chloride ink was chosen as the conducting layer, as it is widely used as an electrode material. As chloride is one of the ions that wants to be measured, Ag/AgCl can be used as a sensing electrode for chloride, the ink selective for this ion. However, in the case of sodium, it is needed selective electrode for this ion, so an ionophore will be used. For the reference membrane, it is also necessary to create a gel-like structure for the potentiometric reaction. Thus, it will be presented and discussed different membranes currently used in sweat research. The chemical and production steps that best fit this project's purpose will be selected.

#### Sodium-selective membrane

For this membrane, it was used Sodium Ionophore X, which is commonly used for this type of



electrode [55]. The principle of this ionophore is based on the charge separations between the organic phase (membrane) and the aqueous phase (sample) [85]. It is stated to have the best stability, sensitivity and explanations for the production steps as seen in literature [80, 86–88] which makes it appropriate for the project.

The selection of the materials depended now on the ionophore's supplier, which was either Sigma Aldrich or Supelco. In the previous project, it was used the first option was due to cost constraints. However, as observed in the literature, the one supplied by Supelco is widely used and more common than the one provided by Sigma Aldrich. Thus, in order to be able to compare the obtained results with more cases in literature, it was chosen this type of Sodium Ionophore X. The materials used and their costs can be observed in Table 3.2.

REAGENTS	Quantity for one electrode	Pack size	Manufacturer	Code in Sigma Aldrich	Price (€)
Selectrophone Ionophore X	1% wt/wt	50 mg	Supelco	71747	137
Bis(2-ethylhexyl) sebacate (DOS)	65.45% wt/wt	5 ml	Supelco	84818	57.1
Na-TFPB	0.55% wt/wt	250 mg	Sigma Aldrich	692360	132
Polyvinyl chloride (PVC)	33% wt/wt	1 g	Supelco	81392	20.8
Tetrahydrofuran (THF)	660 micro L	100 ml	Supelco	87369	40.2
3,4-ethylenedioxythiophene (EDOT)	x	10g	Sigma Aldrich	483028	74.8
poly(sodium 4-styrenesulfonate)	x	5 g	Sigma Aldrich	243051-5G	36.4
<b>TOTAL</b>					<b>387.1</b>

**Table 3.2:** Chemical materials used to produce the sodium-selective membrane

The last two materials on Table 3.2 refer to the production of the solid contact, in this case of PE-DOT:PSS. This membrane allows for a better transfer of the electrons to the conductive membrane, making a more precise measurement of ions concentration. However, the production of this extra membrane is costly and complex to make by hand. As suggested by literature, this ion-selective transducer should be mixed and be placed on top of the electrodes by galvanostatic electrochemical polymerisation. However, it was later proposed that a more efficient way would be to print this layer of PEDOT:PSS during the screen-printing of the sensors. The complexity of building the membranes is minimised and allows for a more straightforward production of this membrane.

However, this addition to the screen-printing process was complex. In addition to time constraints, the solid contact was not added to the electrode in the end. The lack of this ion-selective transducer membrane is not a drawback on the sensor, but it does lose some accuracy when measuring the total concentration of ions. Therefore, it was decided to omit this layer, but it could be included in a later project if a more precise sensor wanted to be produced.

The production process of this membrane is always stated to be the same in all literature that was reviewed, and it follows the next steps [89]:

1. Mix Na Ionophore X (1% wt/wt), Na-TFPB (0.55% wt/wt), PVC (33% wt/wt), and DOS (65.45% wt/wt).
2. Next, 100 mg of the membrane mixture are dissolved in 660  $\mu$ l of tetrahydrofuran.
3. Finally, the ion-selective solutions is sealed and stored at 4 °C overnight.

### Reference membrane

The selection was harder to make for the reference membrane, as almost any type could be used for the project. The standard reference electrode works with the electrode placement in a known electrolyte solution, but in a sweat sensor, it is complex to place the electrode in an aqueous salt solution. Therefore, for this project, it will be much more beneficial to use a gel saturated with salt, such as NaCl or KCl.

In the previous work done by T. Bakker, Polyvinyl Butyral (PVB) was chosen as the type of reference membrane due to costs, production steps and stability over time. The final results obtained when producing this membrane were not the desired ones, as the PVB could not fully dissolve in ethanol, and some bubbles appeared on the surface. Due to this issue, different reference membranes were reviewed to look for other options and compare them with the PVB membrane previously used.

#### pHEMA hydrogel reference membrane

This type of method uses Poli(2-hydroxietil methacrylate (pHEMA) hydrogel on top of an AgCl electrode and an O-ring with a thickness of 1 mm and diameter of 3 mm. It comes to show good stability (one hour of exercise), and the explanation of the production procedure is clearly explained, but the addition of the O-ring to make sure the hydrogel stays on top of the electrode also adds a level of complexity.

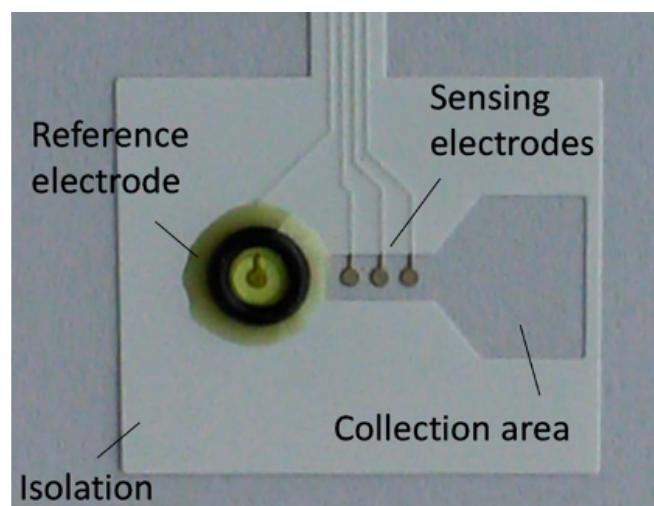


**Figure 3.14:** Sweat patch containing an array of AgCl sensing electrodes and reference electrode. The pHEMA hydrogel layer was drop casted within an O-ring, which was glued on top of the reference electrode. Holes were punched through the collection area to allow the sweat to be absorbed. [82]

#### PVA/KCl membrane-coated Ag/AgCl reference membrane

This method is more similar to the one used in the previous project. However, it uses Polyvinyl Acetate (PVA) instead of Polyvinyl Butyral (PVB) [76]. In this case, the potential stability seemed to rise even after 3 months of storage, making it a perfect suit for the project. It also only needs a very short conditioning duration of 20 minutes to stabilise the potential. Results showed potential changes were negligible for different solutions in a wide concentration range, as well as a stable potential response in a range of pH between 3 to 10 (sweat's pH is around 5) and negligible response to ambient light (see Figure 3.15).

There is also an extra advantage of using this type of membrane. As it is known, the mobility difference of K<sup>+</sup> and Cl<sup>-</sup> in KCl is the least among chlorides, which ends up creating smaller liquid junction potential and a minor correction to the standard potential [56]. Thus, KCl would, in theory, be the best

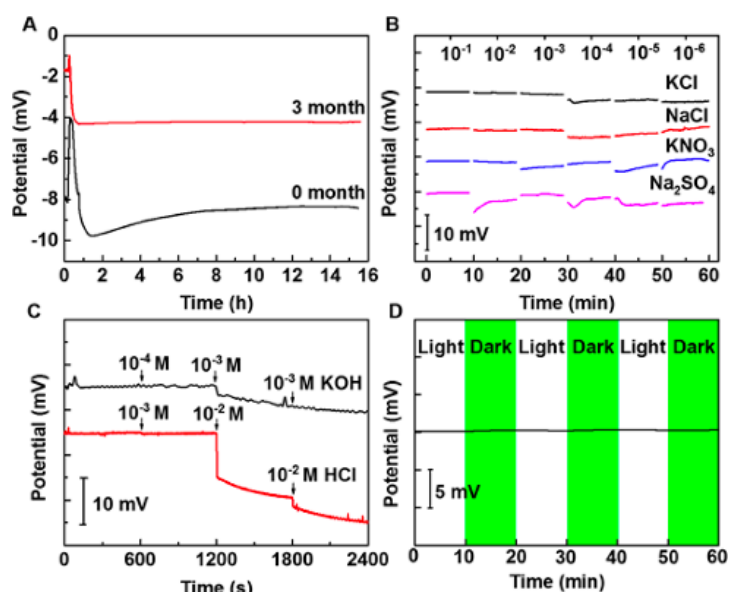


**Figure 3.15:** Potentiometric responses of PVA/KCl-Ag/AgCl solid reference electrode vs double-junction Ag/AgCl/KCl (3 M) containing a 1 M LiAcO salt bridge in (A) 3 M KCl solution and (B) different concentration solutions of ions range from  $10^{-1}$  M to  $10^{-6}$  M. (C) pH response and (D) light sensitivity of PVA/KCl-Ag/AgCl RE. Potential responses in panels B and C have been vertically shifted for clarity of presentation [76]

salt used for the reference membrane. The positive reviews, the excellent stability observed and the low level of complexity in the production steps suggested to use PVA/KCl membrane-coated Ag/AgCl as the reference membrane for this project. Membrane's materials and the cost for each of them can be observed in Table 3.3.

REAGENTS	Quantity for one electrode	Pack size	Manufacturer	Code in Sigma Aldrich	Price (€)
Vinyl acetate	Ratio 1:0.01 by wt with DMPP	1 g	Supelco	48486	81.6
Photoinitiator 2,2-dimethoxy-2-phenylacetophenone (DMPP)	Ratio 0.01:1 by wt with VA	50 g	Sigma Aldrich	196118	67.8
Milled and dried KCl powder	50 wt %	250 g	Supelco	1049360-250	23.5
<b>TOTAL</b>					<b>172.9</b>

**Table 3.3:** Chemical materials used to produce the reference membrane

The production steps are the following [76]:

1. The bottom layer of Ag/AgCl was first prepared by drop-casting 4  $\mu$ L of Ag/AgCl ink onto the reference electrode zone on-chip, which was and left to dry overnight in a glass desiccator.
2. Meanwhile, milled and dried potassium chloride (KCl) powder was prepared for use by annealing for 30 min at 450  $^{\circ}$ C and carefully grinding in a mortar.
3. To prepare the polymer/inorganic salt composite membrane, poly(vinyl acetate) (PVA) and KCl composite was selected. Vinyl acetate monomer and photoinitiator DMPP were mixed in a tube at a ratio of 1:0.01 by weight, and prephotopolymerization in a UV case (UV lamp: 185 nm +254

nm, 250 W) took place for 5 min.

4. 50 wt% KCl powder was added to the previous mixture and well mixed into a white viscous liquid, following by drop-casting of the as-prepared mixture onto Ag/AgCl electrode and irradiation with UV light until the membrane was hard enough.

### 3.2.4. Production steps

Before going into the lab and making the membranes, a lab protocol and a list of equipment were developed to know the necessary lab equipment needed for the purpose. There were several instruments listed in order to build them:

1. **Digital scale.** In order to measure the quantities needed of each reagent to elaborate the membranes. Some of these quantities are very small, so the more accurate it is, the better.
2. **Glass pipette.** Some device for measuring small volumes.
3. **Microsyringe/pipettor.** Some volumes needed for the membranes are tiny (660  $\mu\text{L}$  of THF for the sodium membrane), so a device with higher accuracy would allow for a better result of the membrane.
4. **Beaker.** Necessary to mix all reagents.
5. **Glass desiccator.** Necessary for drying Ag/AgCl ink.
6. **Oven.** For annealing KCl.
7. **Fridge.** Some mixtures need to be cooled down after elaboration.
8. **Mortar.** In order to grind KCl.
9. **UV lamp.** Prephotopolymerization is needed.
10. **Multimeter.** This device is needed to check the potential changes between our membranes and the reference electrode when submerged under a solution.
11. **pH Meter.** To measure the pH of the solutions needed to characterise the reference membrane.

#### Sodium-selective membrane

The steps to build the  $\text{Na}^+$  selective membrane are [89]:

1. Mix  $\text{Na}^+$  Ionophore X (1% wt/wt), Na-TFPB (0.55% wt/wt), PVC (33% wt/wt), and DOS (65.45% wt/wt).
2. Next, 100 mg of the membrane mixture are dissolved in 660  $\mu\text{l}$  of tetrahydrofuran (THF).
3. Finally, the ion-selective solutions is sealed and stored at 4  $^{\circ}\text{C}$  overnight.

When starting to measure the weight for each material, it was noticed that some of them were minimal quantities (5.5 mg for Na-TFPB or 10 mg for Na Ionophore X). The weight scale was supposed to measure these small quantities, but it was hard to add the exact amount. The final quantities used for the membrane are shown in Table 3.4.

MATERIALS	$\text{Na}^+$ Ionophore X	Na-TFPB	PVC	DOS	THF
MASS	19.9 mg	12 mg	722.3 mg	1.45 g	12.82 g

**Table 3.4:** Total quantities of each material for the production of the sodium membrane

Chemicals were all mixed with the solvent, followed by homogeneous mixing using a hot plate stirrer. The final mixture was left at 6 °C to cool down overnight.

### Reference membrane

The production steps for the reference membrane are the following [76]:

1. The bottom layer of Ag/AgCl was already on the sensor as it was screen-printed on the previous step. This step differs from what was suggested in literature [76]: drop-casting 4  $\mu\text{L}$  of Ag/AgCl ink onto the reference electrode zone on-chip. However, the screen-printing technique allows for a more accurate and homogeneous spread of the ink on the electrode, so this step was modified.
2. Meanwhile, milled and dried potassium chloride (KCl) powder was prepared for use by annealing for 30 min at 450 °C and carefully grinding in a mortar.
3. To prepare the polymer/inorganic salt composite membrane, poly(vinyl acetate) (PVA) and KCl composite was selected. Vinyl acetate monomer and photoinitiator DMPP were mixed in a tube at a ratio of 1:0.01 by weight, and prephotopolymerization in a UV case (UV lamp: 185 nm +254 nm, 250 W) took place for 5 min.
4. 50 wt% KCl powder was added to the previous mixture and well mixed into a white viscous liquid, following by drop-casting of the as-prepared mixture onto Ag/AgCl electrode and irradiation with UV light until the membrane was sufficiently hard.

The process followed to build this membrane was the same as for building the sodium-selective membrane. Nevertheless, an issue was encountered when trying to prephotopolymerized poly(vinyl acetate). The process needed a specific UV case where wavelength and power could be set to particular values. However, the lab did not possess such a technology, so instead, it was used a standard UV chamber. The mixture obtained after exposure to UV light of just 2 minutes (instead of the 5 minutes suggested) was a very viscous compound. Thus, the following step of mixing it with KCl was a very tedious task, as the salt could not dissolve whatsoever. It was also added ethanol to use as a solvent, as well as heating the mixture. However, the mixture could still not be homogenised whatsoever.

The PVA/KCl membrane building is novel, and not many research groups have tried it yet. This reference membrane was chosen due to its excellent stability for long term sensors. However, the building process seems to be in the early stages and shows complexity in the different steps. A new approach was necessary for the building of this membrane. Looking back into literature, it was observed how PVB is mainly used as a sweat sensor reference membrane. PVB is a low-cost and rugged polymeric material that has been pioneered to be used for a combination of Ag/AgCl reference electrode as a polymeric reference membrane [55]. As already mentioned, this was the material used in the previous work at TU Delft, where some issues were encountered during the building process. Nevertheless, as Holst Centre possesses more leading-edge facilities than the ones at TU Delft, the building of this membrane had better chances to reach a more stable state than in previous experiments. The building process of this reference membrane is the same on all papers found, and it is the following [85, 90]:

1. A 10 wt.% of stock solution of PVB is prepared by dissolving 78.1 mg of PVB and 50 mg NaCl in 5 ml of methanol to create the reference cocktail.
2. An ultrasonic bath is used to achieve a homogenous solution.
3. The stock solution is stored at 7 °C in order to prevent the evaporation of the solvent.

4. Drop-cast 4  $\mu\text{l}$  of the reference cocktail on top of of the Ag/AgCl reference electrode.
5. Dry overnight before use.

Once PVB was ordered and delivered, the mixing of all chemicals was possible. The laboratory lack a proper ultrasonic dismembrator (Fisherbrand™ Model 120 is suggested in literature [85]), so other methods for mixing the solution needed to be performed. Looking at the available lab equipment, it was decided to perform two different mixings and compare results. The first mixing method was the same as the sodium-selective membrane, using a hot plate stirrer for one hour. The homogenous mixing of the chemicals was achieved. The second method involved using the Branson sonifier, an ultrasonic cell disruptor/homogeniser, which is similar to the one used in literature. However, the former machine was not able to completely dissolve the chemicals together, and there was also some evaporation of methanol. Therefore, mixing using the hot plate stirrer was used.

The final step involved the drop-casting of the sodium-selective membrane and the reference membrane on top of the electrode. For this step, both the older version and the new version of the sweat sensor were used. The placement of the membranes was performed using a precise pipette with a range between 1 and 10  $\mu\text{l}$ . During the process, it was observed how the membranes in the new sensor's version spread around the electrodes onto the PET. This issue did not occur with the other sensors, as the dielectric insulator surrounds the electrodes in this version. This feature will be of crucial relevance in chapter 5 when testing the long-stability of the membranes.

Once the sweat sensor was finally produced, it was ready for the validation process.

### 3.3. Sensor validation

This section focuses on the validation process of the sensor. Once this part of the sweat analysis system was produced, the next step needed to make sure this sensor adequately worked. In this section, the experimental setup will be explained, and the results obtained in the process will be exposed. The sweat sensor was tested taking into account these characteristics:

- Stability of the sensor
- Sensitivity for chloride and sodium
- Response time

#### 3.3.1. Experimental set up

As previously mentioned, the sensor was printed using two different designs: the previous prototype developed by T. Bakker (see Figure 3.8) and a new version for a suitable integration with the sweat collector (Figure 3.9). In addition, in order to test the different characteristics of the sensor, it was necessary to use the read-out circuit developed by T. Bakker for his thesis project [56]. The working principle of this circuit will be further explained in chapter 5. The sweat sensor was validated in a laboratory setting. The measurement setup consisted of:

- The sweat sensor

- The read-out circuit
- A long screw to hold the sensor
- FFC connectors
- Beakers for the different NaCl solutions

As observed in Figure 3.16, it was used a multi-channel measurement setup, capable of running four sweat sensors submerged in different solutions at the same time.

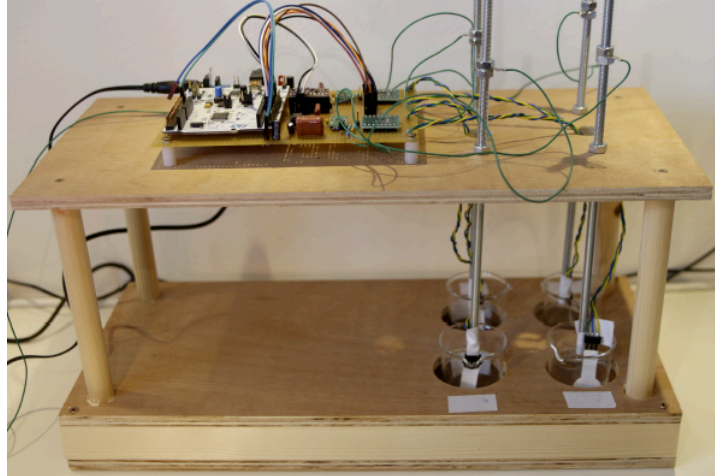


**Figure 3.16:** Multi-channel measurement setup running four experiments at the same time [56].

Regarding the solutions used for testing the sensors, it was concluded to use a solution of water and salt. This water had to be demineralised, as no other ions besides sodium and chloride could be in the solution. Common salt was used as the solute in this solution, contributing to the expected final concentration of  $[\text{Na}^+]$  and  $[\text{Cl}^-]$ . In order to calculate the mass  $M$  of salt needed to reach a final concentration of each ion, the molar concentration formula is used (equation 3.8). In the equation,  $c$  is the molar concentration, and  $V$  is the volume of the solution. The other factor needed is the molar mass  $M_i$  of NaCl, being  $58.4 \text{ g/mol}$ .

$$M = c \cdot V \cdot M_i \quad (3.8)$$

The estimation of the time response of the sensors is also crucial in this study, especially for building the sweat collector. The sensor must have enough time to analyse the sweat on top of the electrodes before it flows away. This crucial time could be estimated by quickly changing it from a solution with a low NaCl concentration to a high one and vice-versa.

For the calculation of the response time, a few sensor theory was needed. The responsiveness of a sensor is usually given by a *Time Constant* and represented by the Greek letter  $\tau$  "tau". However, this constant represents the time required for the sensor to reach 63.2% of its total step change. The response time of the sensor is five times the time constant  $\tau$  (see equation 3.9). The response time is the sensor reading time to reach 99.3% of the total step change.

$$\text{Sensor response time} = 5 \cdot \tau \quad (3.9)$$

Once all these requirements were achieved, the sensor was ready to be tested.

### 3.3.2. Results

In order to test the stability of the sensor, it was submerged into four different solutions with NaCl concentration, from 20 to 80 mmol/L. Results can be observed in Figure 3.17. Each ion sensor show different behaviours:

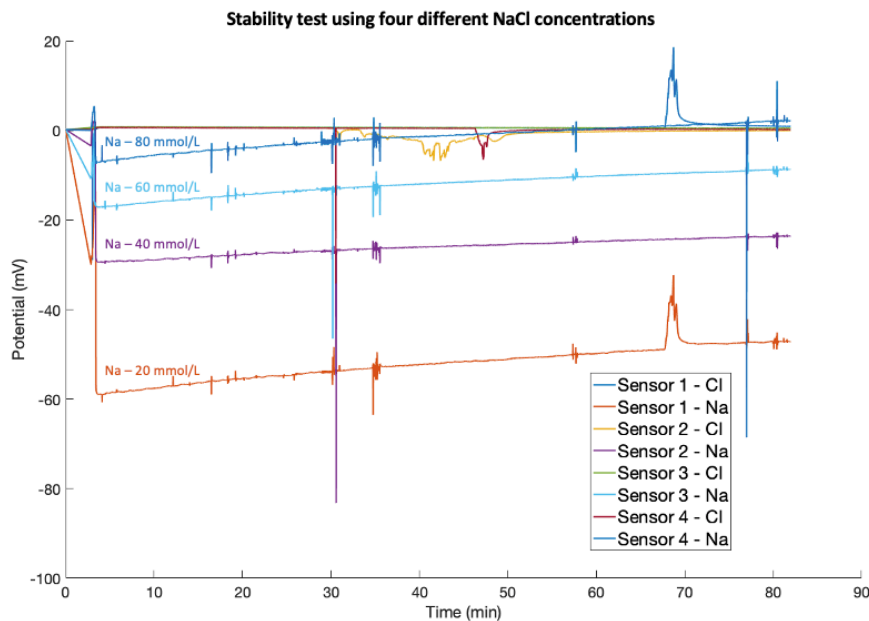


Figure 3.17: Stability test for the sensors using four different NaCl concentrations.

1. **Sodium sensor:** increase in potential as the concentration of NaCl rises. The potential suffers an increment with time of around 10 mV for each concentration.
2. **Chloride sensor:** for all concentrations it stabilizes at zero voltage. Initially, just after sensors are dipped inside the solutions, the voltage in chloride sensors changes, but quickly after that, it goes back to zero. Some sporadic voltage changes are also observed through the test (Sensor 2 after 40 minutes).

The increase in potential for the sodium sensor was not ideal. This voltage should remain constant if small changes in potential wanted to be measured for little variations in sweat concentration. To avoid this issue, pre-wetting of the sensors previously to its usage was tested. This wetting of the electrodes was done using a very small concentration of NaCl with demineralised water. Results showed in Figure 3.18 shows a very stable voltage for four different NaCl concentrations.

Due to the barely existing sensitivity of the chloride electrode to a NaCl solution, possible reasonings for this behaviour were considered. Firstly, as already mentioned, the Ag:AgCl ratio was different between previous sensors produced by T. Bakker and the new ones printed. Whereas T. Bakker used an Ag:AgCl ratio of 60/40, the silver chloride provided by Holst Centre had a ratio of 32/68. However, this ratio of a higher amount of AgCl was recommended by M.A.G. Zevenbergen, author of [82] and researcher at Imec. His experience on different inks for chloride sensing made the Ag/AgCl ink used



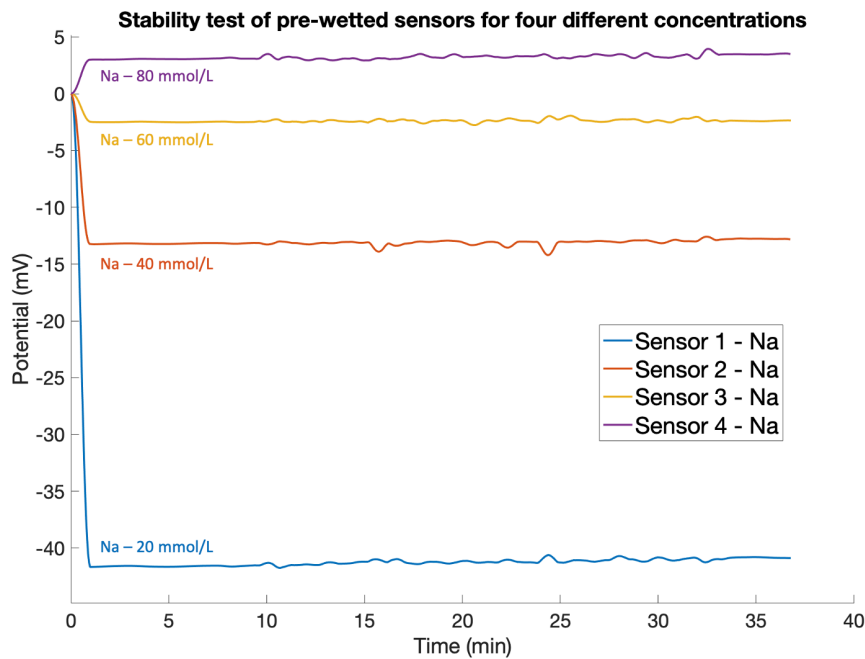


Figure 3.18: Stability test for pre-wetted sodium sensors using four different NaCl concentrations.

in our sensor highly suitable for the project's goal.

Therefore, a few experimental tests were developed to test the sensitivity of the chloride. Firstly, the voltage difference between the reference and chloride electrodes was tested using a voltmeter instead of the read-out circuit. The voltage difference when the electrode was submerged into a NaCl solution also showed a value really close to 0 V. Chloride electrode was also looked into the microscope for possible scratching of the surface, but no imperfections were observed. The last method was to make sure the ink lying on the electrode was sensitive to chloride.

In order to test the homogeneous distribution of the Ag/AgCl layer in the printing process, a simple chemical test was performed. The chloride electrode was compared against an Ag/AgCl reference electrode fully saturated into a 3 M KCl solution. If the sensor electrode layer was not damaged, a potential close to 0 V should be measured when comparing the voltage difference between the reference electrode and our Ag/AgCl electrode. The obtained voltage was over 30 mV, and it was going down slowly to 0 V. This result meant the electrode's Ag/AgCl layer was not completely covering the surface, thus not being sensitive to chloride.

However, the constant voltage drop showed some other conclusions. This decrease suggested the electrodes were indeed damaged and not fully covering the surface of the electrode, but some Ag/AgCl remained on it. In order to try to create a new layer of Ag/AgCl, it was performed a polarization method proposed by A. Kosari (PhD candidate from the Corrosion Technology and Electrochemistry department at the Mechanical, Maritime and Materials Engineering faculty). This method could allow to build a new layer of Ag/AgCl on top of the electrode by coating the existing layer of Ag with AgCl.

The polarization method required the use of a potentiostat, an electronic hardware designed to control the working electrode's potential in a multiple electrode electrochemical cell. The electrodes were submerged inside a solution of 0.1 M HCl, and the opposite edge of the chloride electrode was covered with copper and linked to the working electrode of the potentiostat. In addition, a platinum wire in the solution was attached to the reference and counter electrode to measure the current in the procedure, but remains as an inert element in the chemical process. By inducing a potential in the working electrode,  $\text{Cl}^-$  ions attach to  $\text{Ag}^+$  on the surface of the electrode and begins to form the AgCl. The silver

layer in return starts becoming thinner, so the time and voltage of the polarization process will directly influence on the thickness of both the Ag/AgCl layer [91]. This reaction was initially set to last for 15 minutes at 1.5 V. Figure 3.19 shows the sensitivity of chloride electrode before and after the polarization method was performed. Higher voltage peaks are observed, but the sensitivity still drops back to zero soon after the concentration changes. A longer polarization period (3 hours) was performed, but results showed similar sensitivity behaviour.

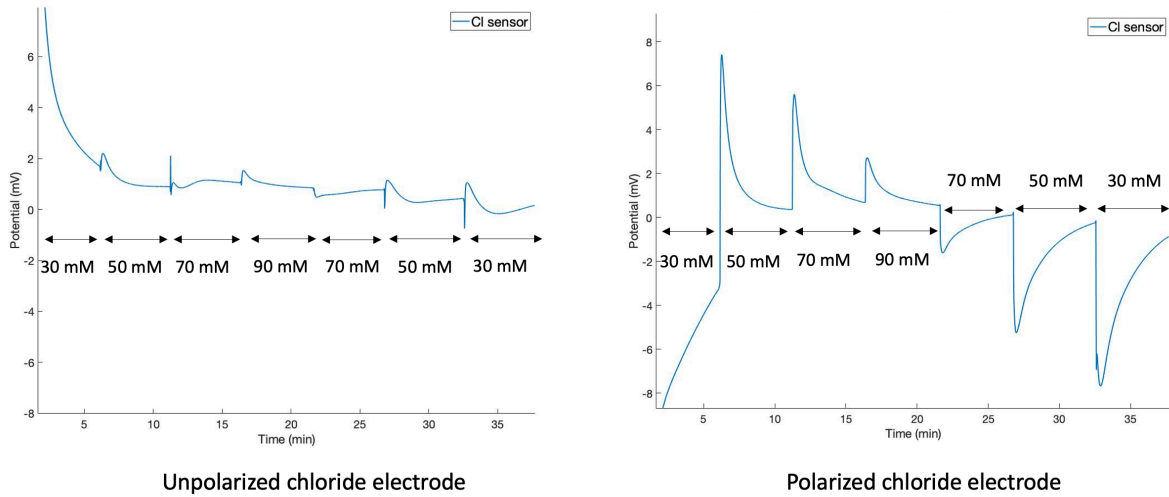


Figure 3.19: Comparison between a polarized and non-polarized chloride electrode

To study the sensitivity of the sensor, they were submerged into six different NaCl concentrations: 20, 40, 50, 60, 80 and 100 mmol/L. As observed from the stability tests, sensors needed some time to reach a constant voltage. Thus, the sensors were previously submerged into demineralised water with a low level of NaCl concentration. The average potential of four sensors for each concentration is shown in Figure 3.20. From the graph, it can be observed how a small concentration (20 mmol/L) is showing a low potential which really differs from the rest of data points. Error bars are shown, but only visible in the 20 mmol/L and 100 mmol/L data points.

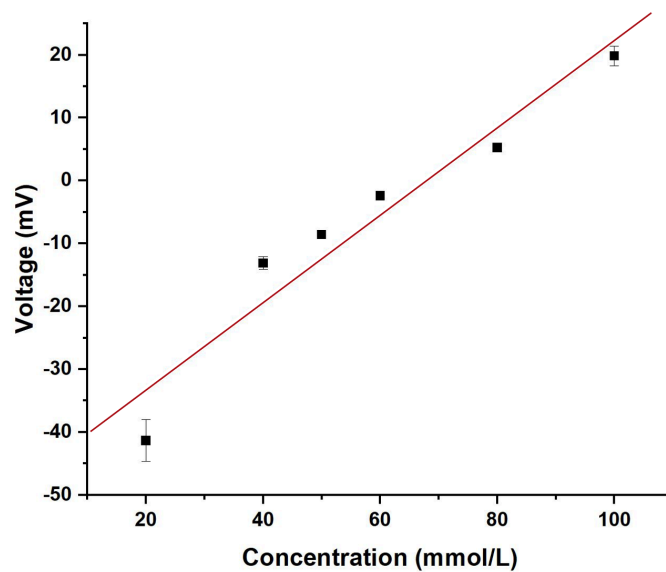


Figure 3.20: Calibration curve for the Na sensor

The last characteristic studied for the sensor was its response time to changes in ion concentrations. As shown in Figure 3.21, the response time of the sensor was studied, going from a low NaCl concentration to a high one and vice-versa. The response time was calculated using five different sensors and averaging the different times obtained. The time constant  $\tau$  of the sensor was estimated to be  $5.6 \pm 0.43$  seconds, giving a response time of  $28 \pm 2.15$  seconds.

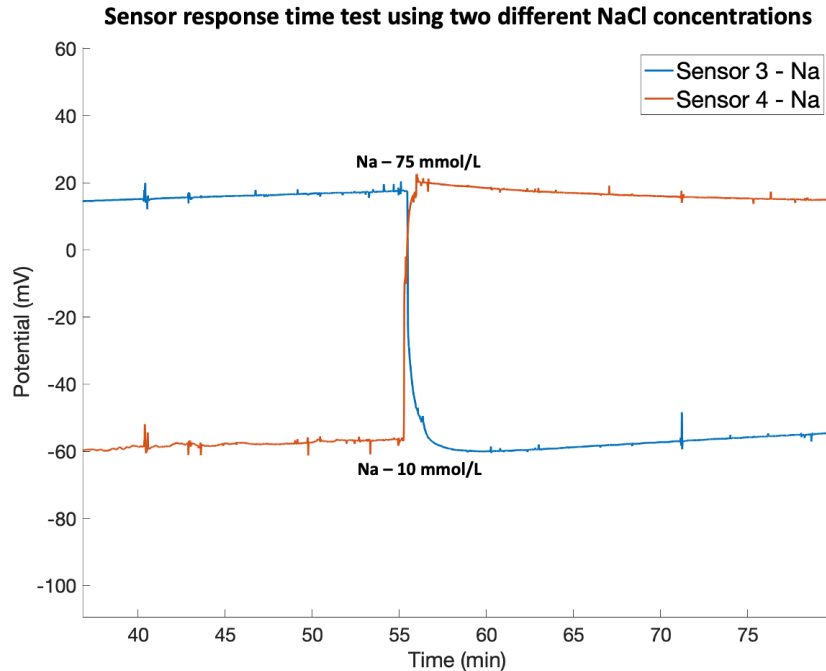


Figure 3.21: Time constant estimation using 10 and 75 mmol/L concentrations.

### 3.4. Discussion

The stability test of the sweat sensor showed some interesting information. As observed in Figure 3.17, there is a measured relationship for the sodium electrode between the potential measured and the concentration of NaCl tested. These differences in potential observed for the Na electrode can allow for the testing of human sweat in order to analyse the exact concentration of Na ions (using the non-linear fitted curve).

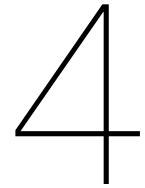
Chloride electrodes are all showing a potential of zero for all concentrations. Comparison of the Ag/AgCl electrode against an Ag/AgCl reference electrode showed that this ink was barely present on the surface of the electrode. This issue could have been due to faulty screen-printing of the Ag/AgCl layer or mechanical damage to the electrodes after they were produced. The polarization method to create a new Ag/AgCl layer did show a higher sensitivity, but a stable Ag/AgCl layer was not achieved.

As observed from Figure 3.20, a low voltage is obtained from low ion concentrations. This behaviour is linked to the higher difficulty of the sensor to analyse low values of saline concentrations. The standard deviation for this point is higher than the rest of data points, which shows the lower accuracy of the sensor for low concentrations. Special attention should be taken for the region 30-60 mmol/L, as those are the common NaCl concentration values found in human sweat. The sensitivity in this specific region is around 0.7 mV per mmol/L, which can allow to analyze sweat NaCl concentration.

---

Finally, the response time calculation provided crucial information for the building of the sweat collector. The sensor needs an average of 30 seconds to analyse the sweat lying on top of the electrodes. The sweat collector should possess the necessary characteristics to provide this time to the sensor to analyse sweat ions accurately.





# Sweat collector

Before sweat can be adequately analysed, there is a previous crucial step: sweat collection. This step has many benefits for the analysis of sweat. It will allow to acquire sweat under controlled conditions and also avoid any contamination of the sample. The sweat collector will also set the necessary microfluidic parameters in order to analyse sweat. Throughout this chapter, literature will be reviewed to select the sweat collection system that better fits this study's desires. Afterwards, the methods followed to build the sweat collector will be exposed. Finally, the results obtained for its validation will be shown.

## 4.1. Sweat collection techniques

Different techniques were developed early in the 20th century in order to collect sweat. These techniques tried to collect sweat from isolated areas using a fabric impermeable to water and dissolved substances. Another method used a chamber saturated in water vapour to collect the sweat from the subject afterwards. Some other experiments tried to enclose the subject inside a tarp to collect the sweat without dilution or evaporation [92]. These initial methods for collecting sweat started to show issues that were later well defined: evaporation on the surface of the skin which can alter the final concentration of sweat constituents, contamination of sweat with skin cells; and a lack of control over where the sweat is collected from [54]. These difficulties are approached in two different ways depending on the research goal and which factors are more important. All body sweat can be collected using a whole body-washdown technique or otherwise from a specific region of the body using different techniques.

### Whole-body washdown technique

The whole-body washdown (WBW) technique measures the overall quantities of sweat secreted during the exercising period. Afterwards, the majority of sweat is collected from recipients, such as plastic bags laying on the floor [93]. Figure 4.1 shows how this technique works on a specific research project: the subject cycles on an ergometer under specific conditions (ambient temperature of 34°C and relative humidity of 60-70 %) while having the patient inside a frame covered with plastic bags all around him. These plastic bags allowed for the conservation of specific conditions and to preserve all sweat dripping to the floor. After each exercise session, the subject was washed down with distilled water to obtain the sweat stuck on the skin surface. The later analysis of sweat allows to measure the final amount of sweat loss as well as the concentration of sweat Na, Cl and K [54].

The WBW method has been chosen in investigations when quantifying the total sweat loss and the body electrolyte balance [93, 94]. This method is primarily limited to laboratory studies in which sweat needs to be collected in significant quantities. In addition, this technique makes almost all constituents of sweat to be affected by contamination [54]. This project focuses on measuring sweat while the

athlete is exercising and not afterwards, so this technique is disregarded.

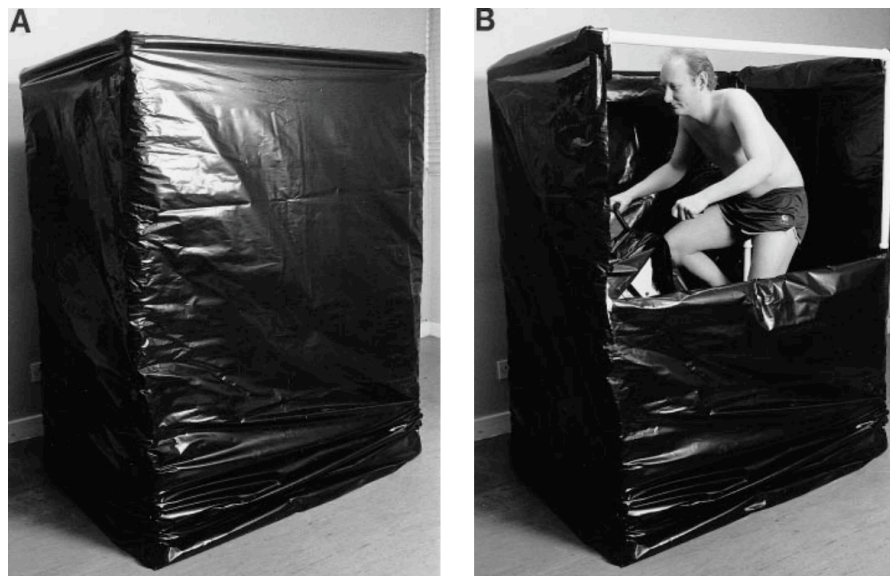


**Figure 4.1:** Whole-body washdown technique. A: intact system; B: a section of the bag has been cut away to show subject cycling on the ergometer. [54]

### Sweat collection in a body region

When collecting sweat in specific regions of the body, it is of main importance to try to have as little epidermal contamination as possible and avoid as much as possible water loss due to evaporation. The methods tried out are broad, and many approaches have been tested out, but not all of them have been successful. Depending on the site of collection, it also shows a great variability regarding the contamination of sweat constituents [50]. Previous work has shown that sweat should be collected in those regions that are highly correlated with whole-body sweating rates [95], as well as to know better which areas will provide sweat at a higher rate. Figure 4.2 shows the different sweating rates in the body divided into regions [81]. The image shows that the back is the area with a higher rate, followed by the forehead and the calves. Thus, it is not surprising that most of the experiments use the person's back to obtain a high sweat volume. The image also shows how the lowest sweating rates are focused on the palm of the hands and cheeks. The glands in these areas are mostly related to hormone secretion and not to the nervous system, so the perspiration does not occur when trying to cool down the body but when feeling emotions.

The need for a precise method for the analysis of sweat constituents shows what criteria needs improvement. Some criteria have already been mentioned, such as the absence of contamination or avoiding the evaporation of sweat. However, other criteria in the methodology were discovered, such as obtaining better reliability of results by placing multiple sweat collectors, the lack of leakage of the sweat sample into and out of the collection area, or the ease of the methodology [32].

Regarding the acquisition of sweat using regional methods, the techniques used can be extensive, and it is worth mentioning some of them due to their outstanding results, accessibility for materials, and ease of acquiring sweat.

Absorbent patches use materials capable of absorbing sweat in large quantities, acting as a sponge. A recent study analysed the effectiveness of using patches over a large area of the body [96]. The experiment carried by Havenith *et al.* was the first one to use absorbent patches over a large area simultaneously. They found that previous studies used small patches to acquire sweat to correlate them to the area studied. Instead, they wanted to measure exact quantities of sweat in the body to compare the results with former studies later on. They used large absorbent patches which covered the whole

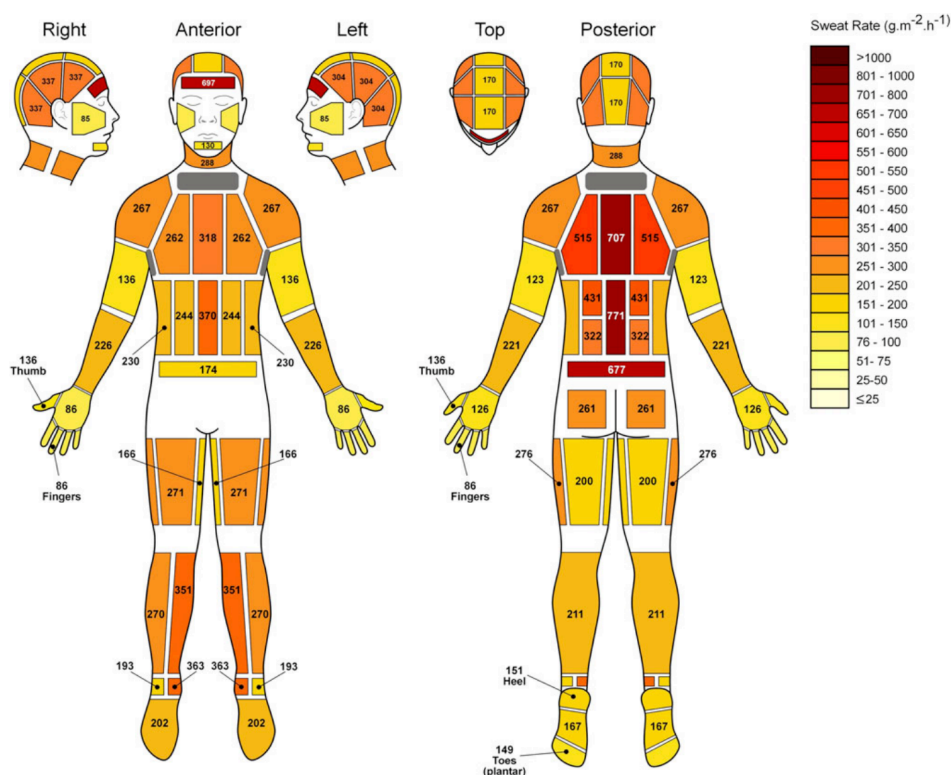


**Figure 4.2:** Absolute regional median sweat rates of male athletes during high intensity exercise [81]

torso and the upper arm area simultaneously. The study showed a very significant correlation ( $P < 0.001$ ) between the data from the patches and the overall sweat loss of the body.

Nevertheless, there were also some concerns regarding the continuity of the measurement using patches. This type of sweat collection helps provide strong evidence for the variation of sweat rates over the body during physical activity. However, absorbent patches get saturated and need replacement, interrupting the continuity of the measurement [17]. Absorbent patches are only able to provide a few data points per experiment on each zone of study [96], which is not sufficient for continuous monitoring of sweat analytes. Thus, this type of sweat collection does not fit the requirements to be used in the analysis of sweat during physical activity.

Another way of collecting sweat consists of the complete coverage of the arm using a plastic bag. This technique is similar to the WBW, but only on the arm instead of the whole body. Thus, these two methods have similar disadvantages that do not fit the goal of this project.

- The arm bag method for collecting sweat has the disadvantage of high contamination risk, especially at the beginning of the process. Studies show there is an increase in external contamination when sweat was collected using an arm bag [97]
- There is a high increase in constituents up to six times the normal values, such as Na, Cl, K, Mn, Zn, or Ca. This issue suggests there is a great alteration of the regional sweating rate due to encapsulation of the arm, creating a microenvironment inside the bag [17, 25, 97, 98].

Thus, this method does not seem appropriate when studying the total amount of electrolytes found in sweat.



The last sweat collecting technique is the wicking of sweat. In this category, it is included all types of devices that wick sweat into some type or microfluidic system in order to analyse it *in situ* or to collect it to study it later on. The process allows absorbing sweat spontaneously into the system by capillary action. This procedure drives liquids to move in a given direction inside a solid.

Sweat collection would be performed without contamination of the sample using capillary action due to its immediate absorption. Furthermore, the number of sweat glands involved in the process could be precisely estimated to predict sweat flow rate and volume during exercise. Knowing these parameters can also be beneficial to estimate whole-body water loss through sweat and electrolytes secreted in the process. These advantages provided by the wicking of sweat make this process the most suitable for building a sweat collector.

#### 4.1.1. Capillary action in sweat collectors

As previously explained, wicking of sweat inside a closed system is thanks to the action of capillary pressure. This type of pressure allows driving the fluid in a given direction inside a solid. The sum of cohesive forces of the liquid's molecules and the adhesive forces that cause the fluid to stick to the solid surface pushes the liquid to move forward [99].

Capillary action can be found in many diverse situations, such as the process of eyes filling with tears or the rapid antigen test. There is an excellent usage of this process, as when a few droplets of fluid are deposited on a fixed matrix, the liquid can follow a specific path previously defined [100]. Capillary pressure can be used to wick sweat inside a closed system. Once inside, it can be driven into collection chambers to analyse it afterwards or into areas where sensors can be placed. This last procedure fits perfectly into the goals of the project, as it would allow analysing a non-contaminated sweat sample while a person is in the perspiration process.



Figure 4.3: Example of the capillary action process in a rapid COVID-19 antigen test [101]

It is not surprising that research groups have recently used capillary pressure to build a sweat collector. This process can be beneficial if sweat wants to be studied during physical activity. It allows to drastically reduce sweat contamination compared to other methods, as well as to work with small and fixed volumes of sweat to be continually monitored.

##### Megaduct® sweat collector

The Macroduct (TELETECH Wescor® Inc., Logan, UT, USA) is a famous commercially available sweat collector that has been used in sweat research since 1986. Placing a plastic capillary-coil device on the forearm wicks the sweat off the skin surface. A more recent version of the Mac product device is the Megaduct (see Figure 4.4). It was developed to increase the volume capacity of the device as well

as to assess certain drugs in sweat [102]. This device can overcome specific issues when collecting sweat, such as the background contamination, the encapsulation of the skin area (undesired rise of skin temperature and sweat rate) as well as to avoid hidromeiosis (progressive decline in sweat rates that occurs when skin is thoroughly wetted or with higher humidity). These advantages are thanks to capillary action by immediately removing sweat from the skin after secretion [103]. These advantages make the Megaduct a device that can theoretically reflect more accurately regional sweat concentrations than other types of sweat collection systems.

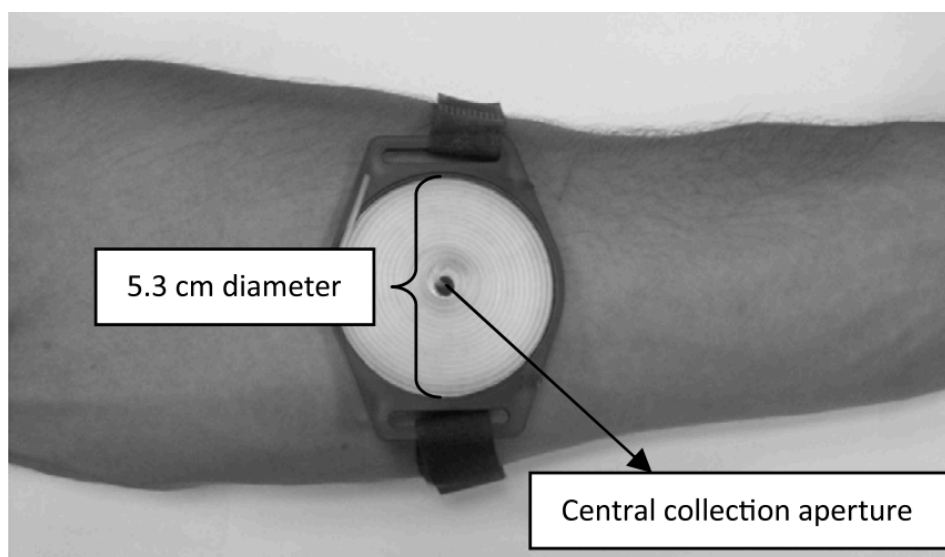


**Figure 4.4:** Megaduct sweat collector (Wescor® Inc., Logan, UT) [102]

However, the Megaduct® is not the ideal sweat collector for measuring sweat during physical activity. A study carried by Ely *et al.* wanted to measure the time it took to fill the reservoir during moderate-intensity exercise (treadmill walking at 1.5 m/s, 4% grade) [102]. The average time for ten healthy men to fill the chamber was over an hour (65 to 75 minutes) with varying exercise intensities ( $\text{VO}_2 = 0.5\text{--}2.0$  L/min), temperatures (20–40 °C) in a controlled 50% humidity environment. The long period to collect 0.5 mL of sweat may be a limitation when analysing sweat constituents. Many studies have demonstrated that the concentration of sweat electrolytes and minerals change in relatively short periods, such as Na and Cl changes within the first 30 minutes [104], acute mineral losses in Fe [105] or Zn [25].

The Megaduct® is an excellent sweat collection approach to avoid sweat encapsulation and hidromeiosis. Nevertheless, different methods are needed if the project aims to measure sweat electrolyte and mineral changes during short periods accurately.

#### **PDMS sweat collector**

A more recent study that also uses the wick effect to get sweat from the skin has shown excellent results for collecting sweat. Y. Zhang *et al.* created a microfluidic device for collecting sweat in chambers to analyse it [106]. The wick effect is achieved by driving the flow through the inlet hole into the microfluidic system. The pressure sum from natural sweat excretion and the oppositely directed capillary pressure drive the sweat inwards. The material used for the collector was chosen to be PDMS. PDMS is naturally hydrophobic, but thanks to air plasma treatment (APT) and a later low-energy polyvinylpyrrolidone (PVP) surface modification, PDMS can remain hydrophilic for more than six months [107].

A relevant new method from this study innovative is the way of collecting sweat. They use hydrophobic valves after the aperture of the sweat collection chambers to retain sweat inside. As previously mentioned, PDMS is naturally hydrophobic. Thus, to obtain these hydrophobic masks, all it has to be

done is place masks when the APT treatment is performed. The unexposed PDMS region under the mask remained hydrophobic and formed the hydrophobic valves in the microfluidic channel. These valves do not allow sweat to flow in the microfluidic channel but go into the chamber. Once the capsule is filled, sweat can break the effect of the hydrophobic valve and continue through the channel onto the next chamber. A more definitive explanation of the process can be seen in Figure 4.5.

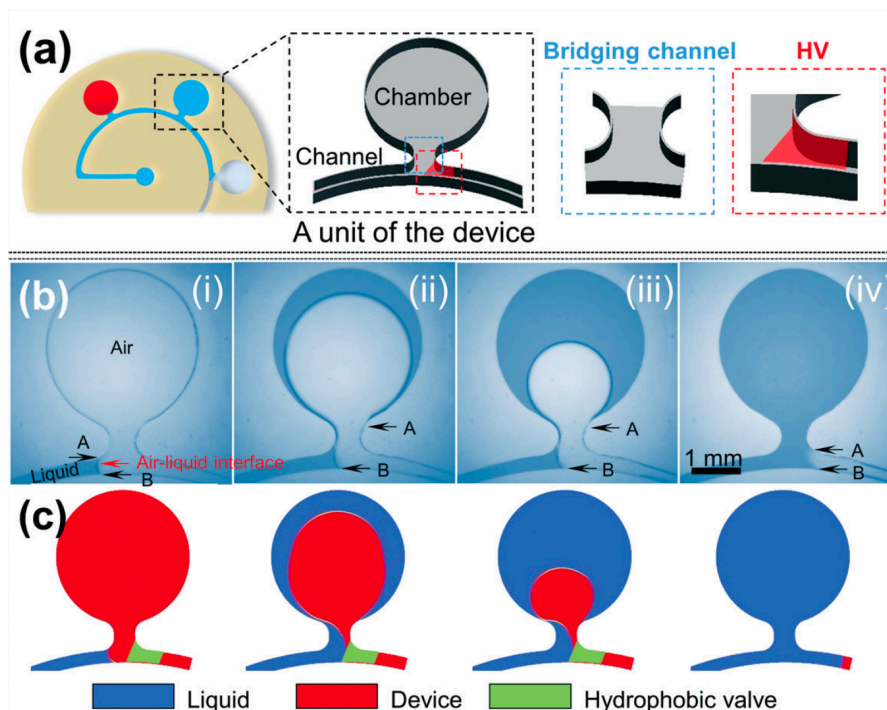


**Figure 4.5:** Working principle of the hydrophobic valve to route liquid into the one-opening chamber in the microfluidic device. (a) Schematic of the one-opening chamber with the hydrophobic valve and a bridging channel in a microfluidic device. (b) Optical images (i–iv) and (c) numerical simulations of the hydrodynamic flow process into the one-opening chamber with a hydrophobic valve [106]

Thanks to the use of capillary action, this device also stands for reducing sweat contamination and evaporation. Previous designs using microfluidic sweat chambers had an outlet for releasing air as the chamber fills out [72, 108]. The usage of an outlet avoids backpressure on the device, but it also favours evaporation of sweat through it. Thus, this novel design can reduce unnecessary sweat evaporation and contamination, making it a very accurate device for sweat analysis. Another great feature is the colourimetric analysis of sweat. This task is thanks to the usage of methyl red as a pH indicator, acting as a chromogen to determine the exact pH of sweat. Considering the advantages of this device, the design of the sweat collector could be modified to fit all goals of this project. An interesting idea would be to place ion-selective electrodes under the collectors, or not having collectors but continually have sweat coming into the sensors and flowing out.

#### 4.1.2. Conclusion

Collection of sweat aims to drive sweat to its accurate analysis avoiding contamination of the sample and under controlled conditions. Depending on the goal of sweat analysis, there are different techniques capable of performing this task. This project aimed to continuously measure small quantities of sweat under controlled conditions, avoiding any contamination. In addition, the collection system had to be designed to reduce the sample flow speed to increase the time for sampling.

Wicking of sweat using capillary action seemed to be the best option for the collection of sweat. Its continuous acquisition allows analysing sweat samples in real-time. Current projects using this tech-

nique also show the advantages of collecting sweat using this method [102, 106]. In addition, it has been observed that microfluidics for this task could be of great help, driving sweat to specific chambers for its analysis and controlling its flow speed. The next chapter will focus on the design, material selection and production of the sweat collector.

## 4.2. Methods

Once literature was reviewed to find the most suitable sweat collection system, it was time to design and build the sweat collector. This chapter will discuss all the decisions taken for obtaining a suitable sweat collector for this project.

### 4.2.1. Design

When designing the sweat collector, the two primary goals were to build it functionally and comfortably for the athlete. Regarding the function of the collector, the idea was relatively simple: absorb sweat without contamination, analyse it taking advantage of the microfluidics characteristics, and release the sweat into the skin. Therefore, these functions can be divided into three sections: inlet hole, analysis area, and outlet zone.

#### Inlet hole

This area is where the wicking of sweat occurs. Sweat can flow inside the microfluidic system thanks to capillary action. However, the flow of sweat is not constant and has three different factors influencing it. Depending on the area of the inlet hole, there will be a different amount of sweat glands able to fill the collector. In addition, depending on which area of the skin the collector is placed, sweat gland density will also variate. Finally, the sweat rate per gland varies during the exercise. These three factors will influence the final volume of sweat and its flow rate.

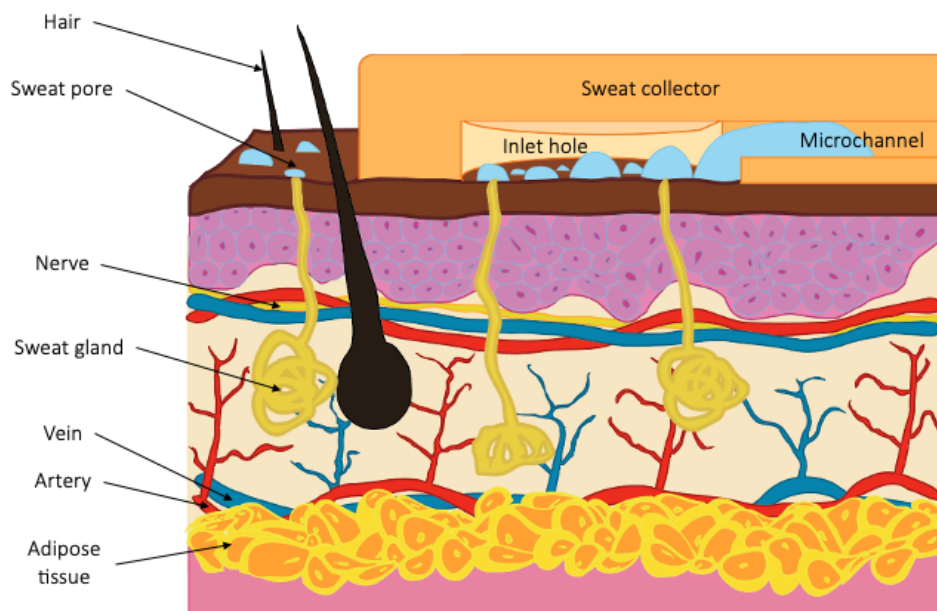


**Figure 4.6:** Lateral view of the skin structure. Sweat is wicked from the inlet hole to the microchannel due to capillary pressure.

The area of the inlet hole ( $A_{hole}$ ) is the variable concerning the amount of sweat going inside the sweat collector. Thus, the radius size had to be optimised. In literature, most collectors using capillary pressure acquire sweat using a relatively small inlet hole (1 mm radius). It was therefore studied the total sweat rate ( $Q_{sweat}$ ) going inside the sweat collector. For these calculations, it was taking as a reference the gland density ( $\rho_{glands}$ ) of the back (100-105 glands/cm<sup>2</sup>) [50] and the average sweat rate per gland ( $Q_{gland}$ ) when acquiring sweat using capillary pressure (approximately 0.04  $\mu$ L/min) [106]. Results showed that the total flow rate was too low (0.2  $\mu$ L/min) to have enough sweat volume for the sensor to analyse. Considering the size of the sensor's electrodes, the inlet hole was set to have a radius of 4 mm. With this bigger radius, the flow rate going inside the collector was over 2  $\mu$ L/min. Equation (4.1) shows the total sweat rate ( $Q_{sweat}$ ) calculations.

$$Q_{sweat} = Q_{gland} \cdot \rho_{glands} \cdot A_{hole} = Q_{gland} \cdot \rho_{glands} \cdot \pi r^2 \quad (4.1)$$

Even though the sweat rate was raised by increasing the inlet hole's radius, it seemed that it would still take a few minutes to cover the sensor's surface with that amount of sweat volume. Looking into literature, studies observed that there is an increase of sweat rate when a portion of sweat glands are sealed [109, 110]. Due to compensatory effects, sweat rate increases exponentially (up to 0.6  $\mu$ L/min per gland) as the adjacent regions of the skin are blocked from the release of sweat. This finding also helped set the size of the inlet hole. It was decided to increase the surface area of the collector around the inlet hole, making a higher number of sweat glands to be sealed (see Figure 4.8).

### Analysis area

In the analysis area, the sweat sensor will be integrated so that sweat can be analysed *in situ*. This area is 0.9 cm in length, 0.5 cm in width and around 200  $\mu$ m in height. This structure aims to provide enough sweat volume to the sensor so the fluid can be appropriately analysed. As previously mentioned, the time constant of the sensor is an important characteristic that needed to be taken into account when designing the analysis area. By widening the microfluidic chamber, the sweat flow is reduced in comparison to the previous channel. Nevertheless, this feature is not enough to slow down the sweat flow in cases of high values of sweat rate, so extra features were designed in the outlet area of the collector.

As observed, only the electrodes were introduced inside the analysis area, as sweat is analysed through them. Therefore, the chamber is big enough to integrate the electrodes, considering their width and height. The rest of the sensor was designed to be lying outside the collector to have the connectors linked to the read-out system using a Flexible Printed Circuit (FFC) 8-pin connector. This external area was also covered using TPU to isolate the whole system correctly.

It was also essential to study the microfluidics in this chamber to understand the behaviour of sweat flow. As the final goal is to analyse the constituents in sweat, a turbulent flow in the system could provide inaccurate results due to the irregular flow of sweat. However, Reynolds number showed a laminar flow ( $Re < 1$ ) behaviour, so it could be concluded that the system possesses an orderly flow regime. This property contributes to obtaining an effective system that can accurately measure the concentration of ions found in sweat. Equation (4.2) shows how the Reynolds number ( $Re$ ) was calculated for the microfluidics system.  $\rho$  is the density of the fluid,  $v$  is the mean speed of the fluid,  $\mu$  is the dynamic viscosity of the fluid and  $D$  is the hydraulic diameter of the pipe. However, as the cross section of the analysis area is a rectangle and not a circumference, this hydraulic diameter is represented as the the cross-sectional area  $A$  of the flow divided by the wetted perimeter  $P$  of the cross-section.

$$Re = \frac{\rho v D}{\mu} = \frac{4 \rho v A}{\mu P} \quad (4.2)$$

### Outlet area

The outlet area has two main functions: slow down the sweat flow and get rid of the already analysed sweat. The first feature is the most important one, as it has the primary objective of providing enough time for the sensor to analyse sweat ions. As previously calculated, the response time of the sensor is about 30 seconds (see Figure 3.21). The time constant of the sensor is a challenge for the collector, which needs to slow down the sweat flow. Different solutions were considered for the outlet area. These possible solutions were divided into two groups depending on whether they had an active or passive working method.

The active methods require some external power for the system to work. It was first considered to have the athlete manipulating the collector every few minutes to push the sweat forward. However, this solution was quickly disregarded as the comfortability of the system would be decreased considerably. Other active methods required electricity inside the system, such as using nozzles [111] or piezoelectricity [112]. The issue of this system is the danger of using electricity in the system, which will be closely in contact with water and the risks that this interaction represents.

Passive methods have the advantage of autonomously working, not requiring any external power. It was first considered to use a system of loops in the microfluidic device. These loops would go up and down, making sweat flow to fight against gravity to advance. However, a more sophisticated method arise when looking into passive valves used in fluid mechanics. This valve is called the Tesla valve, which is worth mentioning separately.

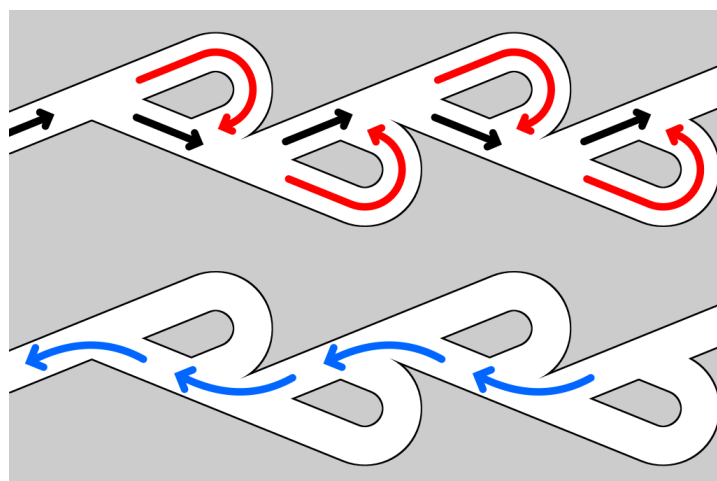


**Figure 4.7:** Principle of operation of a Tesla valve. The upper figure shows flow in the blocking direction: at each stage, part of the fluid is turned around (red) and interferes with the forward flow (black). The lower figure shows flow in the forward direction (blue) [113].

The Tesla valve is a passive check valve that allows fluid to flow in one direction without any moving parts. It was first introduced by Nikola Tesla in 1920 [114], but not until the last few decades it started to be used in pumping/mixing applications and different fields such as analytical chemistry, microelectromechanical systems and biotechnological devices [115]. This valve behaves as a fluidic diode, allowing for preferential forward and reverse flow directions (see Figure 4.7) due to its unique design traits, which impose direction-dependent pressure drops [116]. For our design, in particular, it is of great interest to use its reverse direction, also known as the blocking direction. This valve orientation showed high flow resistance (15 to 40 times higher than the forward direction), which was very convenient for slowing down the fluid flow. This type of passive valve will allow increasing the analysis time of the sensor when sweat flow is elevated. If the flow is not very high, the flow resistance will decrease, allowing sweat to flow easier inside the valve.

Furthermore, the design of the Tesla valve seemed to be easy to replicate except for the small is-

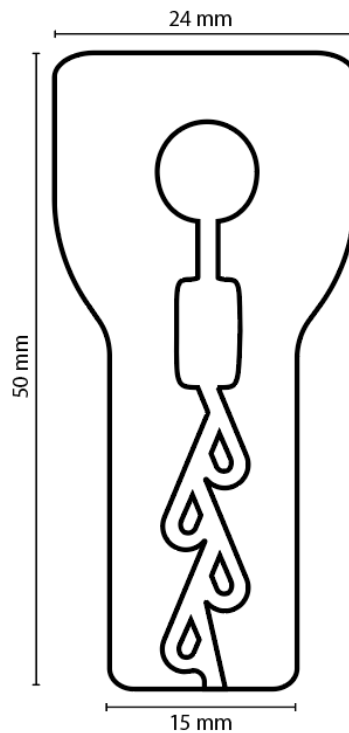


Figure 4.8: Final design for the sweat collector

lands created in the helix region. This independent region could not be cut completely using the laser cutter, as it would become an independent structure from the rest of the system. This issue and how it was solved will be further explained in section 4.2.4

After the Tesla valve, the only left feature to design was the outlet hole. The microchannel was left open at the end, so sweat could be secreted onto the skin once the sensor had analysed it.

After having introduced and explained the three main regions of the sweat collector, the final design can be observed in Figure 4.8. This view corresponds to the middle layer of the collector, being the most complex one and where sweat will be flowing. The design shows the three different features of the collector: inlet hole, analysis area, and outlet area.

#### 4.2.2. Materials and structure

Besides the necessary functionality of the collector, the chosen materials and its structure were vital for its comfortability. The sweat collector had to be as small and straightforward as possible not to discomfort the athlete during the physical exercise period. Therefore, the two main goals were focused on finding a bio-compatible material and determining the simplest structure so sweat could be analysed *in situ*.

In order to find a suitable material, it was looked into literature for the most common ones used. Polydimethylsiloxane (PDMS) is mentioned in many papers as the ideal material for sweat collecting [72, 106]. Other papers use polyethylene terephthalate (PET) as the substrate to create a sweat collection and analysis system [31]. Besides these two materials, Holst Centre also had a significant amount of thermoplastic polyurethane (TPU) available. Thus, this material was also considered, as it is a bio-compatible plastic and used in applications such as the textile industry [117]. In order to choose one of these materials, they were analysed depending on:



- Biocompatibility
- Flexibility
- Availability

All materials showed excellent biocompatibility, and they would not irritate or contaminate the surface of the skin in any way. PET showed lower flexibility properties than the other two materials, and it seemed to be uncomfortable when stuck to the skin. Finally, as PDMS has a time-consuming process to make it, the availability of this material was much lower than for PET and TPU, already available for usage. TPU was therefore used as the material for the collector. These results are summarised in Table 4.1.

MATERIALS	Biocompatibility	Flexibility	Availability
PDMS	++	++	--
PET	++	-	++
TPU	++	+	++

Orange highlighted was used in this study

**Table 4.1:** Analysis of possible materials for the sweat collector

The specific brand used for the thermoplastic polyurethane was DuPont™ Intexar™ TE-11C. As the supplier defines, TPU TE-11C is optimised for high stretch smart clothing applications, such as fitness and health monitoring. The material is a stretchable bilayer, composed of high recovery and a melt adhesive layer. The high recovery layer (100 µm thick) is designed for compatibility with electronic ink printing. The melt adhesive layer (50 µm thick) is used for bonding to fabrics under heat press lamination [118]. For this project, the melt adhesive layer was chosen due to its higher flexibility and easiness to melt and glue to other materials.

The next step was to think and design the structure of the microfluidic system. The main idea was to divide the collector into three layers: top layer (completely sealed), middle layer (for the microfluidic channels) and bottom layer (for the inlet hole). In order to cut the collector into the desire shapes and sizes, the Trotec Speedy 300 was used. This machine uses a CO<sub>2</sub> laser to either cut or engrave different materials such as wood or plastics.

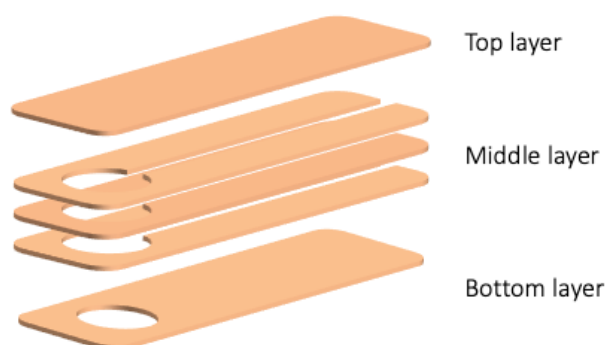


**Figure 4.9:** Sweat collector structure showing the three different TPU layers.

It was observed that TPU had a thickness of just 50 µm, making it too thin to create a microfluidic system inside just two layers. As TPU is a melting adhesive layer, it was first decided to use the Optek vacuum laminator. This machine uses a combination of heat, pressure and an internal roller mechanism to stick different materials together. Initially, three layers of TPU were laminated together to create the middle layer that was afterwards laser cut. The next step was to laser cut the bottom later to create the inlet hole. Finally, all layers were laminated together. However, it was observed in this last lamination step that top and bottom layers stuck together due to the melting process, closing the



inlet hole of the system.

It was looked for new methods to avoid the encapsulation of the system. The next best approach was to glue the different layers of TPU using double sided tape. A few types of commercial glues were available and analyzed for this task:

TAPE	Thickness	Width	Color	Observations
3M 9469PC	0.13 mm	2.54 cm	Transparent	High temperature and solvents compatible
3M 9460PC	0.05 mm	2.54 cm	Transparent	High temperature and solvents compatible
3M 5962 VHB	1.6 mm	12 cm	Black	Extreme conformable acrylic soft foam core and good water seal
3M 300LSE	0.1 mm	A4 size sheets	Transparent	Used in screen protectors
3M 1504	0.11 mm	15 cm	Transparent	Biocompatible

Orange highlighted was used in this study

**Table 4.2:** Analysis of possible double sided tapes

All tapes were tested and glued between two layers of TPU. 3M 5962 VHB was too thick for the collector and hard to work with as it was highly sticky. For 3M 300LSE, the issue was the opposite, being too thin and hard to stick between the two TPU layers. Between 3M 9469PC and 3M 9460PC, the first one seemed like a better option as its thickness allowed to better work with it. The biocompatible tape 3M 1504 was also a great possibility double-sided tape, and as it is already being used in medical applications [119], it was chosen as the double-sided tape for sticking the collector onto the skin.

The initial idea was to use this tape for glueing the top layer with the middle layer. However, due to malfunctioning issues in the Optek vacuum laminator, the lamination of TPU layers was not available anymore. Thus, building the collector's middle layer was rearranged using the 3M tape instead of the laminator. Firstly, two layers of TPU were stuck together using 3M 9469PC. Two additional layers of glue sheets were attached to each side. These layers were then laser cut into the middle layer shape of the collector. Finally, two TPU layers (one bottom and one top) were glued onto each side of the collector to have a sealed system, as shown in Figure 4.10. This method was much more accessible and time-efficient, so it is recommended for future research.

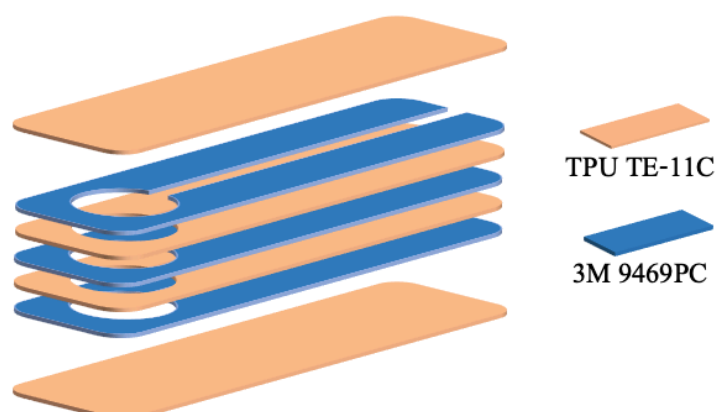


**Figure 4.10:** Schematic of the different layers of TPU and double sided tape.

As it is observed in Figure 4.10, there is no inlet hole in the collector. The idea was first to analyse the hydrophobicity of TPU. If this physical property was too high, there was a chance sweat was unable to flow inside the microfluidic channels. The following subsection will analyse this characteristic using surface treatment.

### 4.2.3. Surface treatment of TPU

In order to study the hydrophobicity of TPU, it was also looked into the possibility of surface treating the TPU bottom layer. This treatment could allow for sweat to be easily collected from the skin due to the negative capillary pressure created [106]. Thus, a few layers of TPU were collected, and surface treated thanks to the facilities provided at Holst Centre.

Surface treatment allows changing the wettability of the material, in this case, TPU. The wettability of a material depends primarily on its surface energy, also referred to as surface tension. This parameter is directly linked to how well a liquid can wet the material, monitored by measuring the contact angle between a liquid and the material's surface. By surface treating TPU, we can increase the material's surface energy, allowing to decrease the contact angle between sweat and TPU (making it more hydrophilic). There are also different surface treatments, but the most used ones are corona and plasma treatment. In this case, plasma treatment was available with different gases, being the most used ones oxygen and nitrogen treatment. In addition to these two types of plasma treatment, TPU was also treated with UV light to have more methods that could be later analysed and compared. Once all TPU sheets were treated with the different techniques available ( $O_2$  treatment,  $N_2$  treatment and UV light), they were laser cut into the bottom layer shape of the collector and sealed using 3M 9469PC tape.

The sweat flow was analysed via video, whose results can be observed in section 4.3. Results came to show that capillary pressure could be strong enough for sweat to go inside the TPU collector without the necessity of surface treatment. Thus, the next step was to reproduce the sweat collector's final design using the previously tested structure.

### 4.2.4. Production steps

This final section will focus on the production steps followed for building the sweat collector. The process aimed to combine the functionality and comfortability achieved with the design and structure of the collector, respectively.

The initial structure consisted of two layers of TPU stuck together using 3M 9469PC double-sided tape. Another layer of tape was added on both top and bottom with the release liner still on. This five-layer structure was the middle layer of the collector, where the microfluidic channels would be created.

The idea was to laser cut the TPU structure using the final design shown in Figure 4.8. However, as previously mentioned, the Tesla valve had independent regions in its design that could not be laser cut as they would get loose. These regions are necessary for the correct function of the valve, dividing the fluid into two directions and interfering with each other to slow down the flow. The final solution consisted of engraving the surface of the structure instead of cutting it. This subtractive manufacturing process allows changing the surface of the object using a laser beam without cutting it. Engraving is a fast method as the material is removed with each pulse of the laser. The depth is dependant on the speed and power of the pulse, as well as the number of times the laser beam is passing on the material [120].

Once the middle layer was engraved with the desired design, the top and bottom layers needed to be attached. Top layer could be immediately glued to the middle layer as no further laser cutting was needed. In the case of the bottom layer, the inlet hole was made using the laser cutter again before attaching it to the middle layer. The process was simple, cutting a circle of 4 mm in radius in the specific spot. Afterwards, this layer could also be glued to the middle layer by detaching the release liner of the

double-sided tape. Even though this glueing process could be performed by hand, the exact placement of the different layers could be achieved using an alignment sheet.

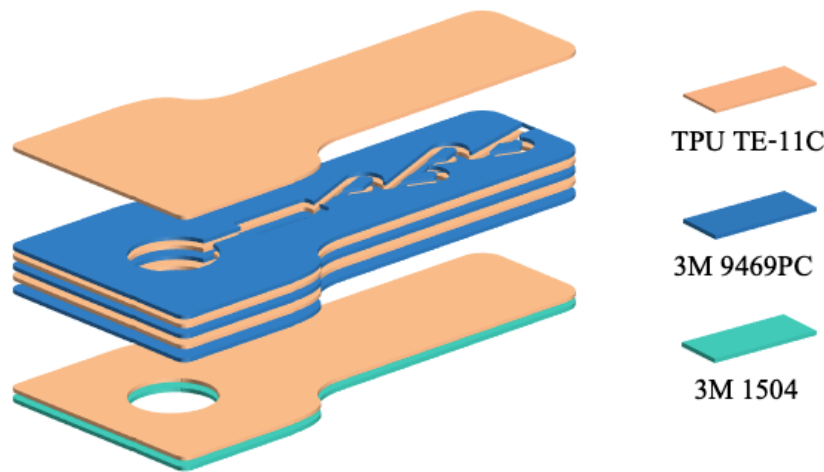


**Figure 4.11:** *Final design and structure of the sweat collector*

The steps completed until this point allowed to test the microchannels of the sweat collector by manually inserting artificial sweat using a needle. However, there was one last step in order to stick the sweat collector onto the skin. For this purpose, a new type of biocompatible double-sided tape was needed to avoid skin irritation. As shown in Table 4.2, 3M 1504 is a thin, transparent and biocompatible double-sided tape that fitted perfectly for this purpose. A new laser cutting process was needed, producing the exact width of the inlet hole through which sweat would be wicked inside the microchannels. The final design and structure of the sweat collector can be observed in Figure 4.11.

This last step meant the end of the sweat collector's production, and it was ready for the validation process.

## 4.3. Collector validation

The objective of validating the sweat collector was to ensure that sweat was going inside the microchannels and flowing into the analysis area. Afterwards, sweat should also be able to exit through the outlet hole. In this section, the experimental setup to validate the collector is explained. Afterwards, the results obtained will be shown using figures.

### 4.3.1. Experimental set up

The validation of the sweat collector followed different experimental tests. Even if TPU is slightly transparent, it is almost impossible to see if sweat was flowing inside the collector due to its transparency. Thus, it was necessary to develop a simple mechanism to see sweat flow inside the collector. A simple method observed in literature used coloured demineralised water to visually check when sweat entered the collector [72]. Throughout the validation of the sweat collector, this method will be used.

Some initial tests were performed to check the hydrophobic behaviour of TPU using artificial sweat. This artificial sweat was a solution with distilled water and sodium chloride (common salt), as it is the main constituent in sweat (see Table 2.1). In order to observe the behaviour of artificial sweat inside

the collector, it was added blue colourant to the liquid. The liquid was inserted inside the microfluidic system using a syringe and a small needle. In order to measure the sweat flow inside the microchannels, video analysis was used. The time ( $t$ ) it took the artificial sweat to get from one mark line to the next one was calculated as the entire process was recorded.

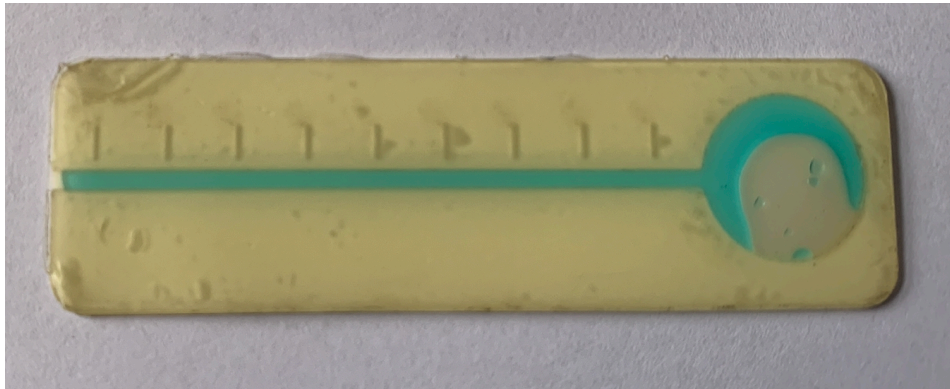


**Figure 4.12:** Sweat collector using double-sided tape without an inlet hole. Dye artificial sweat can be observed flowing inside the microchannel.

First of all, it was tested that the collector allowed sweat flow through its microfluidic channel. In order to do so, a few droplets of artificial sweat with a blue colourant (to easily see it) were injected into the initial chamber using a syringe and a needle. This initial test was a success, observing how sweat was able to flow through the microchannel.

In order to compare the sweat flow between the different collectors, all other variables influencing the test needed to be fixed. The volume inserted in the initial chamber had to be fixed to a particular value and have as little influence as possible on the inside pressure. Thus, a micropipette with  $10 \mu\text{l}$  was used to insert the coloured artificial sweat. The collector was also tilted to an angle of around  $45^\circ$  so gravity could help artificial sweat flow through the microchannel with the same pressure. The proper calculation of flow rate ( $Q$ ) can be seen in Equation (4.3). Where  $V$  is the volume of the microchannel, composed of the surface area  $A$  of the microchannel (integrated into its height  $h$  and width  $w$ ) and the distance  $d$  from one mark line to the next one. Time  $t$  is the time it took for the sweat to cover such a distance (see Figure 4.13 for better understanding).

$$Q = V \cdot t = A \cdot d \cdot t = h \cdot w \cdot d \cdot t \quad (4.3)$$

Once the setup for the experiment was well thought and prepared, tests of the sweat collectors took place. Four different collectors were analysed: non-treated TPU, TPU with  $\text{O}_2$  plasma treatment, TPU with  $\text{N}_2$  plasma treatment and TPU with UV light treatment. Sweat flow was analysed by recording the different tests. Thanks to the trim lines along the microchannel, the flow was calculated using video analysis.

In order to test the final design of the sweat collector, a small test was performed attaching the collector to the skin using biocompatible tape (3M 1504). Its usage during physical activity could give the necessary feedback to check if sweat was flowing inside the microchannels or not. Once again, coloured artificial sweat was introduced in the microchannels of the sweat collector. Once it was filled with this blue substance, the sweat collector was attached to the forehead. The exercise was performed under high humidity conditions and elevated temperatures. Results can be observed in Figure 4.15.

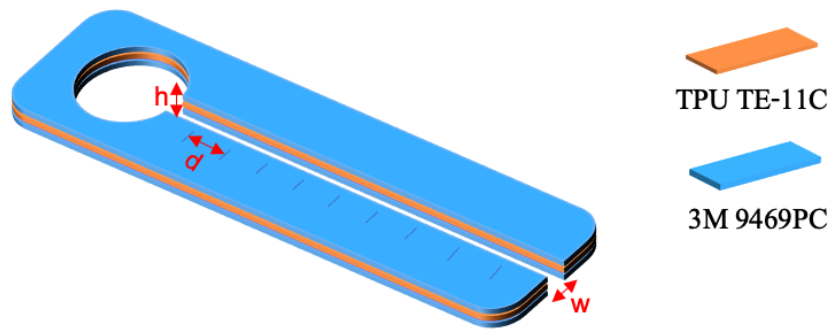


Figure 4.13: Explanatory drawing of the different dimensions of the microchannel in the sweat collector.

### 4.3.2. Results

The results obtained from the experimental tests performed for the sweat collector are presented.

Figure 4.14 shows the sweat flow of the four different collectors. It can be observed that initial sweat flow for non-treated TPU is the highest of all samples. The initial sweat flow for  $O_2$  plasma-treated TPU is also higher than usual. However, artificial sweat flow for all collectors stabilises after a few seconds once the microfluidic channel is wet.

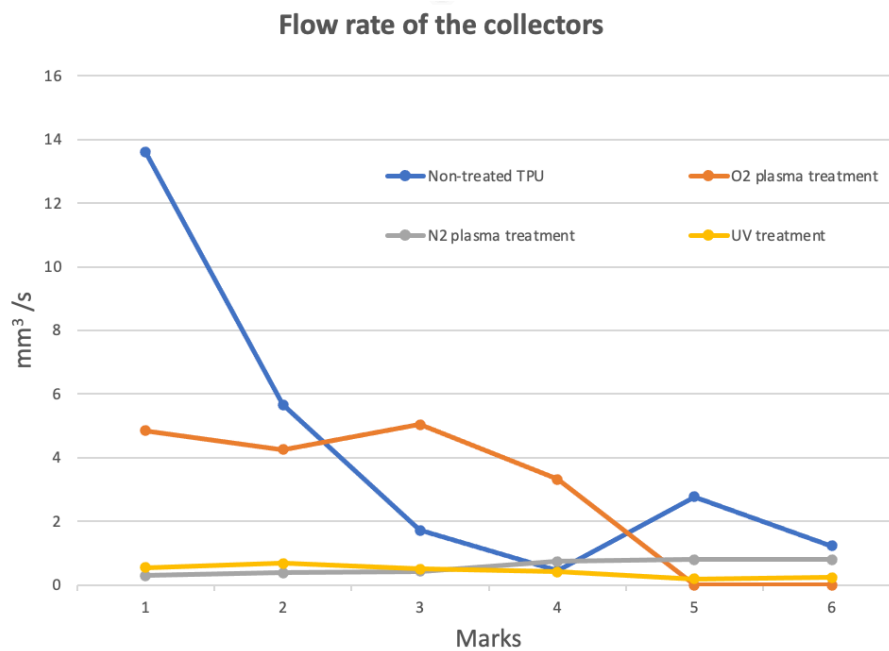


Figure 4.14: Sweat flow rate of the four different collectors.

As observed from Figure 4.15, sweat starts entering the microchannels after 10 minutes of exercise. Dye blue artificial sweat progressively exits the collector through the outlet hole until almost none is left after 30 minutes of physical activity. In the helix regions of the Tesla valves, some artificial dye sweat remained longer than in other regions, but it disappeared eventually.

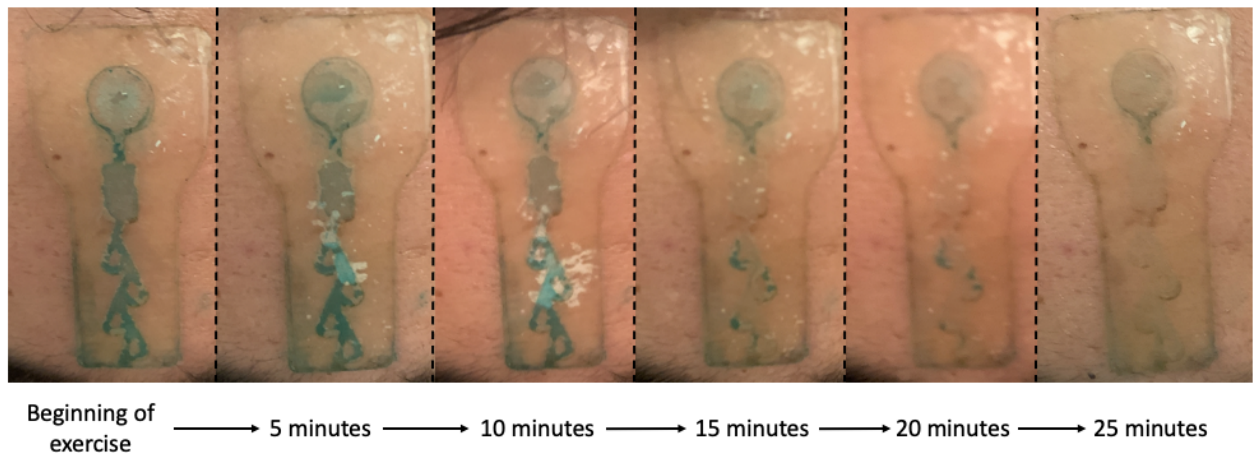


Figure 4.15: Sequential images showing the sweat flow inside the collector during a 30 minute exercise.

## 4.4. Discussion

The hydrophobicity of the TPU collector was first tested. From the results observed in Figure 4.14, some conclusions were derived. Initial flow for the non-treated TPU is opposite to the expected one, as surface treated samples have higher surface energy and thus are more hydrophilic. The reason behind these results is assumed to be related to the sensitivity of the inside pressure. It was observed from the videos taken that any movement of the needle during the insertion of artificial sweat inside the chamber triggered a fast flow of artificial sweat in the microfluidic channel. However, artificial sweat flow from all treated and non-treated TPU stabilises after a few seconds. Thus, surface treatment does not seem suitable, as no significant changes in flow are observed. In addition, surface treatment only lasts for a few days or weeks, a significant disadvantage when trying to obtain a long-lasting sweat collector.

Regarding the final design of the sweat collector, the physiological test showed positive results. Sweat can enter the microchannels of the device and exit it through the outlet hole. The helix regions of the Tesla valve showed to have some resistance to sweat flow. The concave shape of the region, in addition to its vertical position, contributes to an irregular sweat flow. Even though this fact should not slow down sweat flow, a less concave shape on its shape could benefit a more regular flow in the microchannel. In addition, the attachment of the collector to the skin was firm throughout the entire exercise, so it can be concluded that the double-sided tape is strong enough and does not wet during the perspiration process. In addition, its biocompatibility was also tested successfully, as no skin irritation was observed during or after the exercise period.



# 5

## Sweat analysis system

This chapter will be focused on the building and testing of the sweat analysis system. The final system is formed of three components: collector, sensor and read-out circuit. Section 5.1 will focus on the design and production process of the sweat analysis system. This complete integration of the three components aimed to be tested first in the laboratory, to then carry physiological experiments. Finally, the results obtained and a brief discussion will be exposed in section 5.2 and 5.3, respectively.

### 5.1. System integration

The integration of the sweat collector and sensor aims for the analysis of sweat on people. Thus, this sweat analysis patch production had to look for high comfort and provide wearability to the subject. This integration had to maintain the characteristics achieved for the collector and sensor shown in the previous chapters. In addition, this patch had to bear in mind its connection to the read-out circuit. As previously mentioned, this read-out circuit was developed by T. Bakker on his thesis project, and it will be used for this project as well [56]. Thus, this circuit will be briefly explained, and its working principle presented.

#### 5.1.1. Read-out circuit

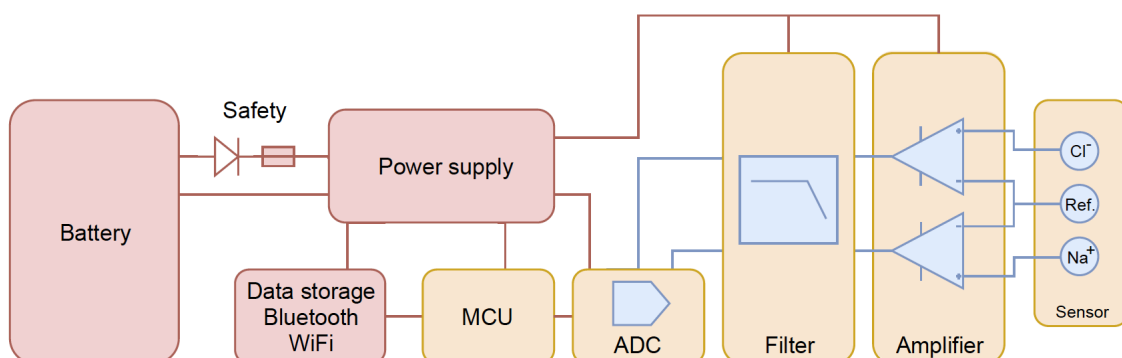


Figure 5.1: Read-out circuit application overview [56]



The read-out circuit is a crucial part of the sensor system since it directly determines the accuracy of the sensor reading, the interference, and the signal-to-noise ratio. This circuit aims to measure a voltage difference between the sensor's reference electrode and the ion-selective electrodes. However, this signal is relatively low, so an amplifier is needed in the circuit. In order to stabilize the output of these sensors, a low pass filter is added to the circuit. In addition to these requirements, an analog-digital converter (ADC) and a microcontroller (MCU) are necessary for the circuit to work correctly. Figure 5.1 shows the components previously defined. The battery, power supply and data storage were not a priority in the study, so there was no focus on these components.

The first idea was to create a single-channel circuit that would only be able to read the signal of a single sensor. However, in order to acquire signals from several sensors, a multi-channel circuit was developed. This read-out is more time-efficient and allows for the comparison between the sensors, as the environmental conditions will be the same for all of them. In addition to the components previously defined, it was decided to use a multiplexer to connect multiple sensors to one instrumentation amplifier. An overview of the hardware used for the final read-out circuit is observed in Figure 5.2.

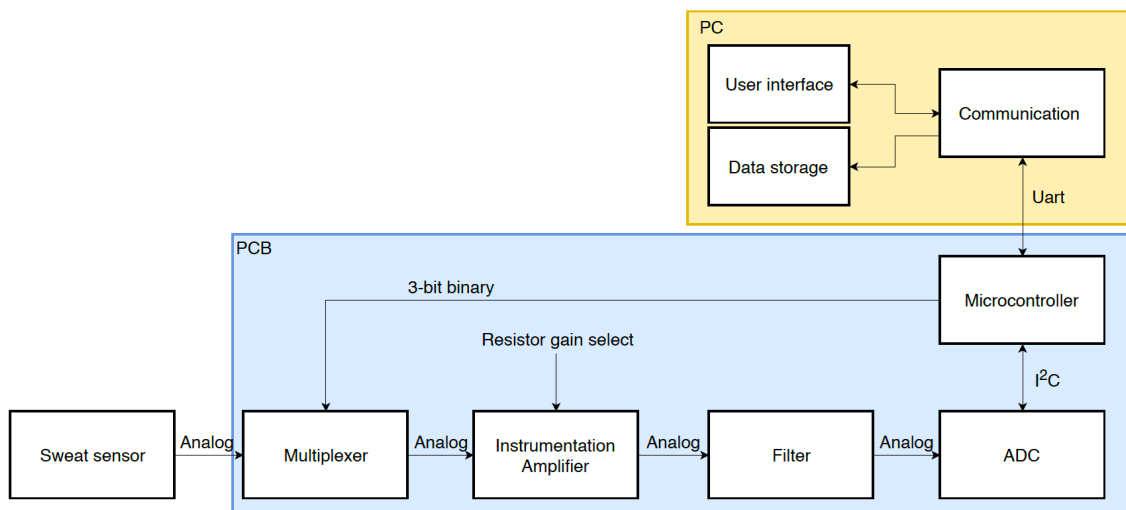


Figure 5.2: Hardware abstraction layer (HAL) of the read-out circuit developed by T. Bakker [56]

This read-out circuit can collect potential differences from four sensors. Tests using this multi-channel circuit were able to collect 20 samples from each sensor were collected every second. These characteristics resulted in a sampling frequency of 160 Hz and a settling time of 125 ms.

Once the read-out circuit was presented and its working principles understood, the first step was focused on the design and structure of the sweat analysis system. The next task involved the production steps necessary to build the device.

### 5.1.2. Design and structure

The design for this integration aimed to create a single patch gathering the sweat sensor and collector. The usage of TPU and double-sided tape for the collector seemed the best option to seal this patch. This slightly bigger patch would still collect and let sweat flow inside the microchannels of the collector. The main task was to attach the sensor to the collector to place the electrodes inside the analysis area. Using strong double-sided tape (3M 9469PC), these two components seemed to have great chances

of working together for the same goal.

As observed in Figure 5.3, the sweat collector's design has been slightly modified for the integration with the sensor. The only difference is the reduction of the area around the inlet hole. This previous characteristic aimed to increase the sweat rate due to compensatory effects when sweat glands were covered [109, 110]. However, adding a more significant TPU layer to integrate the sweat sensor increases this covered surface area, so the sweat collector layers of TPU around the inlet hole were reduced in size.

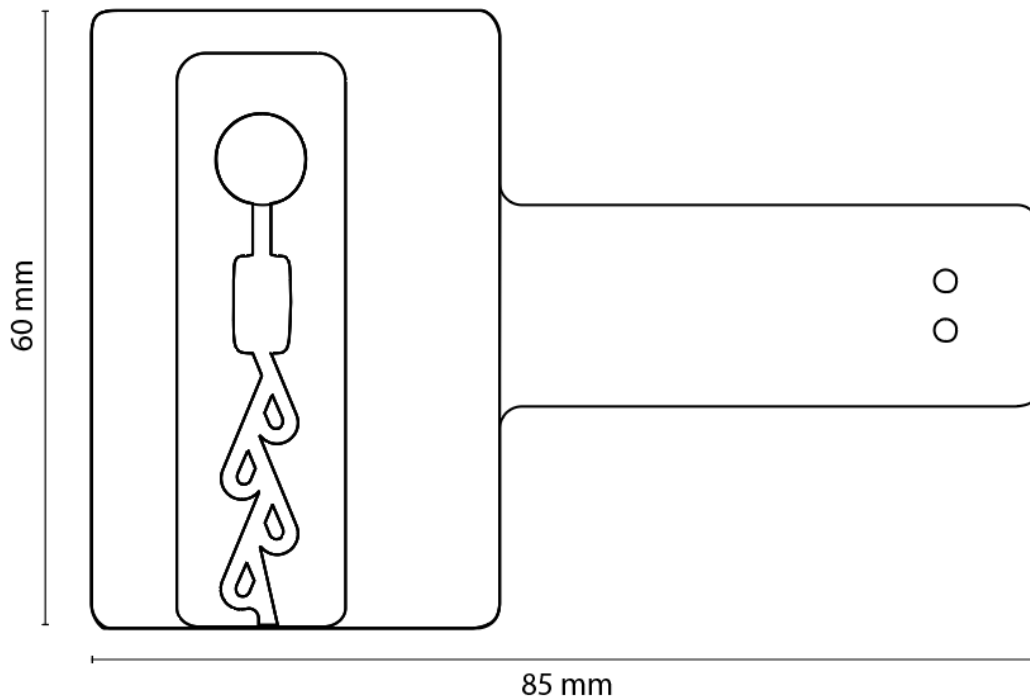


**Figure 5.3:** Final design for the sweat patch

As already mentioned, the design of this sweat patch also aimed for its connection to the read-out circuit. The sweat sensor has three silver paths for the conductive layer. These layers are covered with carbon ink to assure there is no severe deterioration when the sensor is connected to the FFC connector multiple times (see Figure 3.10). This connector then transfers the potential differences obtained at the electrodes to the read-out circuit through insulated wires. In order to make sure the FFC connector did not detach from the sensor during the exercise period, some attachment between the wires and the patch needed to be included in the system.

Figure 5.3 shows the addition of a long stripe of TPU under the carbon connectors of the sensor. In this area, the FFC connector will be attached with the wires heading to the read-out circuit. The two small holes observed on the right side are laser cut to attach the wires to the TPU layer. If the wires were pulled during the exercise period, this tight attachment will exert force on the patch and not the FFC connector, avoiding its detachment. The firm attachment of the patch to the skin by using biocompatible double-sided tape should not detach if some force is exerted on it.

Regarding the structure for the sweat patch, the idea was very similar to the sweat collector's structure. The patch was made out of TPU layers and double-sided tape attached together. Special attention was taken to the analysis area of the collector, as the attachment of the sweat sensor takes place there. To avoid any sweat coming out from this area, tape is used on both sides of the patch. In order to have better withstand the possible forces of the wiring, the bottom patch of TPU is kept with its release liner, with a higher thickness. The same biocompatible tape (3M 1504) attaches the sweat patch to the skin.

The final design and structure of the sweat patch can be observed in Figure 5.4

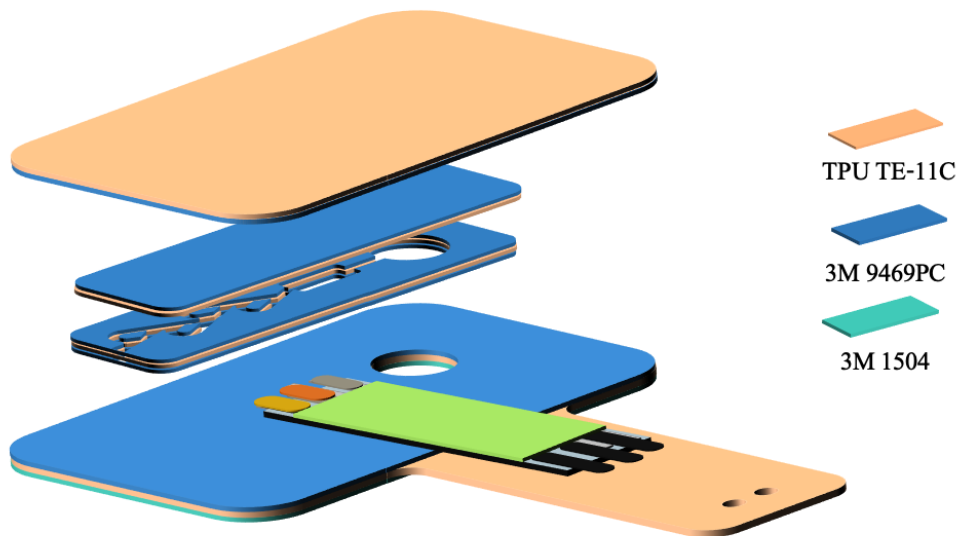


**Figure 5.4:** Final structure for the sweat patch. The sweat sensor is integrated within the collector

### 5.1.3. Production steps

The production steps of the sweat analysis system are very similar to those performed for the sweat collector, using the laser cutter throughout the process. It began by sticking two layers of TPU using 3M 9469PC double-sided tape. Another layer of tape was added on both top and bottom with the release liner still on. This structure was then engraved to form the middle layer of the collector. In this step came the addition of the sensor to the sweat collector. By taking off the release liner of the tape, the sensor could be fixed to the middle layer of the sweat collector. The electrodes were placed just on top of the analysis area so that sweat would flow over them.

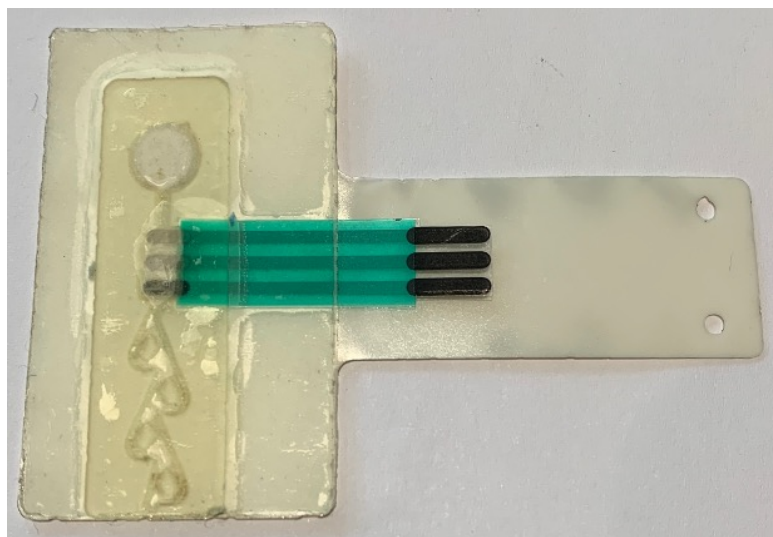


**Figure 5.5:** Sweat patch system. Sweat sensor and collector integrated together.

The top and bottom patches of TPU were used to seal the middle layer of the collector and the

sensor already attached. The top layer of the patch is completely flat, whereas the bottom layer, the inlet hole is laser cut to let sweat flow inside the microchannels. As already mentioned, the bottom TPU patch is kept with the release liner to strengthen this layer. Two small holes are laser cut in this layer to attach the wiring to it. Finally, two additional layers of 3M 9469PC double-sided tape were added to both top and bottom layers to assure no sweat could come out of the analysis area. The produced sweat patch can be observed in Figure 5.5.

## 5.2. Sweat analysis system validation

The validation of the sweat analysis system was divided into two sections. The first one was performed in the lab and aimed to check the correct function of the system using a syringe pump. The second validation experiment was the physiological testing of the system during physical activity.

However, before these experiments were performed, a small test to check the stability and sensitivity of the sensor was carried. This test showed how the sensor was not showing any voltage changes to different ionic concentrations. Three months went by since the last testing of the sensor due to the focus on the sweat collector. Looking into literature for the characteristics of the membranes [85], it was observed how the stability of the sodium membrane strongly decreased within a few weeks (see Figure 5.6A). The long period since the membranes were placed on the electrodes suggested the low stability shown on the sensors.

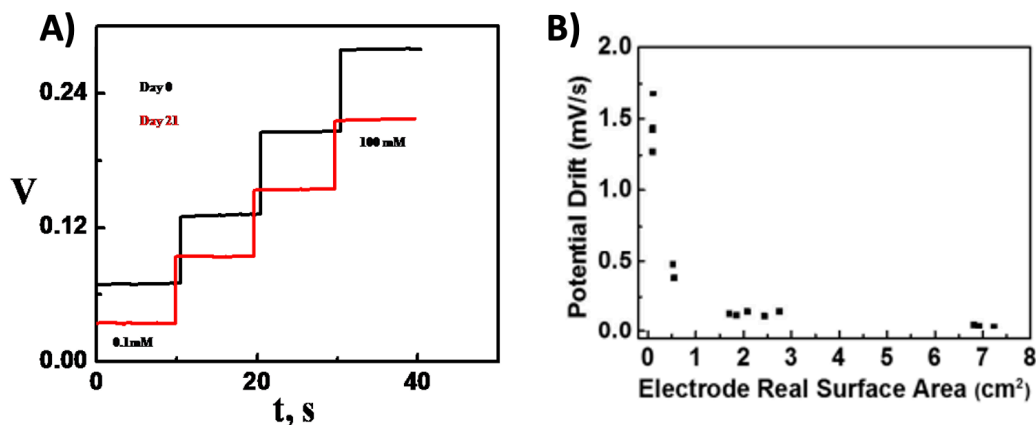


**Figure 5.6:** A) Response of the sodium membrane in a long-term stability test [85]. B) Potential stability dependency on the electrode's surface [76].

However, another factor that is important for the sensor's long-term stability is the surface of the membranes. As shown in Figure 5.6B, the higher the surface of the electrode, the higher stability. This characteristic suggested trying the sensors designed by T. Bakker, which were also screen-printed and the membranes placed on the electrodes. The results obtained showed stability for the sodium sensor. The voltages differences had been slightly reduced compared to the initial measurements done three months prior, but accurate results were still obtained. Thus, this sensor still allowed to keep working with the sweat analysis system.

As the calibration curve was developed a few months prior to the physiological testing of the sensor, a new calibration seemed necessary. Figure 5.7 shows the obtained calibration curve for the sweat sensor, which shared very similar values to the calibration curve of the sensor with smaller electrodes. Error bars are shown but are very small. Bigger differences were observed at 30 *mmol/L* (standard deviation of 3.5%) and 90 *mmol/L* (standard deviation of 2%). This fitting curve shows a saturation of the sensor for high concentrations of sodium.

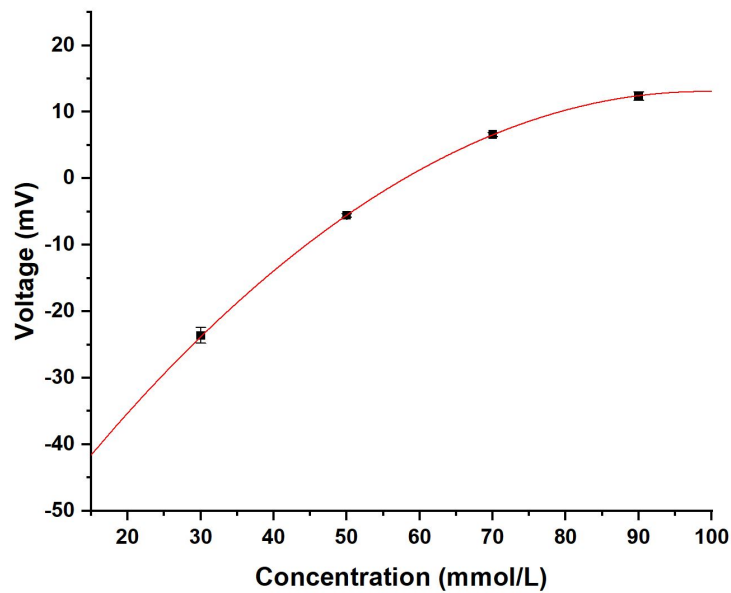


Figure 5.7: Calibration curve for the Na sensor with larger electrodes.

These modifications allowed to continue with the laboratory and physiological experiments using the sweat analysis system.

### 5.2.1. Syringe pump experiment

As previously explained, the validation of the sweat analysis system was first checked with a few lab experiment. This experiment aimed to check if the sweat analysis system could accurately measure artificial sweat concentrations using different flow rates. The experiment had two characteristics that wanted to be tested for the system:

- Stability using different sweat rates
- Sensitivity to different artificial sweat concentrations

To perform this experiment, a syringe pump was used to set different sweat rates. This pump was connected to a syringe inserted inside the sweat patch through the inlet hole. The patch was connected to the read-out system using an FFC connector.

The first objective of this test aimed to test the system's stability to different flow rates using the same salt concentration. In order to test the passive valves, sweat flow in the microchannels during high-intensity exercise period was estimated. As previously calculated using Equation (4.1), normal sweat rates could achieve  $0.04 \mu\text{L}/\text{min}$  per gland. However, higher sweat rates can occur due to compensatory effects [109, 110]. With sweat rates up to  $0.6 \mu\text{L}/\text{min}$  per gland, total sweat rate inside the collector could reach values close to  $30 \mu\text{L}/\text{min}$ . Thus, the syringe pump was initially set to  $10 \mu\text{L}/\text{min}$ . After five minutes, the flow rate was increased to  $20 \mu\text{L}/\text{min}$ , finally increasing it to  $30 \mu\text{L}/\text{min}$  on the last five minutes of the experiment. The artificial sweat concentration remained constant at  $30 \text{ mmol}/\text{L}$ .

As observed in Figure 5.8, the potential remains almost constant when the artificial sweat rate is increased. The system takes a few minutes to start analyzing the artificial sweat, as it has to travel a few millimetres until the substance covers all electrodes.

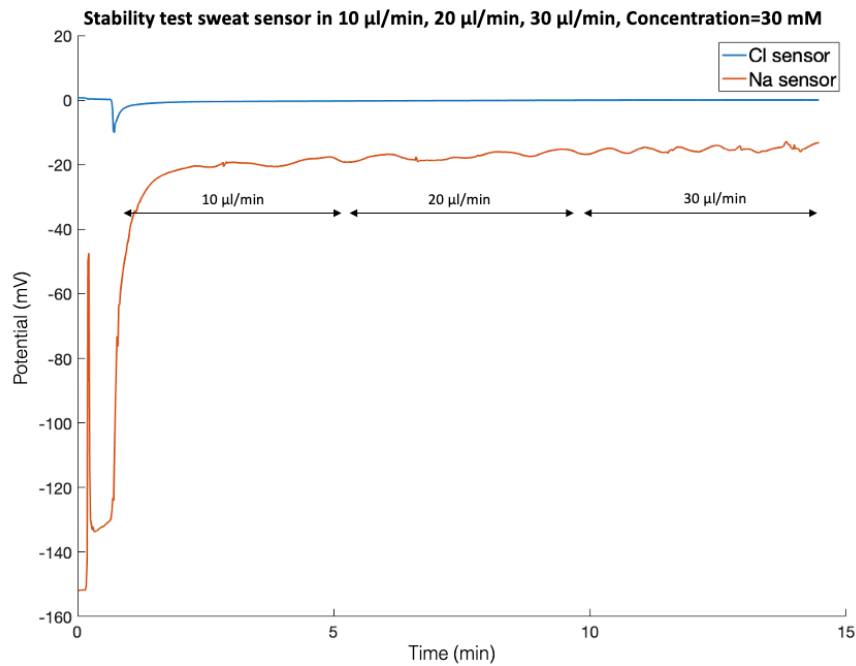


**Figure 5.8:** Stability test sweat sensor in 10  $\mu\text{l}/\text{min}$ , 20  $\mu\text{l}/\text{min}$ , 30  $\mu\text{l}/\text{min}$ , Concentration=30mM

The next test aimed to study the system's sensitivity when different artificial sweat concentrations were introduced in the collector at a constant sweat rate. In this procedure, syringes were changed to introduce a new artificial sweat concentration into the system. Results can be observed in Figure 5.9.

In this test, there is also a tiny period until the voltage stabilizes at 20  $\text{mmol}/\text{L}$ . When the sensor first analyzes a different sweat concentration, there is a slight peak observed for both 50 and 90  $\text{mmol}/\text{L}$ . However, it soon starts to stabilize at its corresponding voltage. It then remains almost constant for the rest of the experiment, with slight variations in voltage of  $\pm 3 \text{ mV}$ . Chloride sensor was tested one more time, showing initial sensitivity when concentration values are changed. However, voltage drops back to zero immediately afterwards.

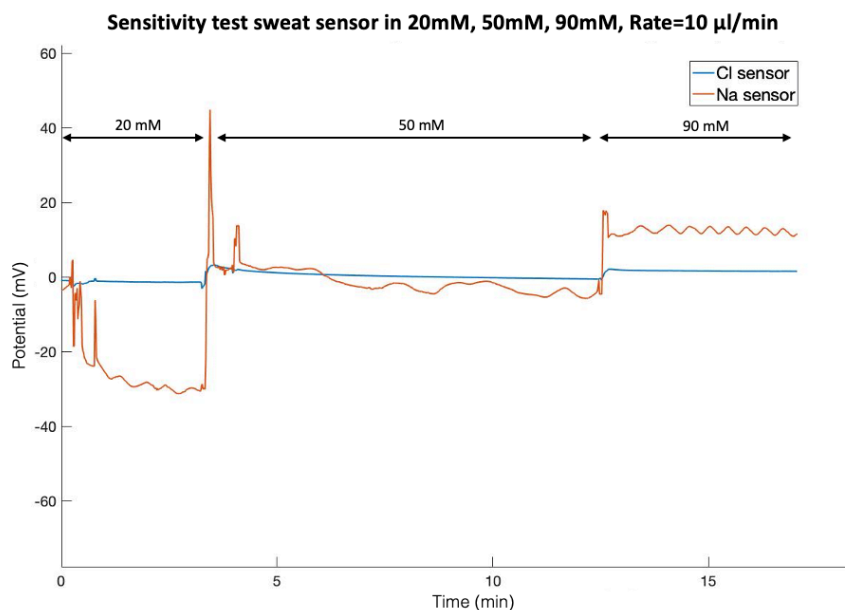


**Figure 5.9:** Sensitivity test sweat sensor in 20mM, 50mM, 90mM, Rate=10  $\mu\text{l}/\text{min}$

In addition to the first sensitivity test, a second experiment was performed to test the sensitivity of the sensor as well as the capacity of the read-out circuit to work with several sensors at the same time. This experiment would test the sensitivity of the sensor for changes in sweat concentration from a low one to high concentration, to then lower it again. This test would allow to show if big differences are observed when the sensor keeps reading changes in sweat concentration. Moreover, working with three sensors at the same time was a first test before performing the physiological experiments. Results from this sensor validation test are observed in Figure 5.10.

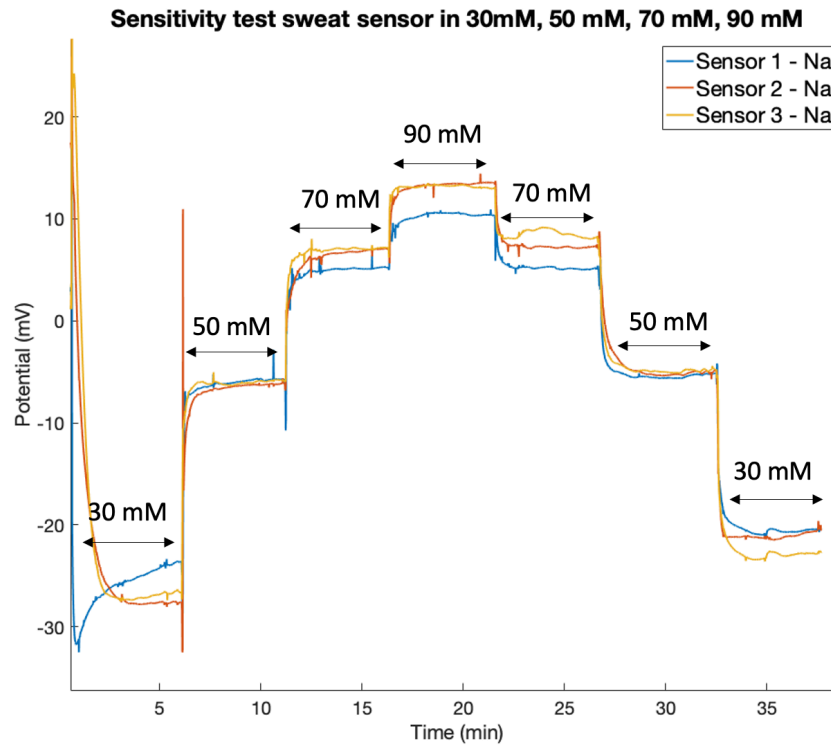


Figure 5.10: Sensitivity test sweat sensor from 30mM to 90mM and back to 30mM

Concentration levels showed almost identical results for all sensors in the 50 mmol/L and 70 mmol/L level. High concentrations (90 mmol/L) and low concentrations (30 mmol/L) show higher differences in potential. The lowest concentration point also shows bigger differences between the first stage of measurement and the second one (SD of 4.1 mV).

### 5.2.2. Physiological experiment

The final testing of the sweat analysis system was performed on humans. This test aimed to check if the positive results obtained for the system in the lab also continued when testing it with real sweat. When testing a new device with humans, the research has to be approved by an Ethics Committee. To do so, this device was included under A. Steijlen's ethics proposal, approved in 2020 under the name: *Sensor technology for unobtrusive athlete monitoring*. In addition, a new device report and a consent form were needed for these physiological experiments.

This physiological experiment also aimed to test the same two characteristics of the system as with the syringe pump experiment:

- Stability of the sensor in a 45-minute physical activity
- Sensitivity through out the exercise

These two characteristics are vital for the correct and accurate analysis of sweat during physical activity. The system will be capable of monitoring the ionic concentration of sweat with precision during long periods of activity. In order to test the system, it was decided to have humans sweating during a high intensity exercise period on a cycling ergometer. During the activity, subjects were not able to ingest any food or water. The physical exercise was divided into three phases:

1. **Warming up phase** - 5 minutes
2. **High intensity physical exercise** - 35 minutes
3. **Cooling down phase** - 5 minutes

It was decided to place three sweat patches for more reliable results, all connected to the read-out circuit. Copper tape was added to the sensors in order to shield them during the physiological experiment, and the grounding of the wires was connected to this tape. The patches were placed on the back due to its high sweating rate and high surface area for patch placement. In addition, absorbent patches were also placed on the back of the subject using a technique observed in literature [121]. Three patches were replaced during the exercise (15, 25 and 35 minutes after exercise begins), to have references of exact sweat concentration during the exercise. The patches would be analyzed later on using the ion chromatography (IC) technique. Finally, sweat rate is recorder using two capsules developed by A. Steijlen.

This final experiment aimed to test the efficiency of the sensor for measuring real sweat during physical activity in real-time. As the acquisition of large data for statistical studies was not needed only three subject were involved in this study. Figure 5.11 shows the sweat system output signal for one of the subjects. The signal of all sensors contained noise which did not allow to analyze the data. A low pass filter with a cut-off frequency of 50 Hz was applied to the signal to get rid of this noise. IC results are compared against sensor 2 due to their mirrored placement on the back (see Appendix C).

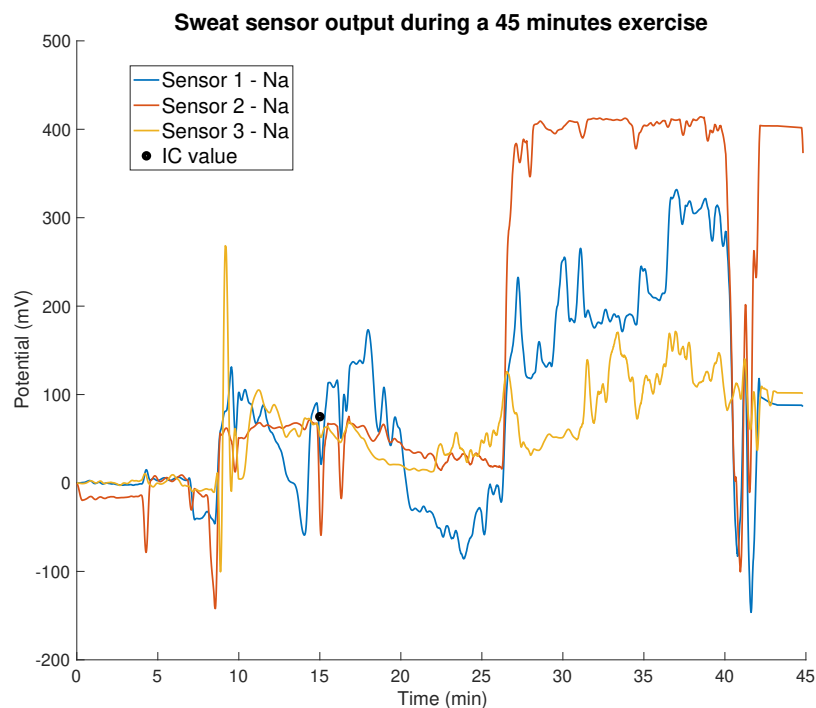


Figure 5.11: Sweat system output signals for the three sensors in a 45 minutes exercise period



From Figure 5.11 several remarks can be made. During the first minutes of exercise, there is still no sweat inside the system, so no changes in voltage are observed. Around minute 8, the voltage from all sensors shows a change in potential due to the introduction of sweat in the analysis area. These first seconds show big changes in potential when sweat concentration abruptly changes. From this point until minute 25, sweat concentration shows small variations in potential difference (in the 60-100  $mmol/L$  region). These readings are very close to the measured sodium concentration in the 15-minute point using ion chromatography (113  $mmol/L$ ). Unfortunately, sweat patches for the other two time periods did not absorb sweat. After minute 25, all sensors showed noise (filtered in the figure), which affected especially the values on sensors one and two, raising to very high and low potential values. The last 5 minutes of exercise (cooling down phase) shows a decrease in sweat concentration for all sensors, despite being affected by noise. Results for the other two subjects and sweat rate measurements can be observed in Appendix A.

Testing of the sweat analysis patch in the laboratory showed that the origin of the noise was coming from the shielding of the sensors. As soon as the grounding established contact with the copper tape, the same noise was appreciated in the data.

A second and last physiological experiment was performed disregarding the shielding of the sensors and leaving the grounding open. For this experiment, only sweat in one subject was tested. Also, due to time constraints, there was no possibility to compare the results with ion chromatography measurements. Nevertheless, the results obtained showed some more positive results. Even though some external noise is still visible (see Figure 5.12), the data obtained was in the same voltage range as for artificial sweat tested in the laboratory (-30 to 20  $mV$ ). Sensor 1 does show unstable voltage after minute 30.

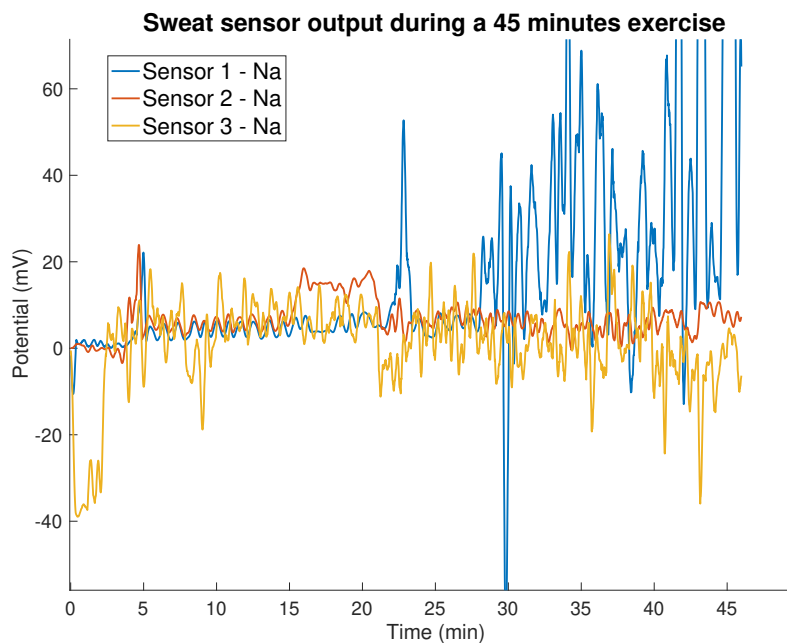


**Figure 5.12:** Sweat system output for all sensors in a 45 minutes exercise period with no shielding of the sensors

Figure 5.13 shows the potential obtained for one of the sensors. Again, initial voltage remains at zero in the beginning of the exercise. As soon as some sweat reaches the membranes (5 minutes after exercising period starts), a change in voltage is shown, which needs a few seconds before stabilizing. Afterwards, the voltage range remains between 5 and 15  $mV$ , an equivalent of 70 to 90  $mmol/L$  of sodium concentration. An alteration of  $\pm 3 mV$  through the entire period of exercise is also observed. There is also a big change in voltage between minutes 15 and 20.

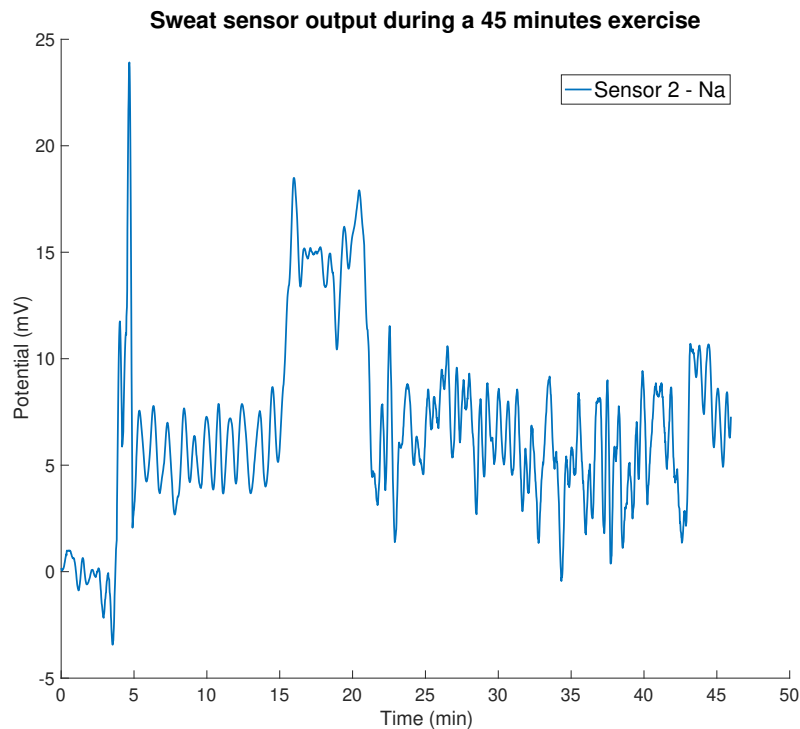


Figure 5.13: Sweat system output signal for sensor 2

## 5.3. Discussion

The first issue observed during these experimental tests concerns the long-stability of the membranes. There is a maximum period for which membranes can still be effective. That period was reached for the new version of the sensor due to the small size of the electrodes. In addition, not having the insulation layer surrounding the electrodes made the membranes' thickness also decrease. As previously mentioned, when drop-casting the membranes on the new version of the sensor, some of the solution spread through the surrounding PET. This fact made the membranes to be thinner. However, a high electrode's surface and membrane thickness was obtained for the older version of the sensor (made by T. Bakker). These characteristics made the sensors remain highly stable even after one hundred days since membranes were placed.

Using the new design for the sweat sensing patch, the stability and selectivity of the system were first tested in the laboratory. The use of the syringe pump showed how the sensor measures a constant sodium concentration even when the flow rate highly increases. This result showed that the sweat analysis system should remain stable and not be influenced by changes in sweating rate when tested on humans during physical activity. The same evaluation was done for changes in sweat concentration. Results showed a positive sensitivity of the sensor to changes in sodium concentration. There is a short period needed by the sensor when concentration quickly changes. The peaks observed after these changes in Figure 5.9 are probably related to the abrupt change from one concentration to the other one. However, these significant changes in concentration are much more constant in human sweat, so the sensor should measure these differences without showing abrupt potential changes.

The physiological experiments carried out showed some positive results. Changes in potential when sweat enters the analysis area of the microchannels and wets the electrodes shows the effective working of the collector. The similar reading between the sweat sensing system and the ion chromatography machine suggests a positive performance of the system. The unusual voltages and noise altered the reading of the sensors in the first physiological tests. This behaviour can be related to the shielding

---

of the sensor, a new addition to the patch for the physiological experiments which was not used in the laboratory experiments. The second physiological test showed voltages very close to usual sweat sodium concentration during exercise. The non-shielding of the sensors can be related to the lower stability of the sensors. Other factors that can influence on the changes in voltage are body temperature, movement of the subject, detachment between sensor and wiring or the wetting of the connector.

# 6

## Final discussion

This chapter discusses the design choices, production techniques, and results for the sweat sensor and collector. This project aimed to study the most suitable materials and designs to develop a sweat sensor system. The final goal was to provide a proof of principle for its health monitoring use during physical activity.

### 6.1. Design and production steps

This project designed and produced the sweat sensor and collector for the sweat analysis system. These two sub-parts with the read-out circuit became the production of the sweat analysis system.

#### 6.1.1. Sweat sensor

The design of the sweat sensor aimed to measure ionic content in sweat using potentiometry as the analytical technique. Three electrodes were used: two of them as working electrodes (for sodium and chloride) and one as a reference electrode.

The first production step was the screen-printing of the sensor. This step showed some initial drawbacks in the complete coverage of the insulation and the carbon layer. A second screen-printing process highly improved the homogeneous spreading of the layers. The use of cutting edge production machines and high-quality inks from Holst Centre provided high-performance sensors.

PET seemed to be an appropriate substrate for the sensor. It provides the necessary stiffness for the printing of the layers, but it is flexible enough for the person's comfort when placed on the skin. Regarding the different inks necessary for the proper working of the sensor, they all were of high quality and provided a high adhesion and resolution between layers.

The only issue encountered in this screen-printing process was the spread of the Ag/AgCl layer. The origin of the problem for the nonexistent sensitivity observed for chloride ions was investigated. After comparing this layer to an Ag/AgCl reference electrode, it was observed that this ink was barely covering the surface of the chloride electrode. There was an error during the production steps of the screen-printing, which only affected the Ag/AgCl layer. Future production of this sensor should consider the correct printing of this layer, as it is crucial for the measurement of chloride ions in sweat.

The second primary production step for the building of the sensor was the development of the membranes for the reference and sodium electrode.

For the reference membrane production, an innovative approach was initially tested that showed excellent stability. However, the production of this PVA/KCl membrane showed to be more complex

than initial expectations. The thick material achieved after production made the drop-casting of the membrane highly complex with the instruments available. The second approach for its production was to use a PVB/NaCl reference membrane, highly used in literature but with lower long-term stability than PVA/KCl. The production of this membrane showed a lower complexity, and it was easier to place on top of the electrodes.

The only drawback encountered on this production step was the spreading of the reference membrane through the PET layer. Future sensor versions should try to surround the electrode with the insulation layer to avoid this spreading. In addition, lower methanol volume (5 ml) should be used to obtain a more dense membrane.

Regarding the production of the sodium-selective membrane, the choosing of Na Ionophore X was the best option currently available. No issues were encountered throughout the production of this membrane, and it showed high selectivity for sodium ions.

Future improvement of this sensor should look for the addition of a solid contact layer in order to offer a faster ion-to-electron transduction and more precise measurement of ion concentration [55]. The addition of PEDOT:PSS layer was intended to be placed on top of the sensors after polymerization of EDOT. Due to the complexity of this process, it was decided to disregard this layer with the inconvenience of having a less accurate sensor. Recommendations for a new sensor version should include this solid contact layer in the screen-printing process for more efficient and faster production.

### 6.1.2. Sweat collector

The design of the sweat collector was focused on its proper functionality and a high comfortability for the person wearing it. The use of TPU as the primary material for the collector has shown to perfectly suit the project's objectives. TPU's hydrophobicity is not a drawback for obtaining high enough capillary pressure to collect sweat inside the microchannels. This advantage avoids the usage of surface treatment on the material, previously done by other research studies [106], but with the disadvantage of only lasting for a few weeks. Regarding the production of the collector, the use of the laser cutter showed a few challenges:

- Small burning on the edges of the collector showed some irregularities in its shape.
- Engraving the microchannels to create Tesla valves created a rough and sticky surface.

In order to improve the laser cutting accuracy, a higher quality laser cutter can provide a more precise laser beam. This upgrade would avoid the irregularities shown on the edges of the sweat collector. Regarding the design of the microchannel, special attention was paid to the creation of the Tesla valves. The small independent islands in this passive valve were not laser cut as they would detach from the rest of the system. Engraving the structure appeared to be the most suitable solution to replicate this structure. However, TPU and double-sided tape stacking made the microchannels obtain a viscous texture due to the remaining glue on its surface. This texture could negatively influence the sweat composition and flow, so the issue was taken care of using ethanol. A few drops of this chemical and rubbing the surface with paper allowed to get rid of the additional glue. Besides these two challenges, the overall working design of the collector showed very positive results in terms of sweat collection and flow.

In addition, all medical tapes showed high performance for the adhesion of TPU layers. Three different tapes were used: 3M 9469PC, 3M 1522 and 3M 1504. The last two tapes were biocompatible and allowed for the attachment of the collector to the skin. This tape showed strong adhesion to the skin during the high sweating period. Neither sweat nor hair prevented the complete attachment of the collector to the skin. Physiological experiments also showed low skin redness during the first minutes after detachment of the collector, but skin reached standard colour soon after. No skin irritation was

observed in any of the subjects. Thus, all double-sided tapes used in the project perfectly suited to the proper functionality and comfortability of the sweat collector.

### 6.1.3. Sweat analysis system

The integration of the sweat sensor and collector showed to be a straightforward problem. As the production of the collector had already been solved, similar method was followed for the integration using TPU and the laser cutting machine. However, initial tests showed the leakage of sweat between the sensor and the TPU layers on top and bottom. This issue was quickly solved by adding two extra double-sided tapes to completely seal the microchannel system and only let sweat out through the outlet hole.

However, after the testing of the sweat analysis system in the physiological experiments, a few remarks were observed:

- The connection between the sensor and the FFC connector is not completely fixed, disconnecting a few times during the exercise due to the person's movement.
- High sweating periods showed liquid close to the wiring.

These drawbacks are all related to the connection between the sensor and the read-out circuit. The limitation of having a wiring connection makes the system lean into possible errors. For our project, a short-term solution was devised to have the most optimal connection. The wiring was attached to the TPU layer using tape, as well as to cover them from possible sweat that could wet them.

Future system improvements should look into solutions to get rid of the wiring, sending the data wirelessly to a computer for later processing. This update would avoid any connection issues and wetting of the wiring.

## 6.2. Results

In this section, the results obtained for the validation and testing of the sensor, collector and sweat analysis system are presented.

### 6.2.1. Sweat sensor

The sensitivity of the sodium electrode to the sweat ion concentration range showed promising results. The region of interest for measuring ion concentration (10 *mmol/L* - 100 *mmol/L*) was easily calibrated, with a sensitivity close to 0.8 *mV* per *mmol/L*. These results are similar to previous sodium electrodes with the same chemical composition [85, 89]. A few remarks can be made on the extremes of this region of interest:

- The sensor shows a more unstable behaviour for low concentrations of NaCl (0-20 *mmol/L* range). The reasoning behind these observations can be related to the high membrane strength to withdraw ions from the solution. The inability to find high enough concentrations of ions can lead to instability in the final sensor readings.
- High concentrations of sodium ions (100 *mmol/L*) show a smaller difference in sensitivity than in lower ion concentration regions. This phenomenon has also been observed in literature [89], which can indicate the saturation of the sensor. In addition, the sensor's response time can also influence the final concentration reading, as with high sweat flow rate, the sensor may not have

enough time to read high amounts of ions in the solution.

The stability of the sensor showed a rise in voltage for more than an hour when submerged in a saline solution. It seems there is a long response time of the sensor when tested for the first time. This behaviour was corrected by previous wetting of the electrodes inside a solution with low NaCl concentration. Afterwards, the sensor showed a much more stable voltage for all NaCl concentrations.

Regarding the fluctuations observed every few minutes on the stability tests, there are a few explanations that can relate to this behaviour:

- Susceptibility of the sensor to slight movements in the wiring or small fluctuations in the saline solution.
- Changes in temperature have also been reported to show fluctuations on the sensor's reading output [56].

Finally, the response time of the sensor in the millimolar range showed a fast behaviour (approximately 30 seconds), coinciding with other research projects focused on sweat analysis [85].

### 6.2.2. Sweat collector

The main success achieved for the sweat collector was its ability to wick sweat into the system thanks to the action of capillary pressure. This action is crucial for collecting sweat, directly dependant on the chemical composition of the materials used and the dimensions of the inlet hole and the microchannels.

- Hydrophobicity of TPU was tested for its capability to guide sweat inside microchannels. Surface treatment using different methods ( $O_2$  treatment,  $N_2$  treatment and UV light) did not show more reliable results than non-treated TPU, so no chemical modifications of the material were necessary.
- Size of the inlet hole and the microchannels were crucial for the proper collection of sweat. Small modifications were necessary to obtain the most suitable dimensions that allowed for the wicking of sweat inside the system and its constant flow inside the microchannels.
- Small dimensions of the microchannels made sweat flow on top of the membranes rather than sideways, allowing for its analysis.

The addition of a passive valve into the system aimed to slow down the sweat flow in the microchannel. Sweat flow inside the microchannel was tested via images, showing the flow division in the helix region. However, the functionality of this valve was not adequately tested. Future work should measure the sweat flow in the outlet hole with and without the Tesla valves to check its working principle reliably.

### 6.2.3. Sweat analysis system

The long-term stability of the membranes was tested after three months since their production. This characteristic showed to be directly dependant on the area of the electrode. In the updated version of the sensor, the surface of the electrodes was reduced to minimize the total dimensions of the sweat analysis patch. However, this sensor showed a drastic drop in sensitivity after three months of production. A thin membrane also seems to show poor long-term stability. The previous version of the sensor with a larger electrode area and thicker membrane showed positive long-term stability, with no significant changes.

Stability and sensitivity tests using specific artificial sweat flow rates showed a positive sensor performance. Reading voltage remains stable even for high flow rates, and changes in ionic concentration are well-differentiated, specially in the middle region of interest (40 *mmol/L* - 70 *mmol/L*). In addition, the difficulty to read a fixed voltage in low ionic concentrations shows the instability of the sensor in this region.

In comparison to sensor readings inside an artificial sweat solution, poorer stability is shown when sweat flows over the sensor. One reasoning behind this behaviour is related to the flow of sweat in a perpendicular direction to the conducting layer. Moreover, these small variations in voltage can also be related to slight sensor movements or changes in temperature.

Physiological experiments were the culmination step for the testing of the sweat analysis system. Noise and altered voltages were observed when shielding the wires of the read-out circuit to the sensor. However, the sensor's filtered output signal already shows the system's ability to read sodium concentration during physical activity. Once sweat enters the analysis area of the collector and a few seconds after the stability of the sensor is reached, the system measures sweat sodium concentrations close to the values set by the ion chromatography method. High voltages in the first experiment were observed to be related to the shielding of the sensor. Avoiding this shielding showed poorer stability but more accurate results. In the second experiment, the sweat sodium concentrations were in the same range as in other literature studies [17]. Once again, deficient reading signals can be avoided by establishing a wireless connection between the sweat analysis patch and the read-out system. In addition, new physiological tests in other environments could be tried out without having the subject in a fixed position throughout the exercise.





## Conclusion and future work

This thesis project focuses on building a reliable sweat sensing system that analyses sweat in real-time during physical activity. The two main contributions to this system relied on the building of a sweat sensor and collector. Several successful experiments showed the positive potential of this system. The sweat sensor managed to analyse sodium ions concentration, and the collector could wick sweat from the skin without its contamination. Also, several issues were encountered, and new approaches had to be defined. A few requirements for this system were set for the project, and their evaluation can provide a final conclusion and some future recommendations.

- *The system should be capable of reliably monitoring a patient for at least one hour of exercise.*

The physiological experiments showed positive stability for long periods of analysis. The region of interest (10 *mmol/L* - 100 *mmol/L*) showed a potential change of approximately 90 *mV*, showing a sensitivity close to 0.8 *mV* per *mmol/L*. In the stability tests for different ion concentrations in a 30 minutes experiment, the system showed stable potentials that differed in a maximum range of 5 *mV*. This range can be translated as a maximum concentration difference of  $\pm 3$  *mmol/L*. However, this range is due to small changes in voltage which show briefly for a few seconds every few minutes. The sensor could reach stability with concentration differences of just  $\pm 1$  *mmol/L*. Physiological experiments showed lower stability, but concentration variations also differed in a maximum range of  $\pm 3$  *mmol/L*.

The improvement of the sensor sensitivity relies on adding a solid contact layer, such as the suggested PEDOT:PSS layer included in the screen-printing process. The stability of the sensor showed to drop when comparing laboratory to physiological experiments. Besides the drawbacks of sensor movement and body temperature, the flow of sweat perpendicular to the direction of the conducting layer could lower the final stability. Future work should try to rearrange the integration of the sweat sensor and collector so sweat can flow parallel to the direction of the sensor.

- *Sweat collection must avoid the contamination of sweat samples.*

The efficient and fast acquisition of sweat into the microfluidic system is crucial for its accurate analysis. The sweat collector in the sweat analysis system proved to positively perform this task thanks to the action of capillary pressure. After a previous cleaning of the skin area, sweat drops inside the inlet hole are quickly absorbed into the microchannels of the TPU system for its analysis. A test to examine this zero-contamination was not performed, but the collector showed exact behaviour to devices used in other studies that claim to avoid this sweat contamination [106]. Recommendations for future work could focus on comparing sweat collected by capillary pressure with other sweat collection techniques to show the efficiency of our method.

- *The system should reduce the sweat flow speed to increase the time for sampling.*

Sensor response time to changes in sweat concentration was effectively estimated to be around 30 seconds. The building of a passive valve after the analysis area of sweat can provide enough time for the accurate analysis of sweat samples. The Tesla valve function remains inactive if the sweat flow is low, but its structure slows down the flow when sweat gland's activity rises. Future research should look for more accurate laser cutting machines that can replicate the helix area of the valve in more detail.

- *The materials and techniques used to build the system should enable the end product to become a comfortable and wearable device.*

The sweat analysis patch is made of biocompatible materials for its comfortable attachment to the skin. Irritation was not found in any of the subjects wearing the patch for almost an entire hour. The building of the end product can be easily reproduced, and it can allow for the production of dozens of sensors in just a few days if all machines and materials are easily accessible. Faster sensor production can be achieved if the membranes are laid on top of the electrodes in the screen-printing process. Alignment sheets could be used for faster and more accurate production of the sweat collector when taping all TPU layers together.

## **Final conclusion**

A new concept for a sweat analysis system in real-time health monitoring during physical activity is provided in this research project. This system focused on producing, validating and testing a sweat sensor and collector, critical components for accurate sweat analysis. The stability and sensitivity of the system for analysing sweat ions were tested in human subjects with promising results. Future research should focus on a more efficient reproducibility of the sweat analysis patch and a wireless data transfer system. Further physiological experiments will provide more insightful information on the relationship between sweat ion concentrations and a person's health status.





# Bibliography

- [1] Keith Suter. "The Importance of Sport in Society". In: *Global Directions* (2014). URL: [www.TheGlobalFactor.com.au/Keith@KeithSuter.com.au](http://www.TheGlobalFactor.com.au/Keith@KeithSuter.com.au).
- [2] *\$100 billion — that's how much Americans spent on sports over the past 12 months - MarketWatch*. URL: <https://www.marketwatch.com/story/heres-how-much-americans-spend-on-sports-in-one-chart-2017-09-11>.
- [3] Centrum voor Beleidsstatistiek. "Sport in focus. The contribution of sport to the Dutch economy in 2006, 2008 and 2010". In: *Statistics Netherlands* (2013).
- [4] Carla L. Dellaserra, Yong Gao, and Lynda Ransdell. "Use of integrated technology in team sports: A review of opportunities, challenges, and future directions for athletes". In: *Journal of Strength and Conditioning Research* 28.2 (2014), pp. 556–573. ISSN: 15334295. DOI: 10.1519/JSC.0b013e3182a952fb.
- [5] Dhruv R. Seshadri et al. "Wearable Devices for Sports: New Integrated Technologies Allow Coaches, Physicians, and Trainers to Better Understand the Physical Demands of Athletes in Real time". In: *IEEE Pulse* 8.1 (Jan. 2017), pp. 38–43. ISSN: 21542287. DOI: 10.1109/MPUL.2016.2627240.
- [6] Ryan Chambers et al. *The Use of Wearable Microsensors to Quantify Sport-Specific Movements*. July 2015. DOI: 10.1007/s40279-015-0332-9.
- [7] T Magdalinski. "Sport, technology and the body: The nature of performance". In: (2009). URL: <https://books.google.com/books?hl=es&lr=&id=NkgpXnrQ6Y8C&oi=fnd&pg=PP1&dq=technology+biology+sports&ots=KniGtPaeKv&sig=23r2EwB2XOATKIPNeU0uwORorms>.
- [8] A. J. Salazar et al. "An initial experience in wearable monitoring sport systems". In: *Proceedings of the IEEE/EMBS Region 8 International Conference on Information Technology Applications in Biomedicine, ITAB*. 2010. ISBN: 9781424465606. DOI: 10.1109/ITAB.2010.5687625.
- [9] Gobinath Aroganam, Nadarajah Manivannan, and David Harrison. "Consumer Sport Applications". In: *Sensors* 19 (2019), pp. 1–26.
- [10] E. Cumps et al. "Injury rate and socioeconomic costs resulting from sports injuries in Flanders: data derived from sports insurance statistics 2003". In: *British Journal of Sports Medicine* 42.9 (Sept. 2008), pp. 767–772. ISSN: 03063674. DOI: 10.1136/bjism.2007.037937.
- [11] Gobinath Aroganam, Nadarajah Manivannan, and David Harrison. *Review on Wearable Technology Sensors Used in Consumer Sport Applications*. Apr. 2019. DOI: 10.3390/s19091983. URL: <https://www.mdpi.com/1424-8220/19/9/1983>.
- [12] Juhani Smolander et al. "Estimating oxygen consumption from heart rate and heart rate variability without individual calibration". In: *Clinical Physiology and Functional Imaging* 31.4 (July 2011), pp. 266–271. ISSN: 14750961. DOI: 10.1111/j.1475-097X.2011.01011.x. URL: <http://www.ncbi.nlm.nih.gov/pubmed/21672133>.
- [13] S. Shenoy. "EMG in sports rehabilitation". In: *British Journal of Sports Medicine* 44.Suppl\_1 (Sept. 2010), pp. i10–i10. ISSN: 0306-3674. DOI: 10.1136/bjism.2010.078725.27.
- [14] Kento Yamagishi et al. "Elastic kirigami patch for electromyographic analysis of the palm muscle during baseball pitching". In: *NPG Asia Materials* 11.1 (Dec. 2019). ISSN: 18844057. DOI: 10.1038/s41427-019-0183-1.
- [15] Demetris Delos, Travis G. Maak, and Scott A. Rodeo. "Muscle Injuries in Athletes: Enhancing Recovery Through Scientific Understanding and Novel Therapies". In: *Sports Health* 5.4 (July 2013), pp. 346–352. ISSN: 19417381. DOI: 10.1177/1941738113480934.

- [16] Joke Schuermans et al. "Proximal Neuromuscular Control Protects Against Hamstring Injuries in Male Soccer Players: A Prospective Study with Electromyography Time-Series Analysis during Maximal Sprinting". In: *American Journal of Sports Medicine* 45.6 (2017), pp. 1315–1325. ISSN: 15523365. DOI: 10.1177/0363546516687750. URL: [https://bjsm.bmj.com/content/51/4/383.2?rss=1&int\\_source=trendmd&int\\_medium=cpc&int\\_campaign=usage-042019](https://bjsm.bmj.com/content/51/4/383.2?rss=1&int_source=trendmd&int_medium=cpc&int_campaign=usage-042019).
- [17] Lindsay B. Baker. "Physiology of sweat gland function: The roles of sweating and sweat composition in human health". In: *Temperature* 6.3 (2019), pp. 211–259. ISSN: 23328959. DOI: 10.1080/23328940.2019.1632145. URL: <https://doi.org/10.1080/23328940.2019.1632145>.
- [18] Mark J. Patterson, Stuart D.R. Galloway, and Myra A. Nimmo. "Variations in regional sweat composition in normal human males". In: *Experimental Physiology* 85.6 (2000), pp. 869–875. ISSN: 09580670. DOI: 10.1111/j.1469-445X.2000.02058.x.
- [19] Marc Parrilla, Maria Cuartero, and Gaston A. Crespo. *Wearable potentiometric ion sensors*. Jan. 2019. DOI: 10.1016/j.trac.2018.11.024.
- [20] HealthLink BC. *Sports-Related Dehydration*. URL: <https://www.healthlinkbc.ca/health-topics/sig56435>.
- [21] Meredith Decker. *The Effects of Hydration on Athletic Performance*. 2011. URL: <https://sportscardiologybc.org/the-effects-of-hydration-on-athletic-performance/%20http://www.kon.org/urc/v10/athletic-training/decker.html>.
- [22] Totum Sport. *The Effect Of Dehydration on Sports Performance*. URL: [https://www.youtube.com/watch?v=Wr0JBu-xnR0&ab\\_channel=TotumSport](https://www.youtube.com/watch?v=Wr0JBu-xnR0&ab_channel=TotumSport).
- [23] Bob Murray, John Stofan, and E.R. Eichner. "Hyponatremia in athletes". In: *Sports Science* 16.1 (2003), p. 88. URL: <https://www.gssiweb.org/sports-science-exchange/article/sse-88-hyponatremia-in-athletes%20http://www.ux1.eiu.edu/~cfje/4900EN/GSSI-88-hyponatremia.pdf>.
- [24] Azar Alizadeh et al. "A wearable patch for continuous monitoring of sweat electrolytes during exertion". In: *Lab on a Chip* 18.17 (Sept. 2018), pp. 2632–2641. ISSN: 14730189. DOI: 10.1039/c8lc00510a. URL: <https://pubs.rsc.org/en/content/articlehtml/2018/lc/c8lc00510a%20https://pubs.rsc.org/en/content/articlelanding/2018/lc/c8lc00510a>.
- [25] Matthew R. Ely et al. "Surface contamination artificially elevates initial sweat mineral concentrations". In: *Journal of Applied Physiology* 110.6 (June 2011), pp. 1534–1540. ISSN: 87507587. DOI: 10.1152/japplphysiol.01437.2010. URL: <https://www.physiology.org/doi/10.1152/japplphysiol.01437.2010>.
- [26] A.S.M. Steijlen et al. "A wearable fluidic collection patch and ion chromatography method for sweat electrolyte monitoring during exercise". In: *Analytical Methods* 12.48 (Dec. 2020), pp. 5885–5892. ISSN: 1759-9660. DOI: 10.1039/D0AY02014A. URL: <https://repository.tudelft.nl/islandora/object/uuid%3A68add158-6e06-401e-8632-e37dd8639223>.
- [27] Chris Woolston. *Moving forward with cystic fibrosis*. May 2018. DOI: 10.1146/knowable-052518-011301. URL: <https://www.knowablemagazine.org/article/health-disease/2018/moving-forward-cystic-fibrosis>.
- [28] Cystic fibrosis foundation. *Sweat Test | CF Foundation*. 2017. URL: <https://www.cff.org/What-is-CF/Testing/Sweat-Test/>.
- [29] Wei Gao, George A. Brooks, and David C. Klonoff. "Wearable physiological systems and technologies for metabolic monitoring". In: *Journal of Applied Physiology* 124.3 (2018), pp. 548–556. ISSN: 15221601. DOI: 10.1152/japplphysiol.00407.2017.
- [30] Juliane R. Sempionatto, Jong Min Moon, and Joseph Wang. "Touch-Based Fingertip Blood-Free Reliable Glucose Monitoring: Personalized Data Processing for Predicting Blood Glucose Concentrations". In: *ACS Sensors* 6.5 (May 2021), pp. 1875–1883. ISSN: 23793694. DOI: 10.1021/acssensors.1c00139.
- [31] Wei Gao et al. "Fully integrated wearable sensor arrays for multiplexed in situ perspiration analysis". In: *Nature* 529.7587 (Jan. 2016), pp. 509–514. ISSN: 14764687. DOI: 10.1038/nature16521. URL: <https://www.nature.com/articles/nature16521>.

- [32] T. C. Boysen et al. "A modified anaerobic method of sweat collection". In: *Journal of Applied Physiology Respiratory Environmental and Exercise Physiology* 56.5 (1984), pp. 1302–1307. ISSN: 01617567. DOI: 10.1152/jappl.1984.56.5.1302. URL: <https://pubmed.ncbi.nlm.nih.gov/6327585/>.
- [33] Jayoung Kim et al. "Noninvasive Alcohol Monitoring Using a Wearable Tattoo-Based Iontophoretic Biosensing System". In: *ACS Sensors* 1.8 (Aug. 2016), pp. 1011–1019. ISSN: 23793694. DOI: 10.1021/acssensors.6b00356. URL: <https://pubs.acs.org/sharingguidelines>.
- [34] Indiana Public Media. *Why Do My Hands And Feet Sweat So Much?* URL: <https://indianapublicmedia.org/amomentofscience/hands-feet-sweat.php>.
- [35] K. Sato et al. "Biology of sweat glands and their disorders. I. Normal sweat gland function". In: *Journal of the American Academy of Dermatology* 20.4 (Apr. 1989), pp. 537–563. ISSN: 01909622. DOI: 10.1016/S0190-9622(89)70063-3.
- [36] Peter Groscurth. "Anatomy of sweat glands." In: *Current problems in dermatology* 30 (2002), pp. 1–9. ISSN: 14215721. DOI: 10.1159/000060678. URL: <https://www.karger.com/Article/FullText/60678>.
- [37] Oliver P. Kreyden and E. Paul Scheidegger. "Anatomy of the sweat glands, pharmacology of botulinum toxin, and distinctive syndromes associated with hyperhidrosis". In: *Clinics in Dermatology* 22.1 (Jan. 2004), pp. 40–44. ISSN: 0738081X. DOI: 10.1016/j.clindermatol.2003.12.029.
- [38] F. Sato et al. "Functional and morphological changes in the eccrine sweat gland with heat acclimation". In: *Journal of Applied Physiology* 69.1 (1990), pp. 232–236. ISSN: 01617567. DOI: 10.1152/jappl.1990.69.1.232.
- [39] Alan M.W. Porter. "Why do we have apocrine and sebaceous glands?" In: *Journal of the Royal Society of Medicine* 94.5 (2001), pp. 236–237. ISSN: 01410768. DOI: 10.1177/014107680109400509. URL: </pmc/articles/PMC1281456/?report=abstract%20https://www.ncbi.nlm.nih.gov/pmc/articles/PMC1281456/>.
- [40] D. L. Costill. "SWEATING: ITS COMPOSITION AND EFFECTS ON BODY FLUIDS". In: *Annals of the New York Academy of Sciences* 301.1 (Oct. 1977), pp. 160–174. ISSN: 17496632. DOI: 10.1111/j.1749-6632.1977.tb38195.x. URL: <https://nyaspubs.onlinelibrary.wiley.com/doi/full/10.1111/j.1749-6632.1977.tb38195.x> <https://nyaspubs.onlinelibrary.wiley.com/doi/abs/10.1111/j.1749-6632.1977.tb38195.x> <https://nyaspubs.onlinelibrary.wiley.com/doi/10.1111/j.1749-6632.1977.tb38195.x>.
- [41] Chang Yi Cui and David Schlessinger. *Eccrine sweat gland development and sweat secretion*. Sept. 2015. DOI: 10.1111/exd.12773. URL: </pmc/articles/PMC5508982/?report=abstract%20https://www.ncbi.nlm.nih.gov/pmc/articles/PMC5508982/>.
- [42] Chang Yi Cui et al. "Forkhead transcription factor FoxA1 regulates sweat secretion through Bestrophin 2 anion channel and Na-K-Cl cotransporter 1". In: *Proceedings of the National Academy of Sciences of the United States of America* 109.4 (Jan. 2012), pp. 1199–1203. ISSN: 00278424. DOI: 10.1073/pnas.1117213109. URL: [www.pnas.org/cgi/doi/10.1073/pnas.1117213109](http://www.pnas.org/cgi/doi/10.1073/pnas.1117213109).
- [43] K. Sato. "The physiology, pharmacology, and biochemistry of the eccrine sweat gland." In: *Reviews of physiology, biochemistry and pharmacology* 79 (1977), pp. 51–131. ISSN: 03034240. DOI: 10.1007/bfb0037089. URL: <https://link.springer.com/chapter/10.1007/BFb0037089>.
- [44] K. Wilke et al. *A short history of sweat gland biology*. June 2007. DOI: 10.1111/j.1467-2494.2007.00387.x. URL: <https://pubmed.ncbi.nlm.nih.gov/18489347/>.
- [45] Kenzo Sato, Minora Ohtsuyama, and Ghyath Samman. "Eccrine sweat gland disorders". In: *Journal of the American Academy of Dermatology* 24.6 (1991), pp. 1010–1014. ISSN: 01909622. DOI: 10.1016/S0190-9622(08)80117-X. URL: <https://pubmed.ncbi.nlm.nih.gov/1869663/>.
- [46] M. M. Ready and P. M. Quinton. "Rapid regulation of electrolyte absorption in sweat duct". In: *The Journal of Membrane Biology* 140.1 (May 1994), pp. 57–67. ISSN: 00222631. DOI: 10.1007/BF00234486.



- [47] G. W. CAGE and R. L. DOBSON. "SODIUM SECRETION AND REABSORPTION IN THE HUMAN ECCRINE SWEAT GLAND." In: *The Journal of clinical investigation* 44.7 (1965), pp. 1270–1276. ISSN: 00219738. DOI: 10.1172/JCI105233. URL: <https://www.jci.org/articles/view/105233/files/pdf>.
- [48] K. Sato and R. L. Dobson. "Glucose metabolism of the isolated eccrine sweat gland. I. The effects of mecholyl, epinephrine and ouabain." In: *The Journal of investigative dermatology* 56.4 (1971), pp. 272–280. ISSN: 0022202X. DOI: 10.1111/1523-1747.ep12261004.
- [49] J. S. WEINER and R. E. VAN HEYNINGEN. "Observations on lactate content of sweat". In: *Journal of applied physiology* 4.9 (Mar. 1952), pp. 734–744. ISSN: 00218987. DOI: 10.1152/jappl.1952.4.9.734. URL: <https://pubmed.ncbi.nlm.nih.gov/14917619/>.
- [50] Nigel A.S. Taylor and Christiano A. Machado-Moreira. "Regional variations in transepidermal water loss, eccrine sweat gland density, sweat secretion rates and electrolyte composition in resting and exercising humans". In: *Extreme Physiology and Medicine* 2.1 (Feb. 2013), p. 4. ISSN: 20467648. DOI: 10.1186/2046-7648-2-4. URL: <http://www.extremephysiolmed.com/content/2/1/41>.
- [51] Scott J. Montain, Samuel N. Cheuvront, and Henry C. Lukaski. "Sweat mineral-element responses during 7 h of exercise-heat stress". In: *International Journal of Sport Nutrition and Exercise Metabolism* 17.6 (Dec. 2007), pp. 574–582. ISSN: 15432742. DOI: 10.1123/ijsnem.17.6.574. URL: <https://journals.humankinetics.com/view/journals/ijsnem/17/6/article-p574.xml>.
- [52] Matthew R. Ely et al. "The effect of heat acclimation on sweat microminerals: Artifact of surface contamination". In: *International Journal of Sport Nutrition and Exercise Metabolism* 23.5 (Oct. 2013), pp. 470–479. ISSN: 15432742. DOI: 10.1123/ijsnem.23.5.470. URL: <https://journals.humankinetics.com/view/journals/ijsnem/23/5/article-p470.xml>.
- [53] W. N. Fishbein, J. W. Foellmer, and J. I. Davis. "Medical implications of the lactate and ammonia relationship in anaerobic exercise". In: *International Journal of Sports Medicine* 11.SUPPL. 2 (May 1990), S91–S100. ISSN: 01724622. DOI: 10.1055/s-2007-1024860. URL: <http://www.thieme-connect.de/DOI/DOI?10.1055/s-2007-1024860>.
- [54] S. M. Shirreffs and R. J. Maughan. "Whole body sweat collection in humans: An improved method with preliminary data on electrolyte content". In: *Journal of Applied Physiology* 82.1 (1997), pp. 336–341. ISSN: 87507587. DOI: 10.1152/jappl.1997.82.1.336.
- [55] Zhengyun Wang et al. "Engineering Materials for Electrochemical Sweat Sensing". In: *Advanced Functional Materials* 2008130 (2020), pp. 1–28. ISSN: 16163028. DOI: 10.1002/adfm.202008130.
- [56] T D Bakker. "Real-time monitoring of sweat of Cystic Fibrosis patients". PhD thesis. Delft University of Technology, 2019, p. 135.
- [57] Eric D.B. Goulet et al. "Measurement of sodium concentration in sweat samples: Comparison of 5 analytical techniques". In: *Applied Physiology, Nutrition and Metabolism* 42.8 (2017), pp. 861–868. ISSN: 17155320. DOI: 10.1139/apnm-2017-0059. URL: <https://cdnsciencepub.com/doi/abs/10.1139/apnm-2017-0059>.
- [58] Christine E. Dziedzic et al. "Variability of measurements of sweat sodium using the regional absorbent-patch method". In: *International Journal of Sports Physiology and Performance* 9.5 (2014), pp. 832–838. ISSN: 15550265. DOI: 10.1123/ijspp.2013-0480. URL: <https://pubmed.ncbi.nlm.nih.gov/24436351/>.
- [59] Eric D.B. Goulet, Tommy Dion, and Étienne Myette-Côté. "Validity and reliability of the Horiba C-122 compact sodium analyzer in sweat samples of athletes". In: *European Journal of Applied Physiology* 112.10 (2012), pp. 3479–3485. ISSN: 14396319. DOI: 10.1007/s00421-012-2331-y. URL: <https://link.springer.com/content/pdf/10.1007/s00421-012-2331-y.pdf>.
- [60] Paul Boisvert and Victor Candas. "Validity of the Wescor's sweat conductivity analyzer for the assessment of sweat electrolyte concentrations". In: *European Journal of Applied Physiology and Occupational Physiology* 69.2 (Mar. 1994), pp. 176–178. ISSN: 03015548. DOI: 10.1007/BF00609413.

- [61] Monica Z. Bruckner. *Ion Chromatography*. URL: [https://serc.carleton.edu/microbelife/research\\_methods/biogeochemical/ic.html](https://serc.carleton.edu/microbelife/research_methods/biogeochemical/ic.html).
- [62] J. Doorn et al. "Ion chromatography for the precise analysis of chloride and sodium in sweat for the diagnosis of cystic fibrosis". In: *Annals of Clinical Biochemistry* 52.4 (July 2015), pp. 421–427. ISSN: 17581001. DOI: 10.1177/0004563214549642.
- [63] Linda M. Thienpont et al. "Validation of candidate reference methods based on ion chromatography for determination of total sodium, potassium, calcium and magnesium in serum through comparison with flame atomic emission and absorption spectrometry". In: *Clinical Biochemistry* 29.6 (Dec. 1996), pp. 501–508. ISSN: 00099120. DOI: 10.1016/S0009-9120(96)00090-2.
- [64] Maria E. Gamboa-Aldeco John O'M. Bockris Amulya K.N. Reddy. *Modern Electrochemistry 2A: Fundamentals of Electrode Processes*. 2001, p. 1522. URL: [https://books.google.nl/books?id=utDyTYpimkUC&redir\\_esc=y](https://books.google.nl/books?id=utDyTYpimkUC&redir_esc=y).
- [65] Santa Monica College. *Electrical Conductivity of Aqueous Solutions*. 2020. URL: [https://chem.libretexts.org/Bookshelves/Ancillary\\_Materials/Laboratory\\_Experiments/Wet\\_Lab\\_Experiments/General\\_Chemistry\\_Labs/Online\\_Chemistry\\_Lab\\_Manual/Chem\\_9\\_Experiments/07%3A\\_Electrical\\_Conductivity\\_of\\_Aqueous\\_Solutions\\_\(Experiment\)](https://chem.libretexts.org/Bookshelves/Ancillary_Materials/Laboratory_Experiments/Wet_Lab_Experiments/General_Chemistry_Labs/Online_Chemistry_Lab_Manual/Chem_9_Experiments/07%3A_Electrical_Conductivity_of_Aqueous_Solutions_(Experiment)).
- [66] ELITechGroup. *Molecular Diagnostics | ELITechGroup: In Vitro Diagnostic Equipment & Reagents*. URL: <https://www.elitechgroup.com/product/sweat-check-analyzer-2%20https://www.elitechgroup.com/products/molecular-diagnostics>.
- [67] Amrita Vishwa Vidyapeetham. *Flame Photometry (Theory) : Inorganic Chemistry Virtual Lab : Chemical Sciences : Amrita Vishwa Vidyapeetham Virtual Lab*. 2012. URL: <http://vlab.amrita.edu/?sub=2&brch=193&sim=1351&cnt=1>.
- [68] BWB Technologies. *How A Flame Photometer Works | BWB Technologies*. 2018. URL: <https://www.bwbtech.com/post/2018/03/08/how-a-flame-photometer-works>.
- [69] Chenwen Lin et al. "Gradient-Based Colorimetric Sensors for Continuous Gas Monitoring". In: *Analytical Chemistry* 90.8 (Apr. 2018), pp. 5375–5380. ISSN: 15206882. DOI: 10.1021/acs.analchem.8b00506. URL: [/pmc/articles/PMC6206500/%20/pmc/articles/PMC6206500/?report=abstract%20https://www.ncbi.nlm.nih.gov/pmc/articles/PMC6206500/](https://pubs.rsc.org/en/content/articlehtml/2020/en/d0en00449a).
- [70] Bin Liu, Jinyin Zhuang, and Gang Wei. *Recent advances in the design of colorimetric sensors for environmental monitoring*. Aug. 2020. DOI: 10.1039/d0en00449a. URL: <https://pubs.rsc.org/en/content/articlehtml/2020/en/d0en00449a>.
- [71] Suresh Kumar Kailasa, Tae Jung Park, and Janardhan Reddy Koduru. "Metal nanoparticles-based colorimetric methods for drug analyses". In: *Nanoarchitectonics in Biomedicine*. Elsevier, Jan. 2019, pp. 619–641. ISBN: 9780128162002. DOI: 10.1016/B978-0-12-816200-2.00003-7.
- [72] Ahyeon Koh et al. "A soft, wearable microfluidic device for the capture, storage, and colorimetric sensing of sweat". In: *Science Translational Medicine* 8.366 (Nov. 2016), 366ra165. ISSN: 19466242. DOI: 10.1126/scitranslmed.aaf2593. URL: [/pmc/articles/PMC5429097/?report=abstract%20https://www.ncbi.nlm.nih.gov/pmc/articles/PMC5429097/](https://pubs.rsc.org/en/content/articlehtml/2020/en/d0en00449a).
- [73] Raja Pavan and Andrew R. Barron. *1.7: Ion Selective Electrode Analysis - Chemistry LibreTexts*. URL: [https://chem.libretexts.org/Bookshelves/Analytical\\_Chemistry/Book%3A\\_Physical\\_Methods\\_in\\_Chemistry\\_and\\_Nano\\_Science\\_\(Barron\)/01%3A\\_Elemental\\_Analysis/1.07%3A\\_Ion\\_Selective\\_Electrode\\_Analysis](https://chem.libretexts.org/Bookshelves/Analytical_Chemistry/Book%3A_Physical_Methods_in_Chemistry_and_Nano_Science_(Barron)/01%3A_Elemental_Analysis/1.07%3A_Ion_Selective_Electrode_Analysis).
- [74] P. T. Bray et al. "Sweat testing for cystic fibrosis: Characteristics of a combination chloride ion-selective electrode". In: *Clinica Chimica Acta* 77.1 (May 1977), pp. 69–76. ISSN: 00098981. DOI: 10.1016/0009-8981(77)90403-X.
- [75] G. Matzeu et al. "An integrated sensing and wireless communications platform for sensing sodium in sweat". In: *Analytical Methods* 8.1 (Jan. 2016), pp. 64–71. ISSN: 17599679. DOI: 10.1039/c5ay02254a. URL: [www.rsc.org/methods](http://www.rsc.org/methods).

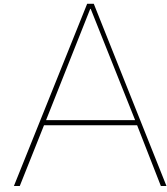
- [76] Shuqi Wang et al. "Wearable Sweatband Sensor Platform Based on Gold Nanodendrite Array as Efficient Solid Contact of Ion-Selective Electrode". In: *Analytical Chemistry* 89.19 (Oct. 2017), pp. 10224–10231. ISSN: 15206882. DOI: 10.1021/acs.analchem.7b01560. URL: <https://pubs.acs.org/doi/full/10.1021/acs.analchem.7b01560>.
- [77] Lindsay B. Baker et al. "Validity and reliability of a field technique for sweat Na<sup>+</sup> and K<sup>+</sup> analysis during exercise in a hot-humid environment". In: *Physiological Reports* 2.5 (2014). ISSN: 2051817X. DOI: 10.14814/phy2.12007.
- [78] James W. Robinson, Eileen Skelly Frame, and George M. Frame II. *Undergraduate Instrumental Analysis*. CRC PRESS, 2014. ISBN: 9780429170331. DOI: 10.1201/b15921.
- [79] Jinbo Hu, Andreas Stein, and Philippe Bühlmann. *Rational design of all-solid-state ion-selective electrodes and reference electrodes*. Feb. 2016. DOI: 10.1016/j.trac.2015.11.004. URL: <https://experts.umn.edu/en/publications/rational-design-of-all-solid-state-ion-selective-electrodes-and-r>.
- [80] Daniel P. Rose et al. "Adhesive RFID sensor patch for monitoring of sweat electrolytes". In: *IEEE Transactions on Biomedical Engineering* 62.6 (June 2015), pp. 1457–1465. ISSN: 15582531. DOI: 10.1109/TBME.2014.2369991.
- [81] Caroline J. Smith and George Havenith. "Body mapping of sweating patterns in male athletes in mild exercise-induced hyperthermia". In: *European Journal of Applied Physiology* 111.7 (July 2011), pp. 1391–1404. ISSN: 14396319. DOI: 10.1007/s00421-010-1744-8. URL: <https://pubmed.ncbi.nlm.nih.gov/21153660/>.
- [82] V. A.T. Dam, M. A.G. Zevenbergen, and R. van Schaijk. "Toward wearable patch for sweat analysis". In: *Sensors and Actuators, B: Chemical* 236 (Nov. 2016), pp. 834–838. ISSN: 09254005. DOI: 10.1016/j.snb.2016.01.143.
- [83] Zahra Taleat, Alireza Khoshroo, and Mohammad Mazloum-Ardakani. *Screen-printed electrodes for biosensing: A review (2008-2013)*. 2014. DOI: 10.1007/s00604-014-1181-1.
- [84] Jirayu Sitanurak et al. "T-shirt ink for one-step screen-printing of hydrophobic barriers for 2D- and 3D-microfluidic paper-based analytical devices". In: *Talanta* 205 (2019). ISSN: 00399140. DOI: 10.1016/j.talanta.2019.120113. URL: <https://reader.elsevier.com/reader/sd/pii/S0039914019307398?token=680ED8110B84BCECC7F2352085B78BA27F26C9D1B187761E41634C5FFE1242CB9C531671655D5C4626FD2F0CA1826AD4&originRegion=eu-west-1&originCreation=20210903081713>.
- [85] Amay J. Bandodkar et al. "Epidermal tattoo potentiometric sodium sensors with wireless signal transduction for continuous non-invasive sweat monitoring". In: *Biosensors and Bioelectronics* 54 (Apr. 2014), pp. 603–609. ISSN: 18734235. DOI: 10.1016/j.bios.2013.11.039.
- [86] Shinichi Komaba et al. "All-solid-state ion-selective electrodes with redox-active lithium, sodium, and potassium insertion materials as the inner solid-contact layer". In: *Analyst* 142.20 (2017), pp. 3857–3866. ISSN: 13645528. DOI: 10.1039/c7an01068k. URL: <https://pubs.rsc.org/ko/content/articlehtml/2017/an/c7an01068k>.
- [87] Wenya He et al. *Integrated textile sensor patch for real-time and multiplex sweat analysis*. Tech. rep. 2019. URL: <http://advances.sciencemag.org/>.
- [88] Qingbo An et al. "A multichannel electrochemical all-solid-state wearable potentiometric sensor for real-time sweat ion monitoring". In: *Electrochemistry Communications* 107 (2019). ISSN: 13882481. DOI: 10.1016/j.elecom.2019.106553. URL: <https://www.sciencedirect.com/science/article/pii/S1388248119302164>.
- [89] Sam Emaminejad et al. "Autonomous sweat extraction and analysis applied to cystic fibrosis and glucose monitoring using a fully integrated wearable platform". In: *Proceedings of the National Academy of Sciences of the United States of America* 114.18 (May 2017), pp. 4625–4630. ISSN: 10916490. DOI: 10.1073/pnas.1701740114. URL: <https://www.pnas.org/content/114/18/4625%20https://www.pnas.org/content/114/18/4625.abstract>.
- [90] Tomàs Guinovart et al. "A reference electrode based on polyvinyl butyral (PVB) polymer for decentralized chemical measurements". In: *Analytica Chimica Acta* 821 (Apr. 2014), pp. 72–80. ISSN: 18734324. DOI: 10.1016/j.aca.2014.02.028.

- [91] Xianbo Jin et al. "The electrochemical formation and reduction of a thick AgCl deposition layer on a silver substrate". In: *Journal of Electroanalytical Chemistry* 542. January (2003), pp. 85–96. ISSN: 15726657. DOI: 10.1016/S0022-0728(02)01474-2.
- [92] D B Dill et al. "SALT ECONOMY IN EXTREME DRY HEAT". In: *Journal of Biological Chemistry* 100.3 (1933), pp. 755–767. ISSN: 0021-9258. URL: <http://www.jbc.org/>.
- [93] S. ROBINSON and A. H. ROBINSON. "Chemical composition of sweat". In: *Physiological reviews* 34.2 (Apr. 1954), pp. 202–220. ISSN: 00319333. DOI: 10.1152/physrev.1954.34.2.202.
- [94] Food Institute of Medicine, Committee on Mineral Requirements for Cognitive Nutrition Board Committee on Military Nutrition Research, and Physical Performance of Military Personnel. *Mineral requirements for military personnel: Levels needed for cognitive and physical performance during garrison training*. 2006, pp. 1–496. ISBN: 0309101263. DOI: 10.17226/11610. URL: [https://books.google.nl/books?hl=es&lr=&id=RbIug-ZHemUC&oi=fnd&pg=PA323&dq=Haymes+EM.+Mineral+sweat+losses+during+exercise.+In:+Institute+of+Medicine,+editor.+Mineral+requirements+for+military+personnel.+Washington+\(DC\):+National+Academies+Press%3B+2006.+](https://books.google.nl/books?hl=es&lr=&id=RbIug-ZHemUC&oi=fnd&pg=PA323&dq=Haymes+EM.+Mineral+sweat+losses+during+exercise.+In:+Institute+of+Medicine,+editor.+Mineral+requirements+for+military+personnel.+Washington+(DC):+National+Academies+Press%3B+2006.+)
- [95] Lindsay B. Baker et al. "Exercise intensity effects on total sweat electrolyte losses and regional vs. whole-body sweat [Na<sup>+</sup>], [Cl<sup>-</sup>], and [K<sup>+</sup>]". In: *European Journal of Applied Physiology* 119.2 (2019), pp. 361–375. ISSN: 14396319. DOI: 10.1007/s00421-018-4048-z. URL: <http://dx.doi.org/10.1007/s00421-018-4048-z>.
- [96] George Havenith et al. "Male and female upper body sweat distribution during running measured with technical absorbents". In: *European Journal of Applied Physiology* 104.2 (2008), pp. 245–255. ISSN: 14396319. DOI: 10.1007/s00421-007-0636-z.
- [97] Ruth van Heyningen and J. S. Weiner. "A comparison of arm□bag sweat and body sweat". In: *The Journal of Physiology* 116.4 (Apr. 1952), pp. 395–403. ISSN: 14697793. DOI: 10.1113/jphysiol.1952.sp004713. URL: <https://pubmed.ncbi.nlm.nih.gov/14946709/>.
- [98] K. J. Collins and J. S. Weiner. "Observations on arm□bag suppression of sweating and its relationship to thermal sweat□gland "fatigue"". In: *The Journal of Physiology* 161.3 (May 1962), pp. 538–556. ISSN: 14697793. DOI: 10.1113/jphysiol.1962.sp006902. URL: <https://www.ncbi.nlm.nih.gov/pmc/articles/PMC1359611/>.
- [99] Tammi L. van Neel and Ashleigh B. Theberge. "Programmable capillary action controls fluid flows". In: *Nature* 595.7865 (June 2021), pp. 31–32. ISSN: 0028-0836. DOI: 10.1038/d41586-021-01708-2. URL: <https://www.nature.com/articles/d41586-021-01708-2>.
- [100] Nikola A. Dudukovic et al. "Cellular fluidics". In: *Nature* 595.7865 (June 2021), pp. 58–65. ISSN: 0028-0836. DOI: 10.1038/s41586-021-03603-2. URL: <https://www.nature.com/articles/s41586-021-03603-2>.
- [101] SYNLAB. *Antigen test for SARS-CoV-2 corona virus detection*. URL: <https://www.synlab.com/news-publications/sars-cov-2/default-title-1%20https://www.synlab.com/news-publications/sars-cov-2/antigen-tests-for-sars-cov-2-detection>.
- [102] M. R. Ely et al. "Evaluation of the Megaduct sweat collector for mineral analysis". In: *Physiological Measurement* 33.3 (Mar. 2012), pp. 385–394. ISSN: 09673334. DOI: 10.1088/0967-3334/33/3/385. URL: <https://iopscience.iop.org/article/10.1088/0967-3334/33/3/385%20https://iopscience.iop.org/article/10.1088/0967-3334/33/3/385/meta>.
- [103] Joy N. Hussain, Nitin Mantri, and Marc M Cohen. "Working up a good sweat - The challenges of standardising sweat collection for metabolomics analysis". In: *Clinical Biochemist Reviews* 38.1 (2017), pp. 13–34. ISSN: 18380212. URL: <http://www.hmdb..>
- [104] S. ROBINSON et al. "Effect of skin temperature on salt concentration of sweat." In: *Journal of applied physiology* 2.12 (1950), pp. 654–662. ISSN: 00218987. DOI: 10.1152/japphysiol.1950.2.12.654. URL: <https://www.cabdirect.org/cabdirect/abstract/19512900155>.
- [105] MARY F. WALLER and EMILY M. HAYMES. "The effects of heat and exercise on sweat iron loss". In: *Medicine & Science in Sports & Exercise* 28.2 (Feb. 1996), pp. 197–203. ISSN: 0195-9131. DOI: 10.1097/00005768-199602000-00007. URL: <http://journals.lww.com/00005768-199602000-00007>.

- [106] Yingxue Zhang et al. "Skin-interfaced microfluidic devices with one-opening chambers and hydrophobic valves for sweat collection and analysis". In: *Lab on a Chip* 20.15 (Aug. 2020), pp. 2635–2645. ISSN: 14730189. DOI: 10.1039/d0lc00400f. URL: <https://pubs.rsc.org/en/content/articlehtml/2020/lc/d0lc00400f>. URL: <https://pubs.rsc.org/en/content/articlelanding/2020/lc/d0lc00400f>.
- [107] Samu Hemmilä et al. "Rapid, simple, and cost-effective treatments to achieve long-term hydrophilic PDMS surfaces". In: *Applied Surface Science* 258.24 (Oct. 2012), pp. 9864–9875. ISSN: 01694332. DOI: 10.1016/j.apsusc.2012.06.044.
- [108] Sung Bong Kim et al. "Soft, Skin-Interfaced Microfluidic Systems with Wireless, Battery-Free Electronics for Digital, Real-Time Tracking of Sweat Loss and Electrolyte Composition". In: *Small* 14.45 (Nov. 2018), p. 1802876. ISSN: 16136810. DOI: 10.1002/smll.201802876. URL: <http://doi.wiley.com/10.1002/smll.201802876>.
- [109] Jungil Choi et al. "Thin, Soft, Skin-Mounted Microfluidic Networks with Capillary Bursting Valves for Chrono-Sampling of Sweat". In: *Advanced Healthcare Materials* 6.5 (Mar. 2017), p. 1601355. ISSN: 2192-2659. DOI: 10.1002/ADHM.201601355. URL: <https://onlinelibrary.wiley.com/doi/full/10.1002/adhm.201601355>. URL: <https://onlinelibrary.wiley.com/doi/abs/10.1002/adhm.201601355>. URL: <https://onlinelibrary.wiley.com/doi/10.1002/adhm.201601355>.
- [110] Peter B. Licht and Hans K. Pilegaard. "Severity of compensatory sweating after thoracoscopic sympathectomy". In: *Annals of Thoracic Surgery* 78.2 (Aug. 2004), pp. 427–431. ISSN: 00034975. DOI: 10.1016/j.athoracsur.2004.02.087.
- [111] V. Tesař. "Microfluidic Valves for Flow Control at Low Reynolds Numbers". In: *Journal of Visualization* 4.1 (2001), pp. 51–60. ISSN: 13438875. DOI: 10.1007/BF03182455.
- [112] Agnes Beate Bußmann et al. "Piezoelectric titanium based microfluidic pump and valves for implantable medical applications". In: *Sensors and Actuators, A: Physical* 323 (June 2021), p. 112649. ISSN: 09244247. DOI: 10.1016/j.sna.2021.112649.
- [113] Cmglee. *Tesla valve principle*. 2021. URL: [https://commons.wikimedia.org/wiki/File:Tesla\\_valve\\_principle.svg](https://commons.wikimedia.org/wiki/File:Tesla_valve_principle.svg).
- [114] Nikola Tesla. *Valvular Conduit*. 1920. URL: <https://patents.google.com/patent/US1329559A/en>.
- [115] Erik Stemme and Göran Stemme. "A valveless diffuser/nozzle-based fluid pump". In: *Sensors and Actuators: A. Physical* 39.2 (1993), pp. 159–167. ISSN: 09244247. DOI: 10.1016/0924-4247(93)80213-Z. URL: <https://www.sciencedirect.com/science/article/pii/092442479380213Z>.
- [116] Piyush R. Porwal et al. "Heat transfer and fluid flow characteristics in multistaged Tesla valves". In: *Numerical Heat Transfer; Part A: Applications* 73.6 (Mar. 2018), pp. 347–365. ISSN: 15210634. DOI: 10.1080/10407782.2018.1447199. URL: [https://www.tandfonline.com/doi/abs/10.1080/10407782.2018.1447199?casa\\_token=4o4tGoNDuUwAAAAA:rv\\_10B3KoDiGrSaYWRFj0YqisbUa7Zp01qpdgg91hQbYrHxOP80gE-PdpgNEfv50J7PssrW\\_L15](https://www.tandfonline.com/doi/abs/10.1080/10407782.2018.1447199?casa_token=4o4tGoNDuUwAAAAA:rv_10B3KoDiGrSaYWRFj0YqisbUa7Zp01qpdgg91hQbYrHxOP80gE-PdpgNEfv50J7PssrW_L15).
- [117] Michael Korger et al. "Testing thermoplastic elastomers selected as flexible three-dimensional printing materials for functional garment and technical textile applications". In: *Journal of Engineered Fibers and Fabrics* 15 (June 2020), pp. 1–10. ISSN: 15589250. DOI: 10.1177/1558925020924599. URL: <https://journals.sagepub.com/doi/full/10.1177/1558925020924599>.
- [118] Dupont. *TPU – Insulectro*. URL: <https://insulectro-pe.com/collections/tpu>.
- [119] Gamma Sterilization Compatible et al. "3M Medical Materials & Technologies". In: September (2018), pp. 2–3.
- [120] Sculpteo. *Laser engraving definition*. URL: <https://www.sculpteo.com/en/glossary/laser-engraving-definition/>.

- [121] Lisa Klous et al. "The effect of short and continuous absorbent patch application on local skin temperature underneath". In: *Physiological Measurement* 42.4 (May 2021), p. 045006. ISSN: 13616579. DOI: 10.1088/1361-6579/abf364. URL: <https://iopscience.iop.org/article/10.1088/1361-6579/abf364%20https://iopscience.iop.org/article/10.1088/1361-6579/abf364/meta>.





## Additional results of physiological experiments

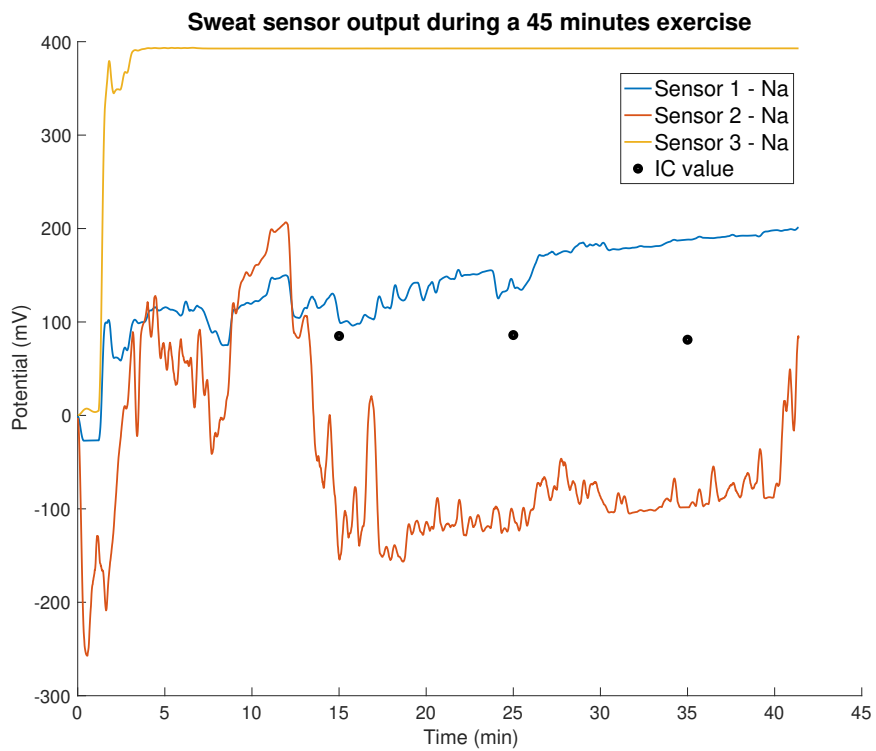


**Figure A.1:** Sweat system output for all sensors in a 45 minutes exercise period for subject 2



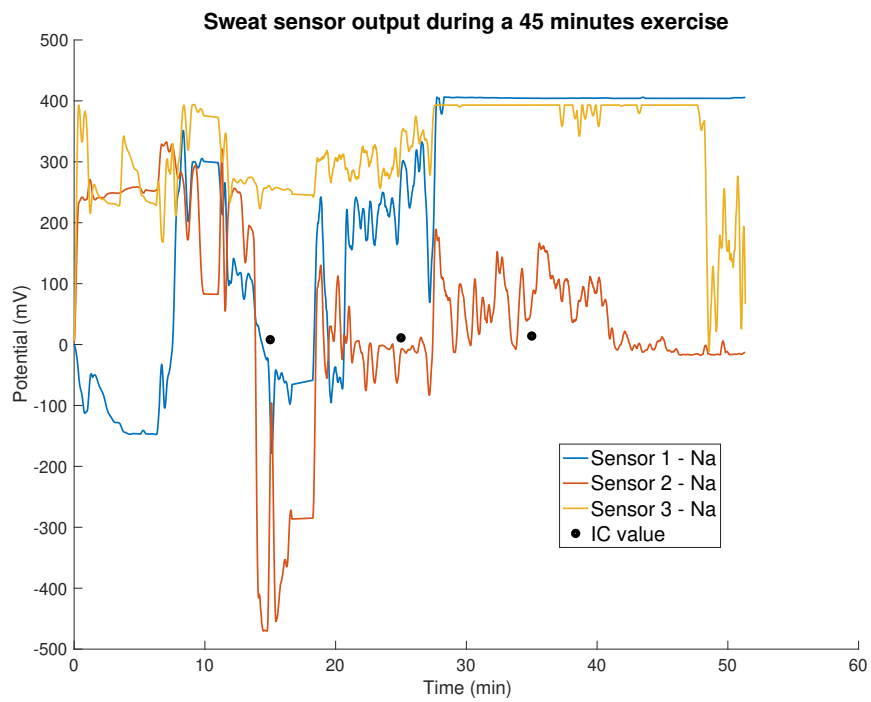


**Figure A.2:** Sweat system output for all sensors in a 45 minutes exercise period for subject 3

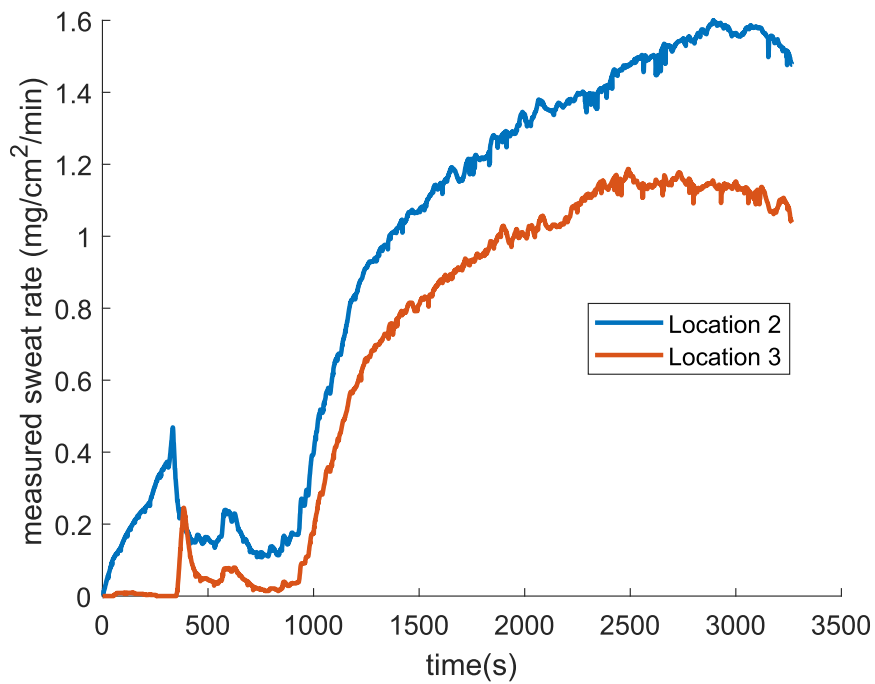


**Figure A.3:** Sweat rate for subject 1

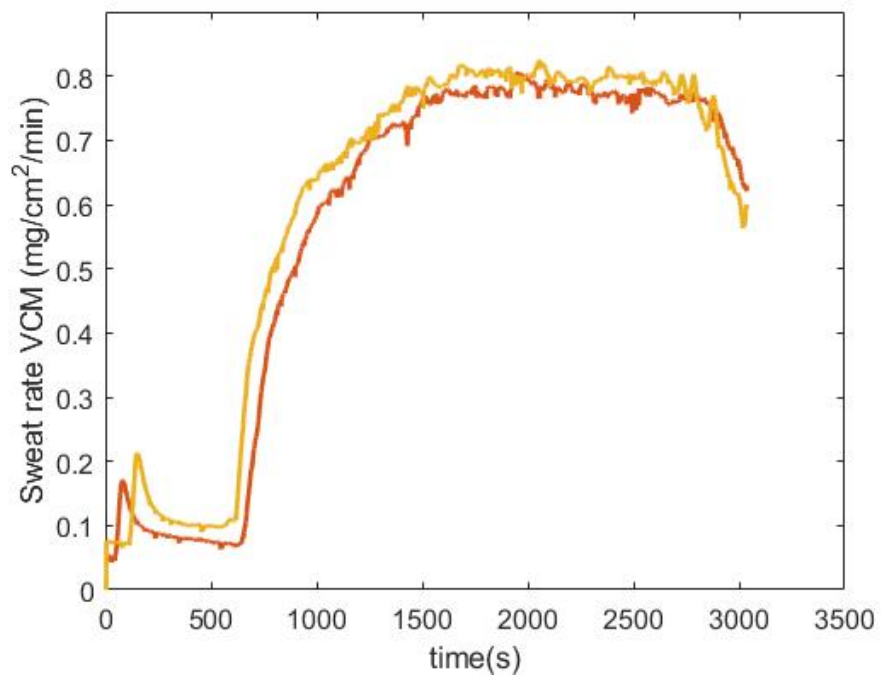


Figure A.4: Sweat rate for subject 4



# B

## Read-out software code

```
#include "mbed.h"
#include "Adafruit_ADS1015.h"
#define SERIAL_BAUD_RATE 115200

I2C i2c(PB_9, PB_8); // I2C pins
Adafruit_ADS1115 adc(&i2c, 0x48); // Library optimized for more efficient sampling
Serial pc(SERIAL_TX, SERIAL_RX); // debug tx, rx
Ticker sample; // Interrupt
Timer timer; // Timer for samples
int32_t sensor[8] = {0,0,0,0,0,0,0,0}; // Sweat sensors
int16_t single_temp = 0; // Temperature sensor
bool channel=0; // Read-out channel (0 or 1)
bool read_e=0; // If read_e=1, start of collecting data
unsigned int sensor_count=0; // Sensor sampled
unsigned int next_sensor=0; // Sensor next sample
unsigned int sample_count=0; // Numbers of samples in a row from the same sensor

DigitalOut a1(LED1); // Indication light

BusOut C_a(D3, D4, D5); // Databus to select channel Multiplexer 1
BusOut C_b(D7, D9, D11); // Databus to select channel Multiplexer 2

void get_data()
{
    read_e = 0;
    if(sample_count<19) {
        sensor[sensor_count] = sensor[sensor_count]+adc.readADC_Differential(channel); //load
        sampled data, ask for next sample
        sample_count++;
        return;
    }
    sample_count=0; //After 20 samples, a new sensor has to be selected
    channel=0;
    next_sensor = (sensor_count+4)%8;
    if(next_sensor<4) { Switch from multiplexer and sensor
        next_sensor++;
        channel=1;
        if(next_sensor>3) {
            next_sensor=0;
        }
    }
}
```

---

```
sensor[sensor_count] = sensor[sensor_count]+adc.readADC_Differential(channel); //load
    sampled data, ask for next sample at other channel
if(next_sensor>3) {
    C_a = (sensor_count+1)%4; //Select channel of multiplexer 1
}
if(next_sensor<4) {
    C_b = (sensor_count+1)%4; //Select channel of multiplexer 2
}
int mseconds = timer.read_ms();
pc.printf("%6d,%6u,%6d", sensor_count,mseconds,sensor[sensor_count]); //Send through Uart
    the sensor number, time of the sample and sensor value of 20 samples
pc.printf("\r");
pc.printf("\n");
sensor[sensor_count]=0; //Reset sensor value
sensor_count = next_sensor; //This is the sample that is know beeing sampeld due to the
    optimized library
}

void time_read()
{
    read_e = 1; //Start sampling
}

int main()
{
    i2c.frequency(800000);
    pc.baud(SERIAL_BAUD_RATE);
    adc.setGain(GAIN_ONE);
    sample.attach_us(time_read, 6250); //Specifying the repeat interval of the sampling
    timer.start();
    while(1) {
        if(read_e>0) {
            get_data(); //After interupt, load data and start new sampling
            a1 = channel; //Indicat via led after succesfull run through get_data()
        }
    }
}
```

---

C

## Pictures of physiological experiments

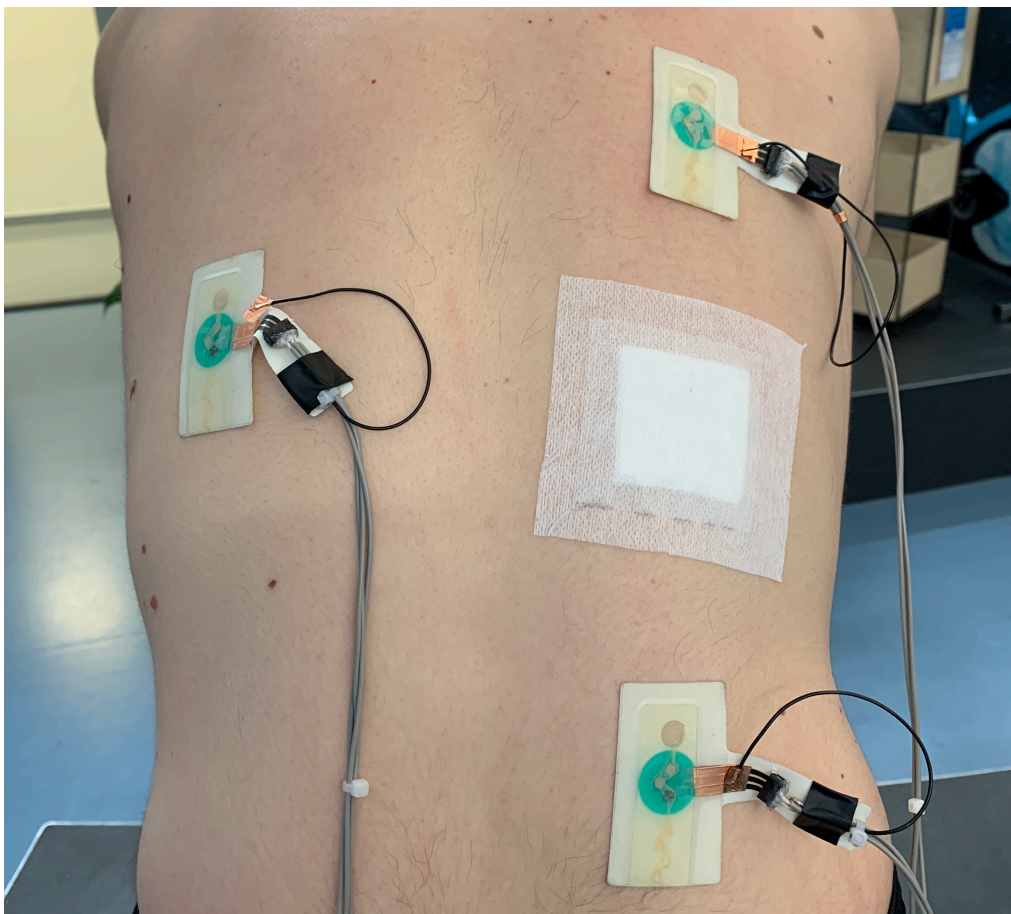


**Figure C.1:** All three sensors and the sweat patch attached to the back of the subject

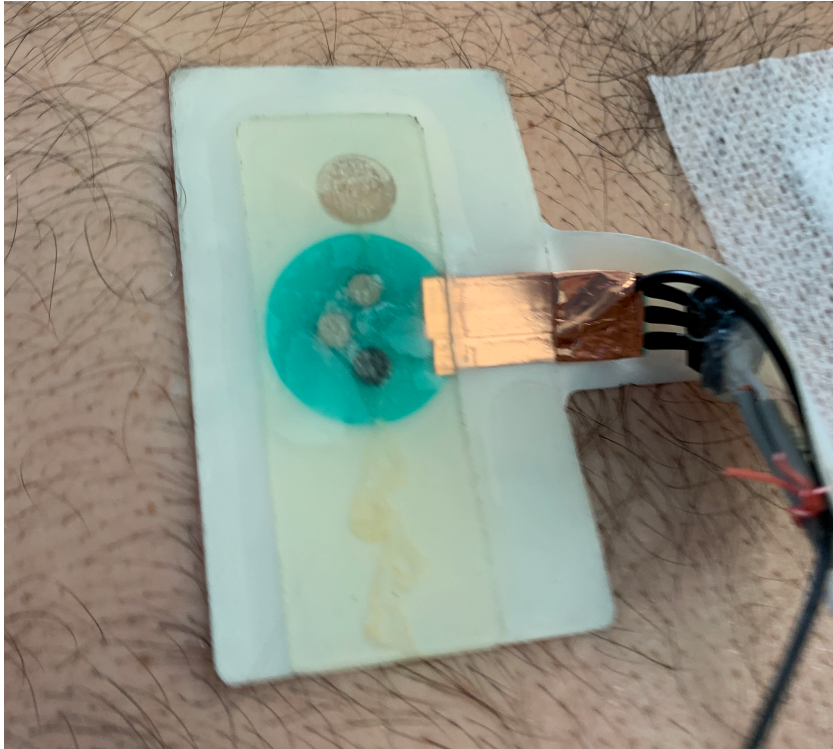


**Figure C.2:** *Strong adhesion of the sensor in a subject with abundant body hair*

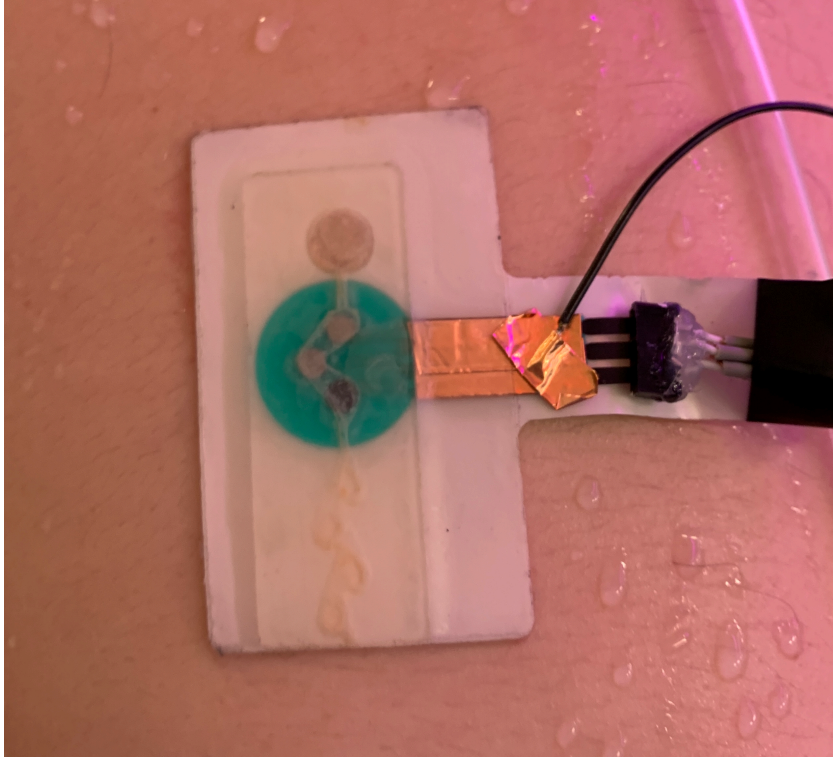


**Figure C.3:** *Sweat sensing patch during the exercise period*

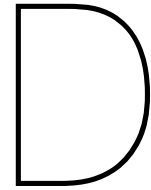




**Figure C.4:** *Slight skin irritation right after detachment of the patch*







# Informed consent form and study information

## Consent Form for [Sweat collection and analysis]

Please tick the appropriate boxes

Yes No

### Taking part in the study

I have read and understood the study information dated [02/10/2021], or it has been read to me. I have been able to ask questions about the study and my questions have been answered to my satisfaction.  Yes  No

I consent voluntarily to be a participant in this study and understand that I can refuse to answer questions and I can withdraw from the study at any time, without having to give a reason.  Yes  No

I understand that taking part in the study involves a physical exercise to stimulate sweat production, the collection of my sweat and its ion concentrations will be measured. The information is recorded by making notes and sweat samples and by logging the measurements from the devices.  Yes  No

### Risks associated with participating in the study

I understand that taking part in the study involves the following risks: skin irritation by the sweat analysis device and physical exhaustion.  Yes  No

### Use of the information in the study

I understand that information I provide will be used for reports and publications.  Yes  No

I understand that personal information collected about me that can identify me, such as [e.g. my name or where I live], will not be shared beyond the study team.  Yes  No

### Future use and reuse of the information by others

I give permission for the anonymized data and sweat ion concentrations that I provide to be archived in a secured storage system so it can be used for future research and learning.  Yes  No

### Signatures

\_\_\_\_\_  
Name of participant

\_\_\_\_\_  
Signature

\_\_\_\_\_  
Date

I have accurately read out the information sheet to the potential participant and, to the best of my ability, ensured that the participant understands to what they are freely consenting.

\_\_\_\_\_  
Researcher name

\_\_\_\_\_  
Signature

\_\_\_\_\_  
Date

### Study contact details for further information:

Luis del Río

T: +34 609 602 509

E: l.delriogarcia@student.tudelft.nl

## Informed consent form

### Study information

**Title of Research:** Ionic sweat analysis for health monitoring in real-time exercise  
**Researchers:** Luis del Río  
**Affiliation:** Delft University of Technology, the Netherlands  
**Contact:** l.delriogarcia@student.tudelft.nl  
**Date:** 02/10/2021

#### **Purpose of the research**

The purpose of this study is to check the functionality of a sweat analysis system previously produced. This sweat analysis system can measure ionic concentrations in sweat during physical activity. The differences in concentrations during the exercise could be of great help on the monitoring of the health status of the athlete.

#### **What does participation in the research involve?**

The participation in this research study involves an approximate 45-minute exercise on a cycle ergometer. This period will allow you to sweat in great quantities so ionic concentrations can be analysed by a system taped to your back.

Before the start of the study, you will be asked to come wearing sport clothing to the testing area. As the participant will sweat in great quantities, you should also bring a towel and water.

Afterwards, you will be asked to take off your shirt so the sensors can be placed on your back. During the exercise period, no water intake is allowed, so you should drink before starting the physical activity. The placement and connection of the sensors should last around 10 minutes.

The exercise period will start with a 5-minute warm up so you can get used to cycle on the ergometer. During the intensive exercise period (~35 minutes), you will be constantly cycling so the sweating on your back is assured. You may be asked to maintain your heartbeat or the bike's cadence above a certain value. The physical activity will finish with a 5-minute cooling down period.

#### **Time required:**

The complete study will take an approximal time of one hour. In this time, it is also included the preparation time for placing all sensors and the familiarization of the subject to the cycling ergometer.

#### **Risks:**

There are no anticipated risks associated with this study. The sensors attached to your skin are made using medical tape. Chances are very low, but some skin irritation may appear. The physical test is challenging but not harder than an average spinning class.

**Benefits:**

You will not directly benefit from participating in this study. The study will contribute to research on monitoring the health status of patients during physical activity through sweat.

**Confidentiality of data:**

Should you agree to take part, your participation will be completely confidential. You have the right to stop participating at any time and can have your data removed up to three months after the data gathering. All information gathered in the survey will be stored securely in compliance with the standards set by the European Union General Data Protection Regulation (GDPR). No one outside the research group will have access to the data. Data will be kept by the research group and will be completely anonymized (no link between the data and the consent form). Upon analysis and publication, the anonymized data will be stored and made available open access for other researchers to analyse.

**Right to withdraw from the study:**

Participation in the study is completely voluntary. If at any time you do not wish to continue your participation, you are free to withdraw from the study without any penalties.

**How to withdraw from the study:**

You can end your participation by stopping the teaching activity at any time. If you want to withdraw your participation after completing a session, please contact Luis del Río (see email information above).

**Questions?**

For questions, concerns, or complaints, please contact Luis del Río (see email information above).

